Uncertainty and Sensitivity in Regional Earthquake Loss Estimation

by

Phani Rama Krishna Jammalamadaka

Bachelor of Technology in Civil Engineering
Indian Institute of Technology, Madras (2001)

Submitted to the Department of Civil and Environmental Engineering
in partial fulfillment of the requirements for the degree of

Master of Science in Transportation
at the

MASSACHUSETTS INSTITUTE OF TECHNOLOGY

September 2003

Author .....
Department of Civil and Environmental Engineering
August 15, 2003

Certified by .....
Joseph M. Sussman
JR East Professor
Thesis Supervisor

Certified by .....
Daniele Veneziano
Professor of Civil and Environmental Engineering
Thesis Supervisor

Accepted by .....
Heidi Nepf
Chairman, Departmental Committee on Graduate Studies

Uncertainty and Sensitivity in Regional Earthquake Loss Estimation

by
Phani Rama Krishna Jammalamadaka

Submitted to the Department of Civil and Environmental Engineering
on August 15, 2003, in partial fulfillment of the requirements for the degree of
Master of Science in Transportation

Abstract

The objectives of this thesis are: (a) assess the uncertainties in various components of the regional earthquake loss estimation process, and (b) perform sensitivity analysis to obtain the relative influence of different factors on the final losses and get a measure of the uncertainty in the losses.

Specifically, we quantify uncertainty on the following components of loss estimation: (a) ground motion attenuation, (b) site amplification, (c) building inventory and fragility, (d) bridge fragility, and (e) loss of function and its recovery over time. Sensitivity of the losses is evaluated by varying each parameter or model within its uncertainty range.

The analysis is done in the context of earthquake scenarios in the New Madrid Seismic Zone (NMSZ), using the earthquake loss estimation methodology developed by Kunnumkal (2002).

Thesis Supervisor: Joseph M. Sussman
Title: JR East Professor

Thesis Supervisor: Daniele Veneziano
Title: Professor, Civil and Environmental Engineering

Acknowledgements

I express my sincere gratitude to my advisors, Professor Daniele Veneziano and Professor Joseph Sussman for their advice, support and patience. This research would not have been a success without their expertise. I owe a lot to them.

I would like to thank Professor Robert Whitman, Professor Reginald DesRoches and Professor Howard Hwang for their feed-back on some parts of this research.

I am thankful to my under-graduate advisor, Professor Meher Prasad, for his guidance and support. He would always remain a source of inspiration for me.

I thank Sumit Kunnumkal and Erdem Karaca, who worked on this project along with me, for their friendship and help. I learnt a lot from their sincerity and dedication.

I would also like to express my thanks to Mid-America Earthquake Center and National Science Foundation for their financial support of this research.

In addition, I would like to thank all my friends for their support.

Finally, I would like to thank my dear parents, siri and all my relatives for their love and support.

Contents

List of Figures

List of Tables

1 Introduction

The process of estimating losses produced by large scenario earthquakes is affected by many uncertainties. Even when the source parameters such as the epicentral location and magnitude are fixed, significant uncertainties remain on the resulting ground motion, the inventory, the response of the infrastructure and the consequent economic impacts. These uncertainties are partly due to the inherent randomness of the physical phenomena involved and partly to our lack of knowledge. A reason for the limited knowledge is that there have been very few major earthquakes in the recent past. One aim of this thesis is to assess the uncertainties associated with the models and parameters that are used in regional earthquake loss estimation. This assessment is made through a review of existing data sources. The other aim of this thesis is to perform sensitivity analysis of the losses by using alternative models and parameters within their respective range of uncertainty. The results of the sensitivity analyses can then be used to quantify uncertainty on the losses, through uncertainty propagation analysis. This uncertainty propagation is however outside the scope of the present study.

We specifically assess uncertainty in the following components of loss estimation: (a) earthquake ground motion/intensity attenuation, (b) site amplification, (c) building inventory, (d) building fragility, (e) bridge fragility, and (f) loss of function and recovery of social function. For ground motion and damage characterization, we use two alternative approaches, the "macroseismic" approach and the "engineering" approach. The macroseismic approach is a traditional method based on the characterization of ground motion intensity and building fragility in terms of a macroseismic intensity measure. By contrast, the engineering approach uses instrumental measures of ground shaking intensity such as peak ground acceleration or response spectra.

Sensitivity analysis is done by perturbation of the components mentioned above. In addition, we study the sensitivities to some of the transportation network functionality

and economic parameters relevant to loss estimation. The loss estimation methodology used in this thesis is the one developed by Kunnumkal (2002).

This thesis focuses mainly on assessing the uncertainties in the input models and parameters that are applicable for earthquakes in the New Madrid Seismic Zone (NMSZ). The NMSZ is specifically considered here because it is an economically active region and acts as a conduit for a large fraction of the flow of goods that take place in the U.S. Damage to the physical infrastructure in NMSZ could thus cause widespread losses to the U.S. economy.

The thesis is organized as follows:

Chapter 2 reviews existing earthquake loss estimation models and includes a detailed description of the methodology of Kunnumkal (2002). It describes the sources for inventory and economic data, the models used in various components of the methodology and the analytical framework.

Chapter 3 describes the different types of uncertainties involved in earthquake loss estimation and assesses the uncertainty of various component models and parameters.

Chapter 4 describes the framework for sensitivity analysis and the associated results.

Chapter 5 summarizes the main findings of this study and suggests areas for future research.

2 Earthquake Loss Estimation Models

There have been a number of studies in the past aimed at quantifying the direct and indirect impacts of earthquakes. HAZUS (2000), Werner et al. (2000), Cho et al. (2000), Sohn et al. (2001), Gupta (2001) and Kunnumkal (2002) represent the state of the art techniques in earthquake loss estimation. All of them evaluate system wide impacts, but operate at different geographical scales. Cho et al. (2000), Gupta (2001) and Kunnumkal (2002) are the only methodologies that integrate the transportation network damage with the disruption of the economic sectors. In the first section of this chapter, a brief review of the earthquake loss estimation models is presented. The second section consists of a detailed description of the methodology developed by Kunnumkal (2002), which is used in the Sensitivity Analysis in Chapter 4.

2.1 Brief review of earthquake loss models

HAZUS (2000)

HAZUS (2000) is a methodology that uses detailed inventory databases (default) for all the states in the U.S. at the census tract level. It calculates the direct and indirect economic and social losses. As the methodology does not incorporate transportation network analysis, the indirect economic losses that are calculated do not account for the disruption in the traffic flows after an earthquake. The analysis is limited to a census tract or county discretization due to the data intensiveness.

Werner et al. (2000)

Werner et al. (2000) developed a metropolitan-level loss estimation methodology which calculates both the direct losses due to the damage to the highway components and the indirect losses due to the increase in travel time from transportation network damage. The methodology incorporates the recovery of the transportation network over time. However, it does not consider the vulnerability of the non-transportation infrastructure as it considers the demand for the transportation network to be exogenous. Thus, the losses do not account for the reduced transportation demand, which could result from the

damage to the economic sectors. The applicability of the model beyond the metropolitan scale is limited by the data intensiveness and the computational requirements.

Cho et al. (2000)

Cho et al. (2000) is a comprehensive metropolitan-level loss estimation methodology which models the interactions between the economy and the transportation network in the region of interest. The methodology also considers the reduced transportation demand due to the disruption of the economic sectors and the reduced transportation capacity after an earthquake. The losses evaluated are both the direct losses to the infrastructure and the indirect losses due to the increased transportation costs and business interruption. Limitation with the methodology is the data intensiveness, computational complexity, specificity to southern California and the use of proprietary models.

Sohn et al. (2001)

Sohn et al. (2001) model the inter-regional flows and the inter-industry interactions at a national level. They estimate the indirect losses due to the disruption of the transportation network in the form of increased transportation costs and the induced changes in the final demands. Their network model considers cross-hauling (the flow of the same commodity in both directions between two regions) and non-linear link travel times. They model the vulnerability of the transportation network but not that of the building infrastructure. Therefore, they do not model the reduced transportation demand due to the damage to the economic sectors. The recovery process of the transportation network is not modeled in detail.

Kunnumkal (2002)

This methodology is an improvement on the methodology developed by Gupta (2001). Kunnumkal (2002) considers the damage to the infrastructure elements, their loss of functionality and their recovery with time. The dependence of the functionality and the recovery of various economic sectors on the regional transportation system and other lifelines are also modeled, although in a coarse manner. Inter-industry interactions are modeled by using an input-output model. In addition, inter-regional interactions are

modeled by using a transportation network model. The methodology considers alternative approaches, engineering and macro seismic (which have been introduced in Chapter 1), for estimation of the direct damage to the infrastructure elements. Other loss measures calculated in the methodology include the increased transportation costs due to network disruptions, direct social losses in the form of injuries and casualties, and indirect social losses due to the unmet domestic demand. The methodology is essentially deterministic as it does not incorporate uncertainties in most of the input models and parameters. However, computational requirements limit the methodology to the use of linear link cost functions and the omission of factors such as cross-hauling.

Table 2-1 shows comparisons of the different earthquake loss estimation methodologies that are reviewed here.

2.2 Detailed description of the methodology of Kunnumkal (2002)

In the methodology, the conterminous U.S. is divided into many analysis regions, which are connected by the road transportation network. Each analysis region typically consists of a number of counties or in the Shelby County of the New Madrid region, census tracts. The nodes of the transportation network are the highway intersections and the links are the highway segments connecting the nodes, along with the bridges on them. Each county is associated with the highway node that is closest to its centroid. All the counties that are associated with the same highway node form an analysis region. The building stock associated with an analysis region is assumed to be concentrated at the centroid (the location of the mean of the geometric centroids of the counties associated with an analysis region, weighted by the counties' population) of the analysis region. The exports/imports from/to an analysis region are assumed to take place through the highway node associated with that analysis region.

	HAZUS (2000)	WERNER ET AL. (2000)	CHO ET AL. (2000)	SOHN ET AL. (2001)	KUNNUMKAL (2002)
Geographic Scale	Regional	Metropolitan	Metropolitan	National	National
Lowest geographical unit	Census tract	Traffic Analysis Zone	Traffic Analysis Zone	EQAZ, 2-5 EQAZ's per state	Census Tract
Detail in transportation network	None included for transportation network flow modeling	Detailed inventory of urban road system	Detailed inventory of L.A. region roads	Interstate highway network	Interstate highways augmented by some state and county roads
Infrastructure Earthquake Vulnerability	For most building infrastructure including lifelines	Only for highway bridges, approach fills, and roadways	Explicitly modeled for highway bridges and industries	Only for highway bridges	Buildings, highway pavements and bridges
Recovery of components	Yes, detailed recovery models	Yes, for highway components only	Yes, for economic sectors only	No	Yes, explicitly modeled
Modeling approach	Engineering	Engineering	Engineering	Engineering	Macro-seismic and Engineering
Direct Losses	Yes	Yes, only for highway components	Yes	No	Yes, for building stock, highway pavements and bridges
Indirect losses due to business interruption	Yes	Yes, limited to costs of travel delays	Yes	Yes, excluding indirect losses due to the damage to the economic sectors	Yes
Industrial interactions (through input-output models)	Yes, detailed input-output modeling for indirect losses	None, transportation demand is assumed to be exogenous	Yes, detailed input-output models	Yes, input-output models for industrial interactions	Yes, input-output models for industrial interactions
Prediction of network flows	None, there is no transportation flow modeling involved	Yes, detailed artificial intelligence approach	Yes, urban transportation planning method	Yes, optimization based algorithms minimizing transportation costs	Yes, optimizing transportation network costs
Freight/Traveler	None	Both	Both	Freight	Freight
Indirect losses in transportation network	None	Increase in travel time	Increase in travel cost and effect on the economy	Increase in travel cost and effect on economy	Yes, increased transportation costs due to network damage

Table 2-1: Comparison of the various earthquake loss estimation models

Immediately after a scenario earthquake, the damage and the functionality of the building infrastructure and the road transportation network components are estimated, as a function of the distance from the epicenter. Suitable ground motion/intensity attenuation and infrastructure vulnerability models are assumed for the damage and initial functionality calculations. The production and consumption rates in different economic sectors are estimated under the constraints of the reduced transportation network and economic sector functionalities as a function of time after the earthquake. Functionalities of the various economic sectors are updated with time, taking into account the associated dependence on the functionalities of the lifelines and the residential sector. Indirect economic losses due to the "lost" productions and "lost" consumptions are estimated along with the increased transportation costs during the recovery period of all the economic sectors. Direct losses due to the damage to the building and transportation infrastructure are also estimated.

Next, we describe the way in which the data regarding the population, inventory, economic data and local geological conditions are obtained for each analysis region.

2.2.1 Inventory and economic data

- Building Inventory: The building inventory at the county level is obtained from HAZUS (2000), which is aggregated to the analysis regions.
- Contents Inventory: The contents inventory is assumed to be 75% of the corresponding building inventory, based on the data in ATC-13 and HAZUS (2000).
- Population: The population at the county level is obtained from the 1990 U.S. Census of Population and Housing. The county level data is aggregated to the analysis regions.
- Transportation Network: Only the road transportation network is considered, which includes mainly the highways. In the New Madrid region, there is a finer classification as some of the state highways are also included in the analysis. The highway inventory is obtained from NTAD (Bureau of Transportation Statistics (2000)). Bridges on highways are considered only in the New Madrid region for

analysis. Bridge inventory given in NBI (Federal Highway Administration (FHWA (1995)) is used.

- Geological Conditions: For the New Madrid region, the geological information is obtained from Toro and Silva (2001). Outside the New Madrid region, hard rock conditions are assumed.
- Economic data: 13 economic sectors are considered, as given in Okuyama et al. (1999). The domestic consumptions and productions are obtained at the national level from Sohn et al. (2001), which are disaggregated to the analysis region level.

2.2.2 Component models

Kunnumkal (2002) uses both the engineering and macroseismic approaches (introduced in Chapter 1) for choosing the parameters in the ground motion/intensity attenuation and fragility models. The various models considered are:

- Ground motion/intensity attenuation: Bollinger (1977) with out site effects is used in the macroseismic approach. Toro and Silva (2001) is the attenuation relation used in the engineering approach.
- Building fragility:
    - In the macroseismic approach, 6 building classes (timber, unreinforced and reinforced masonry, reinforced concrete, heavy and light steel) are considered. The fragility parameters are based on the information given in ATC-13 and FEMA (1990). Soil effects are not considered for the damage calculation.
    - In the engineering approach, the fragility parameters and the seismic vulnerability classes are based on HAZUS (2000). Soil effects are considered in this approach.
- Link (pavement) fragility: Classification and fragility information from ATC-13 is used to calculate the link damages.
- Bridge fragility: Fragility models in HAZUS (2000), DesRoches (2002) and Hwang et al. (2000a) are considered.
- Functionality-Interaction and Recovery Parameters:

- The initial functionality of each occupancy class is calculated by considering the variability in the functionality of individual buildings in the occupancy class.
- The recovery parameters for buildings and links are from ATC-13. In case of bridges, the parameters are based on Hwang et al. (2000b).
- Effects of the loss of function of the utilities and transportation on the functionality and recovery rates of different economic sectors are from Kunnumkal (2001) (the details of this model are given in Chapter 3).

- Transportation flow model: The (undamaged) link capacities are based on the Average Daily Traffic (ADT) data from FHWA (1995). Passenger flows and cross-hauling are not considered in the analysis. The effect of secondary roads is modeled by the re-routing parameter (ρ). The highway link capacity is set as the minimum of the pavement and bridge capacities. However, the bridge capacities are not allowed to be less than ρ times the undamaged link capacity.

2.2.3 Analytical framework

The loss estimation methodology developed by Kunnumkal (2002), includes the following 4 steps:

Step 1: Damage and functionality initialization

A scenario earthquake is assumed and the damage to buildings, lifelines, pavements and bridges is calculated as a function of the distance from the epicenter, by assuming certain ground motion/intensity attenuation relations. The initial functionalities of all the economic sectors and the transportation network components are calculated.

Step 2: Node-Network iterations

i. For each analysis region, the productions of each economic sector are calculated as a function of the reduced functionality of the economic sectors. The productions are calculated as:

$$X^{k,r} = X^{k,r}_{preEQ} * F^{k,r}_{actual} \qquad \forall k, r \tag{2-1}$$

where

$X_{preEQ}^{k,r}$ is the pre-earthquake production rate of sector k in analysis region r.

$X^{k,r}$ is the production rate of sector k in analysis region r at the time instant considered.

$F_{actual}^{k,r}$ is the actual functionality of economic sector k in analysis region r at the time instant considered.

The post-earthquake consumption rates are assumed to be the same as the pre-earthquake consumptions, i.e.,

$$c^{k,r} = c_{preEQ}^{k,r} \quad \forall k, r \tag{2-2}$$

where

$c_{preEQ}^{k,r}$ is the pre-earthquake domestic consumption rate of sector k in analysis region r.

$c^{k,r}$ is the domestic consumption rate of sector k in analysis region r at the time instant considered.

ii. Some of the supply shocks in the analysis regions due to the reduced functionalities of the economic sectors are assumed to be absorbed by the availability of excess inventories or foreign imports. These buffering effects are modeled by assuming a certain slack in the sectorial production capacities in all the analysis regions. It is assumed that productions can be increased up to the slack limit to offset the reduced functionalities of the sectors in the earthquake affected regions. The productions are increased to minimize the difference in the total production and the total demand (industrial demand and the domestic consumption) of all the commodities at the national level, under the constraint that the production of each economic sector cannot exceed its slack limit. A linear programming formulation of the above problem is given below:

$$\min \sum_k \left\| d^k \right\| \tag{2-3}$$

s.t.

$$(I - A)X_f^{national} - c^{national} + d = 0 \tag{2-4}$$

$$0 \le f^k \le slack^k \quad \forall k \tag{2-5}$$

where

I is the identity matrix.

A is the input-output matrix.

$X_f^{national}$ is the vector of the increased national production rates of the economic sectors.

$c^{national}$ is the vector of the national domestic consumption rates of the economic sectors.

$slack^k$ is the slack in the production of sector k.

f^k is the factor by which production rate of the economic sector k is increased to minimize the difference between the productions and the total demands at the national level.

$\|d^k\|$ is the absolute difference between the production rates and the demand rates of sector k at the national level.

iii. The f^k's obtained by solving the LP problem (2-3) are applied uniformly to all the analysis regions. The productions and consumptions of the analysis regions are then aggregated at the associated highway nodes. The productions and consumptions at the highway nodes are given by:

$$X^{k,i} = \sum_{r \in R_i} X^{k,r} * f^k \quad \forall k, \forall i \tag{2-6}$$

$$c^{k,i} = \sum_{r \in R_i} c^{k,r} \quad \forall k, \forall i \tag{2-7}$$

where

$X^{k,i}$ is the production rate of sector k associated with highway node i.

$X^{k,r} * f^k$ is the increased production rate of the sector k in analysis region r.

$c^{k,i}$ is the domestic consumption rate of sector k at node i.

$c^{k,r}$ is the domestic consumption rate of sector k at analysis region r.

R_i is the set of the analysis regions that are associated with highway node i.

iv. A multi-cost-multi-commodity flow problem is then solved on the network to satisfy the nodal requirements by routing the commodities at the least cost. The corresponding problem's linear programming formulation is:

$$\min \sum_k \sum_{(i,j)\in L^+} c_{ij}^k x_{ij}^k \tag{2-8}$$

s.t.

$$\sum_{j:(i,j)\in L^+} x_{ij}^k - \sum_{j:(j,i)\in L^+} x_{ji}^k = b^{k,i} / \lambda^k \quad \forall k, \forall i \tag{2-9}$$

$$\sum_k x_{ij}^k \le u_{ij} \quad \forall (i,j) \in L^+ \tag{2-10}$$

$$x_{ij}^k \ge 0 \quad \forall (i,j), k \tag{2-11}$$

where

c_{ij}^k is the cost of transporting a unit of commodity k on link (i, j), which is taken to be the link length.

x_{ij}^k is the flow of commodity k on link (i, j) in vehicle units (trucks/day).

$b^{k,i}$ is the net export/import rate of commodity k at node i in \$.

λ^k is the factor used to convert the commodity values to vehicle units for commodity k (\$/truck).

u_{ij} is the link capacity (trucks/day).

L^+ is the set of all links, including the virtual links. Each highway node is connected to a virtual node by an undirected link, called virtual link. Virtual links and the virtual node are introduced into the methodology because of the following reason. Even though the net exports and imports over the whole transportation

network balance out (supply equals demand) in pre-earthquake conditions, one can typically expect the demand to be greater than the supply due to the disruption in the production of the industrial sectors after an earthquake. This net deficit/excess in the real network is associated with the virtual node. Virtual links serve as conduits for the flows from all the nodes to or from the virtual node. They are associated with high costs (to limit the flows on these links as the objective is to minimize cost) and high capacities (so that very high net deficits/excesses can be handled by the augmented network).

The objective function (2-8) minimizes the total cost of routing all the commodities on the network. Constraint (2-9) is the flow balance constraint at each node. Constraint (2-10) is the capacity constraint on the flow on each link. Constraint (2-11) is the non-negativity constraint on the commodity flows.

v. The actual export/import rate of commodity k from node i, say $b^{k,i}_{actual}$, would be different from the net exports/imports, $b^{k,i}$, because the value $b^{k,i}$ includes the flows on virtual links, which are not actually sent from or received at any node. The actual export/imports are given by:

$$b^{k,i}_{actual} = \lambda^k \left(\sum_{j:(i,j)\in L} x^k_{ij} - \sum_{j:(j,i)\in L} x^k_{ji} \right) \forall k, \forall i \qquad \textbf{(2-12)}$$

where

L is the set of all the real links.

vi. In this step, the net exports/imports are adjusted such that they become as close to the actual exports/imports as possible. This is done by the following L.P. at each node:

$$\max \; -C_1 \sum_k d^{k,i} + C_2 \sum_k X'^{k,i} + C_3 \sum_k c'^{k,i} \qquad \textbf{(2-13)}$$

s.t.

$$(I - A)X'^{i} - c'^{i} \pm d^{i} = \pm b^{i}_{actual} \qquad \textbf{(2-14)}$$

$$0 \le X'^{k,i} \le X^{k,i} \quad \forall k \tag{2-15}$$

$$0 \le c'^{k,i} \le c^{k,i} \quad \forall k \tag{2-16}$$

$$d^{k,i} \ge 0 \tag{2-17}$$

where:

C_1, C_2, C_3 are given non-negative constants.

$d^{k,i}$ is the difference between the actual and net export rates of commodity k at node i.

$X^{k,i}$ is the maximum possible production rate of sector k at node i considering the reduced functionality due to the damage at the node. $X^{k,i}$ is from equation (2-6).

$X'^{k,i}$ is the adjusted production rate of sector k at node i.

$c^{k,i}$ is the maximum domestic consumption rate of sector k from at node i. This is from equation (2-7).

$c'^{k,i}$ is the adjusted consumption rate of sector k at node i.

The coefficients C_1, C_2, C_3 in equation (2-13) are the weights of the variables in the objective function and determine how the deficit is apportioned between the economic sectors and the population. The negative sign of C_1 in equation (2-13) means that the value of $d^{k,i}$ is set as close as possible to zero, implying that the adjusted consumptions and productions are set close to the actual export/imports that are dictated by the network. A greater value of C_3 relative to C_2 means that the domestic consumptions are set to be close to their maximum possible values, but the productions are allowed to get adjusted more to obtain the required exports/imports.

If the value of $d^{k,i}$ is less than an allowable positive tolerance, then it is assumed that the node is able to adjust its production/consumptions and is said to be balanced. Otherwise, the node is said to be unbalanced.

vii. If there are any unbalanced nodes, steps (iv-vi) are repeated with modified nodal net exports given by:

$$b^{k,i} = b^{k,i}_{actual} - d^{k,i} \tag{2-18}$$

If there are no unbalanced nodes, then the node-network iterations are terminated. The production and consumption rates of the analysis regions that correspond to the highway node i are then calculated as:

$$X'^{k,r}_{nof^k} = X^{k,r} \frac{X'^{k,i}}{X^{k,i}} \quad \forall r \in R_i, \forall k \tag{2-19}$$

$$X'^{k,r}_{withf^k} = X^{k,r} \frac{X'^{k,i}}{X^{k,i}} * f^k \quad \forall r \in R_i, \forall k \tag{2-20}$$

$$c'^{k,r} = c^{k,r} \frac{c'^{k,i}}{c^{k,i}} \quad \forall r \in R_i, \forall k \tag{2-21}$$

where

$X'^{k,r}_{nof^k}$ is the production rate of sector k at region r at the end of the node-network iterations, which does not include the increased production factor f^k.

$X'^{k,r}_{withf^k}$ is the production rate of sector k at region r at the end of the node-network iterations, which includes the increased production factor f^k.

$X^{k,r}$ is the production rate of sector k at region r prior to the node-network iterations, from equation (2-1).

$c'^{k,r}$ is the domestic consumption rate of sector k at region r at the end of the node-network iterations.

$c^{k,r}$ is the domestic consumption rate of sector k at region r prior to the node-network iterations.

Step 3: Loss calculation

1. **Direct losses:** At the time instant t = 0^+, i.e., immediately after the earthquake, the direct losses due to the damage to the buildings, contents, highway pavements and bridges are calculated.

2. **Indirect losses:**

Production Loss: The loss due to the reduction in actual production during a time interval (Δt) is calculated in two different ways. One loss calculation includes the increased productions due to slack in the production capacity, while the other does not include the increased productions. The production loss calculated when using the first method is given by

$$IDL_{prod}(\Delta t)_1 = \Delta t \sum_k \sum_r (X^{k,r}_{preEQ} - \overline{X'^{k,r}_{nof^k}}) \tag{2-22}$$

where

$IDL_{prod}(\Delta t)_1$ is the indirect loss associated with the loss of production of the economic sectors during the time interval of length Δt, where the post-earthquake productions considered in the loss calculation do not include the increased productions due to slack in the production capacity.

$\overline{X'^{k,r}_{nof^k}}$ is the average production rate of the economic sector k in region r during the time interval Δt, this is calculated based on equation (2-19).

The production loss obtained from the second method is

$$IDL_{prod}(\Delta t)_2 = \Delta t \sum_k \sum_r (X^{k,r}_{preEQ} - \overline{X'^{k,r}_{withf^k}}) \tag{2-23}$$

$IDL_{prod}(\Delta t)_2$ is the production loss of the economic sectors during the time interval of length Δt, where the post-earthquake productions are calculated taking into account the increased production of the economic sectors due to slack in the production capacity.

$\overline{X'^{k,r}_{withf^k}}$ is the average production rate of the economic sector k in region r during the time interval Δt, which is calculated based on equation (2-20).

Consumption Loss: The loss due to the decreased consumption is calculated as

$$IDL_{cons}(\Delta t) = \Delta t \sum_k \sum_r (c^{k,r}_{preEQ} - \overline{c'^{k,r}}) \tag{2-24}$$

$IDL_{cons}(\Delta t)$ is the indirect loss associated with the reduced domestic consumption (unmet final demand) during the time interval Δt.

$\overline{c'^{k,r}}$ is the average domestic consumption rate of the economic sector k in region r during the time interval Δt.

The indirect losses calculated during different time intervals are added over time to get the total indirect losses.

3. **Increased transportation costs:** Increased transportation costs are estimated as the ratio of the cost of transporting commodities on the damaged network to the cost of transporting the same commodities on the undamaged network. The transportation cost corresponding to the undamaged network and the damaged network are obtained by routing the net exports from all the highway nodes that are obtained after step (2-vii) on an undamaged and damaged network respectively. The multi-cost-multi-commodity flow formulation given in equation (2-8) is used for the network routing. The increased transportation cost is given as:

$$IDL_{transp} = \frac{TC_{damaged}}{TC_{undamaged}} \tag{2-25}$$

where:

$TC_{damaged}$ is the total transportation cost on the damaged network.

$TC_{undamaged}$ is the total transportation cost on an undamaged network.

Step 4: Functionality update

A recovery model is used to update the functionalities of the various occupancy classes, pavements and the bridges as a function of the time after the earthquake. The functionalities are updated considering the interactions between the functionalities of the different occupancy classes.

Steps 2 to 4 are repeated until all the infrastructure elements have recovered completely.

In this chapter, we have compared some of the models that are considered to represent the state of the art in earthquake loss estimation. In addition, we have described in detail the methodology of Kunnumkal (2002), which is used as the basis for the sensitivity analysis that we perform in Chapter 4. In the next chapter, we assess the uncertainty in various components of regional earthquake loss estimation.

3 Uncertainty Assessment

This chapter assesses uncertainty on the main models and parameters that are used in regional earthquake loss estimation, with focus on the Central and Eastern United States (CEUS) region. Specifically, we consider uncertainty on ground motion attenuation, building inventory, building and bridge vulnerability, loss of functionality, and the recovery of social function over time. First we briefly discuss the types of uncertainty that one encounters in loss estimation. Then we assess the uncertainty in various components of loss estimation.

3.1 Uncertainty types

Given an earthquake location and intensity, regional earthquake loss estimation usually involves the following main components: (1) characterization of the exposed inventory, (2) estimation of the ground motion/intensity attenuation and site amplification, (3) estimation of the level of damage, (4) calculation of the monetary losses, given the level of damage to the infrastructure. All of the above components in loss estimation are associated with uncertainties, which propagate to the final loss estimates. These uncertainties are partly due to: (a) inherent randomness in the physical phenomena involved, and (b) imperfections in the models and parameters used in loss estimation. Inherent randomness, also called aleatory uncertainty, is associated with the variability in the result of a redo-able experiment. Model imperfections result due to the lack of sufficient knowledge about physical phenomena and/or due to the idealizations/simplifications made in modeling complex phenomena. Imperfections in the parameters arise due to the limited availability of statistical data. In this thesis, we refer to this type of uncertainty as epistemic (knowledge-related) uncertainty, as imperfections in the models and parameters would not arise if one had complete knowledge of the involved phenomena. There is a basic difference between these two types of uncertainty. Model and parameter imperfections can be reduced with the availability of additional statistical data or by gaining a better understanding of the involved phenomena through additional analyses or experiments. On the other hand,

aleatory uncertainty is intrinsic to the phenomena and hence cannot be decreased with additional knowledge.

In loss estimation studies, the distinction between aleatory and epistemic uncertainties may not be very relevant. However, it is important that these studies include all sources of uncertainties that may exist in various models and parameters. As stated by Hanks and Cornell (1994), "What is aleatory uncertainty in one model can be epistemic uncertainty in another model, at least in part. And what appears to be aleatory uncertainty at the present time may be cast, at least in part, into epistemic uncertainty at a later date. As a matter of practical reality, the trick is to make sure that uncertainties are neither ignored nor double counted. The possibilities of doing so with parametrically complex models are large".

In this thesis, unless otherwise stated, when we say 'uncertainty', we are referring to the total (aleatory + epistemic) uncertainty.

3.1.1 Illustration

In this section, we illustrate the different types of uncertainty by considering one of the components of loss estimation viz., the estimation of the direct losses due to the building damage. In earthquake loss estimation, it is a common practice to group buildings with similar seismic resistance characteristics into seismic vulnerability classes. Damage functions, which are used to estimate the level of damage, are developed for each of the seismic vulnerability classes as a function of the ground motion intensity/magnitude. Given the earthquake magnitude, location and the geological conditions of the exposed building infrastructure in the study area, following steps are employed to estimate the building losses: (1) assignment of the buildings in the study area to different seismic vulnerability classes, (2) calculation of the direct building losses to each seismic vulnerability class by using the corresponding damage function. The types of uncertainty that one usually encounters in the mapping of the buildings to different vulnerability classes are illustrated through the following example.

Example

Consider the building classification scheme of HAZUS (2000), which is reproduced in Table 3-1. This classification is broadly based on the primary structural material, the type of the structural framing system and the height of the building. HAZUS (2000) further classifies buildings of the same structural class into structural sub-classes based on their quality of construction: High-code, Moderate-code, Low-code and Pre-code, are the four sub-classes used in HAZUS (2000) to designate conformity of the buildings to modern building code provisions. For example, buildings that belong to the "Low-rise Unreinforced Masonry (URML)" class and designed to the low-code seismic design standards fall into the "Low-rise Low-code Unreinforced Masonry ($URML_{lowcode}$)" vulnerability class. Table 3-2 shows a recommended mapping between the Uniform Building Code (UBC) seismic zone ('Seismic Zone 4' is the geographical region that is expected to have the highest level of seismicity and 'Seismic Zone 0' is expected to have the lowest level of seismicity), the age of construction and the sub-class category, as recommended in HAZUS (2000). For example, in Seismic Zone 4, buildings constructed after 1975 are considered to be conforming to the modern Code provisions, i.e., they are assumed to be in the High-code sub-class.

Suppose we are interested in estimating the direct losses to the residential sector in a study area. Suppose that all the residential buildings are of the Wood-Frame type. Also suppose that one has information on the age of these buildings and no other indicator of the building quality specifically. Let 10% of the buildings be constructed before 1940 and 90% be Post-1980. Assuming that the study area corresponds to UBC Seismic Zone 4, we might conclude from Table 3-2 that 90% of the buildings are High-Code and the remaining are Moderate-Code. However, the reality could be that 45% and 55% belong to the High-Code and Moderate-Code sub-classes, respectively. This discrepancy could come from the fact that only 50% of the buildings built after 1980 strictly followed the building code provisions. As a result, we would underestimate the direct losses by using our assumed 90% / 10% split. Here we see how the lack of complete knowledge of the quality of construction leads to (epistemic) uncertainty in the final loss estimates.

No.	Label	Description	Height			
			Range		Typical	
			Name	Stories	Stories	Feet
1	W1	Wood, Light Frame (≤ 5,000 sq. ft.)		1 - 2	1	14
2	W2	Wood, Commercial and Industrial (> 5,000 sq. ft.)		All	2	24
3	S1L	Steel Moment Frame	Low-Rise	1 - 3	2	24
4	S1M		Mid-Rise	4 - 7	5	60
5	S1H		High-Rise	8+	13	156
6	S2L	Steel Braced Frame	Low-Rise	1 - 3	2	24
7	S2M		Mid-Rise	4 - 7	5	60
8	S2H		High-Rise	8+	13	156
9	S3	Steel Light Frame		All	1	15
10	S4L	Steel Frame with Cast-in-Place Concrete Shear Walls	Low-Rise	1 - 3	2	24
11	S4M		Mid-Rise	4 - 7	5	60
12	S4H		High-Rise	8+	13	156
13	S5L	Steel Frame with Unreinforced Masonry Infill Walls	Low-Rise	1 - 3	2	24
14	S5M		Mid-Rise	4 - 7	5	60
15	S5H		High-Rise	8+	13	156
16	C1L	Concrete Moment Frame	Low-Rise	1 - 3	2	20
17	C1M		Mid-Rise	4 - 7	5	50
18	C1H		High-Rise	8+	12	120
19	C2L	Concrete Shear Walls	Low-Rise	1 - 3	2	20
20	C2M		Mid-Rise	4 - 7	5	50
21	C2H		High-Rise	8+	12	120
22	C3L	Concrete Frame with Unreinforced Masonry Infill Walls	Low-Rise	1 - 3	2	20
23	C3M		Mid-Rise	4 - 7	5	50
24	C3H		High-Rise	8+	12	120
25	PC1	Precast Concrete Tilt-Up Walls		All	1	15
26	PC2L	Precast Concrete Frames with Concrete Shear Walls	Low-Rise	1 - 3	2	20
27	PC2M		Mid-Rise	4 - 7	5	50
28	PC2H		High-Rise	8+	12	120
29	RM1L	Reinforced Masonry Bearing Walls with Wood or Metal Deck Diaphragms	Low-Rise	1-3	2	20
30	RM2M		Mid-Rise	4+	5	50
31	RM2L	Reinforced Masonry Bearing Walls with Precast Concrete Diaphragms	Low-Rise	1 - 3	2	20
32	RM2M		Mid-Rise	4 - 7	5	50
33	RM2H		High-Rise	8+	12	120
34	URML	Unreinforced Masonry Bearing Walls	Low-Rise	1 - 2	1	15
35	URMM		Mid-Rise	3+	3	35
36	MH	Mobile Homes		All	1	10

Table 3-1: Structural Classification in HAZUS (2000) - *Source HAZUS (2000)*

UBC Seismic Zone (NEHRP Map Area)	Post-1975	1941 - 1975	Pre-1941
Zone 4 (Map Area 7)	High-Code	Moderate-Code	Pre-Code (W1 = Moderate-Code)
Zone 3 (Map Area 6)	Moderate-Code	Moderate-Code	Pre-Code (W1 = Moderate-Code)
Zone 2B (Map Area 5)	Moderate-Code	Low-Code	Pre-Code (W1 = Low-Code)
Zone 2A (Map Area 4)	Low-Code	Low-Code	Pre-Code (W1 = Low-Code)
Zone 1 (Map Area 2/3)	Low-Code	Pre-Code (W1 = Low-Code)	Pre-Code (W1 = Low-Code)
Zone 0 (Map Area 1)	Pre-Code (W1 = Low-Code)	Pre-Code (W1 = Low-Code)	Pre-Code (W1 = Low-Code)

Table 3-2: Suggested mapping of the sub-classes to the *UBC* Seismic Zone and Building Age - *Source HAZUS (2000)*

The above knowledge-related (epistemic) uncertainty could be reduced by collecting information on the quality of construction, for example, through surveys of individual buildings in the study area. Surely, such surveys would require time and economic resources, which could be large if one is dealing with an extended study area.

Next, we assess the uncertainty in various component models of earthquake loss estimation.

3.2 Ground motion attenuation and site amplification

3.2.1 Macroseismic attenuation

This section describes and compares the attenuation relations for Modified Mercalli Intensity (MMI) for the CEUS.

Cornell and Merz (1974)

As part of a seismic risk analysis of Boston, Massachusetts, Cornell and Merz (1974) proposed an attenuation relation for the northeastern U.S. They developed the attenuation relation based on the isoseismal maps from several large historical events in the region. The mean MMI at distance R miles from the epicenter is given by

$$I_{site} = I_0 ; R < 10 \text{ miles}$$

$$I_{site} = 3.1 + I_0 - 1.3\ln(R);\ R \geq 10 \text{ miles} \quad \textbf{(3-1)}$$

Cornell and Merz (1974) observe that the value of 1.3 for the coefficient of $\ln(R)$ in Equation (3-1) agrees well with the intensity data available for the 1811 New Madrid earthquake and the 1886 Charleston earthquake. They also mention that for West Coast events the same coefficient is about 2.0, suggesting a faster decay of intensity with distance. Cornell and Merz (1974) obtain a standard deviation of 0.5 MMI for the difference between observed and predicted intensities.

Gupta and Nuttli (1976)

Gupta and Nuttli (1976) used 8 data points that are given in Nuttli (1973), which are from the isoseismals of the November 9, 1968, southern Illinois earthquake and the December 16, 1811, New Madrid, Missouri earthquake to obtain their attenuation relation. The epicentral MMI values of the southern Illinois earthquake and the 1811 New Madrid earthquake are estimated to be 7 and 11 respectively. Gupta and Nuttli (1976) compare their relationship with that of Cornell and Merz (1974) and Howell and Schultz (1975) and find good agreement between the three relations. Based on these comparisons, they comment that the attenuation characteristics of ground motion in the central and eastern U.S., whether northeastern or southeastern, are very similar.

Bollinger (1977)

By analyzing the intensity data of Dutton (1889), Bollinger (1977) assigned an epicentral MMI of 10 to the Charleston, South Carolina earthquake of 1886. Bollinger (1977) performed a regression analysis on 780 intensity-distance observations. He notices that the regression technique used avoids the subjective step of contouring the intensity data.

The standard deviation of the difference between the observed and predicted intensities is 1.2 intensity units; hence is much greater than in the Cornell and Merz (1974) study. Bollinger (1977) says that his attenuation relationship is probably valid for epicentral distances greater than 10-20 km. He compares it with other published relations for the CEUS and finds that Howell and Schultz (1975) relation is at about the 85-percent

fractile of his relation, Cornell and Merz (1974) relation is at the 70-percent fractile and the relation of Gupta and Nuttli (1976) is at the 80-percent fractile.

Anderson (1978)

By analyzing the isoseismal lines of 66 Eastern United States earthquakes, Anderson (1978) estimated the distribution of the distances (R's) for each combination of the site intensity and the epicentral intensity. He found that the probability distributions of $\log_{10}(R)$ were consistent with the Gaussian shape. Anderson (1978) says that the standard deviation of $\log_{10}(R)$ is typically 0.3, implying large uncertainties in the estimates obtained from the data.

Chandra (1979)

Chandra (1979) obtained an attenuation relation from the isoseismal maps of about 20 earthquakes in the CEUS and southern Canada. The relation was derived by using an iterative least squares procedure, where the estimate of the epicentral intensity of each earthquake in the data set was updated at each iteration. Thus, the epicentral intensity of an earthquake was estimated based on all the isoseismal contours that were available for that earthquake and not on the maximum reported intensity. Chandra (1979) says that improved estimates of the epicentral intensities are obtained by using this iterative procedure.

Comparison of the attenuation relations

Figure 3-1 compares the median drop in MMI with distance given by the attenuation relations of Cornell and Merz (1974), Gupta and Nuttli (1976), Bollinger (1977), Anderson (1978) and Chandra (1979). As can be seen, except for the relation by Chandra (1979), the MMI drops given by the other four relations are zero till 10km. At distances greater than 10 km, the estimates by Bollinger (1977) are below those from other relations by about 0.5-1.0 units. This is mainly due to the lower value of the constant term a in the median relation of Bollinger (1977) compared to the value of the same term in Cornell and Merz (1974), Gupta and Nuttli (1976) and Anderson (1978), which are of the form

$$I_{site} - I_0 = a - bR - c\ln(R) \tag{3-2}$$

The above comparisons give an indication of the epistemic uncertainty in the macroseismic attenuation in the CEUS.

Comments

It is well known that the attenuation relations that are primarily based on the isoseismal radii are biased (the bias varies with the epicentral distance) and overestimate the MMI values at specified distances. Such relations should not be used unless suitable adjustments are made to correct for the bias. For example, LLNL (1984) applies a downward correction by 0.5 MMI units to the attenuation of Gupta and Nuttli (1976). Campbell (1986) comments that the intensity estimation in Bollinger (1977), which is based on individual damage reports rather than isoseismal data, is consistent with the way the expressions relating strong-motion parameters and MMI (for example, Trifunac and Brady (1975), Murphy and O'Brien (1977) and Bernreuter (1981)) are developed.

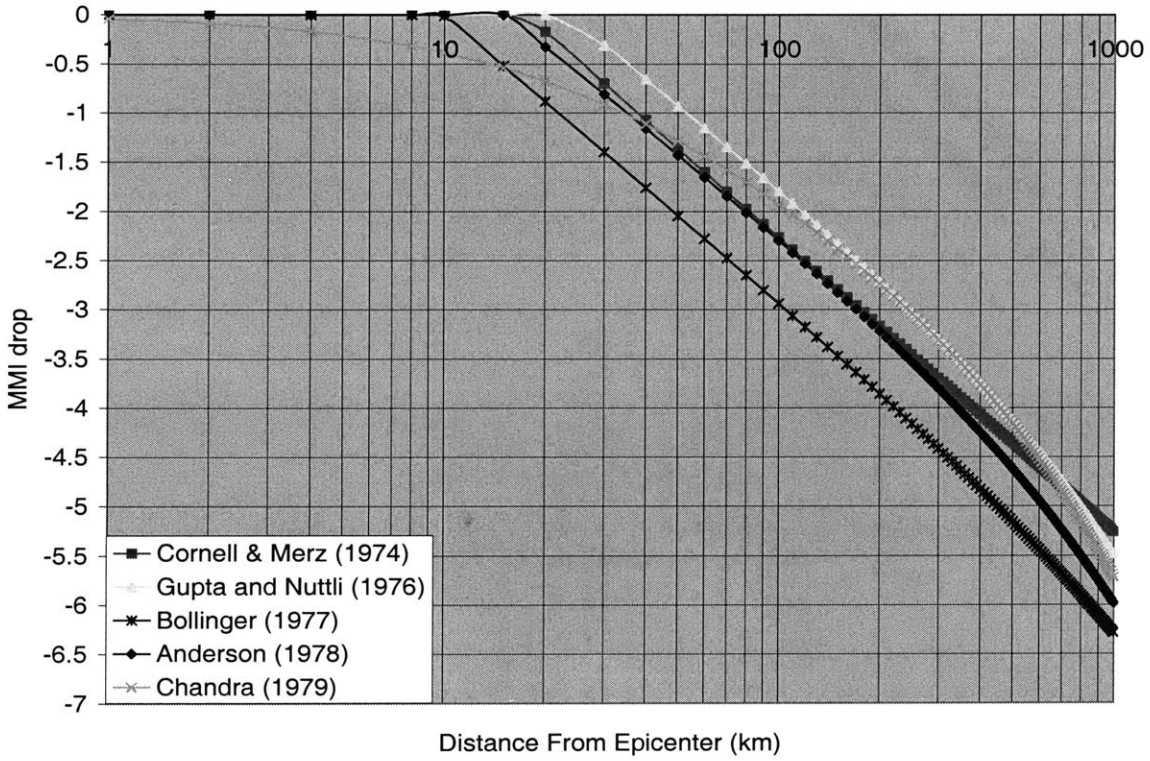

Figure 3-1: Comparison of some macroseismic attenuation relationships for the CEUS

Therefore, it is suggested that an appropriate macroseismic attenuation relation that could be used in earthquake loss estimation studies in CEUS is that given by Bollinger (1977).

3.2.2 Engineering attenuation

This section compares ground motion attenuation relations for engineering parameters such as Peak Ground Acceleration (PGA) and 5% damped Spectral Acceleration (SA), in the CEUS.

Little instrumental data is available regarding the ground motion attenuation of large earthquakes in the CEUS. Therefore, many of the proposed attenuation relationships for the CEUS are based on theoretical models and simulated ground motions. In some cases, the synthetic ground motion data is augmented by the empirical data. Next we describe a set of models that may be considered representative of current knowledge about ground motion attenuation in the CEUS.

Atkinson and Boore (1995)

Atkinson and Boore (1995) give estimates of PGA, PGV and spectral acceleration at 0.5 Hz to 20 Hz, on hard rock (NEHRP site class A). The estimates are developed for an earthquake magnitude range of 4.0 M to 7.25 M and a hypocentral distance range of 10 km to 500 km. Values of the median attenuated quantities are given in tabular form for different distance and epicentral magnitude combinations. In addition, the authors provide simple quadratic fits to their numeric results. These quadratic relations are developed by the regression of a subset of the median simulated ground motion data. The subset consists of all the hypocentral distances ($\leq$ 500 km) for earthquakes with M > 6.5. For small earthquakes, the hypocentral distances considered in the regression are up to 25 km. As a result, for small magnitudes (M < 5.5) the simplified expressions over-predict their simulated ground motion data for distances greater than 30km. Figure 3-2 shows a comparison of the ground motion estimates given by the two representations.

Atkinson and Boore (1995) use the recordings from the Eastern Canada Telemetric Network (ECTN) for small to moderate earthquakes and isoseismals from some of the past earthquakes to constrain their stochastic double-corner point source model. They find that their relations are in good agreement with empirical data for earthquakes between 4M and 5M. They also find that their estimates are consistent with the ground motion data from the Saguenay (5.8 M) and Nahanni (6.8 M) earthquakes.

Atkinson and Boore (1997) compare the ground motion estimates given in Atkinson and Boore (1995) with other attenuations relations proposed for the CEUS. They find that the low frequency (< 3 Hz) predictions from the attenuation relation in EPRI (1993) are much larger than the predictions from Atkinson and Boore (1995). However, at larger frequencies (> 10 Hz), Atkinson and Boore (1995) predicts significantly larger amplitudes of ground motion compared to EPRI (1993) predictions. The main reason for

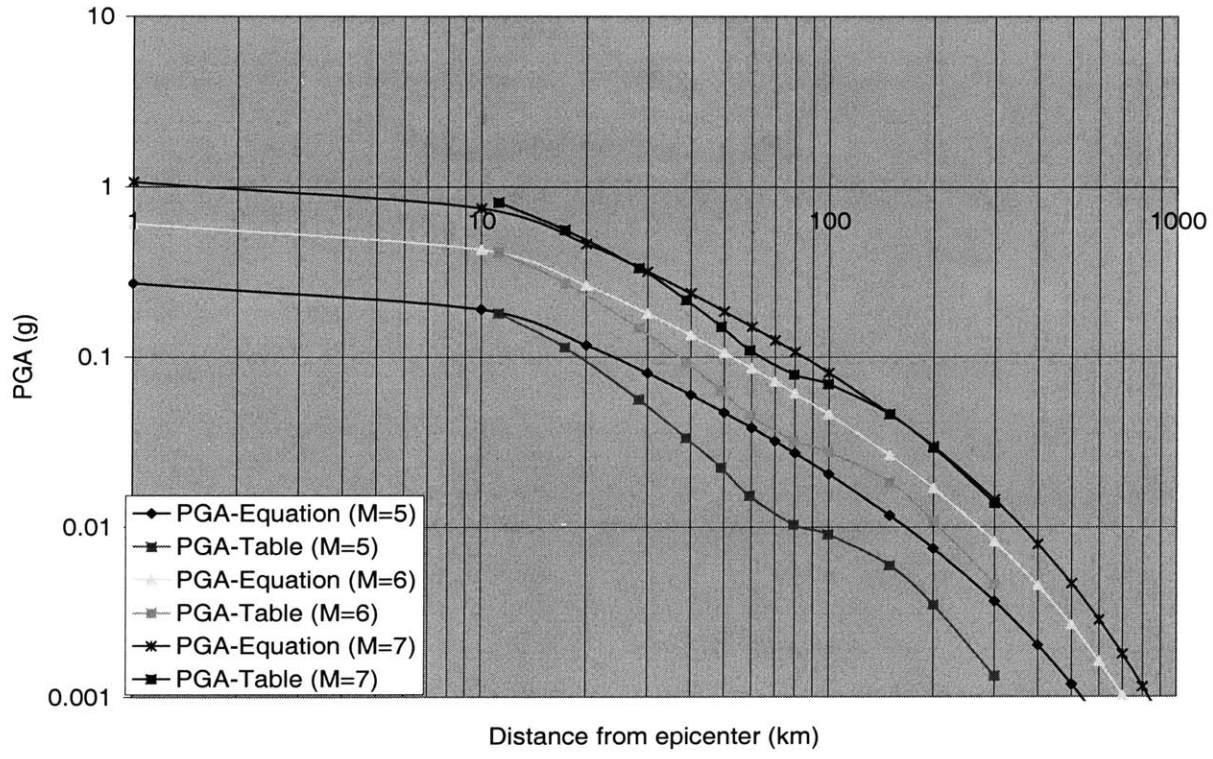

Figure 3-2: Comparison of the ground motion estimates given by the two alternative representations of Atkinson and Boore (1995) (NEHRP site class A)

these differences is cited as the difference in the source model (the EPRI relation uses the single corner Brune source model) and the duration of motion used by the two studies. Atkinson and Boore (1997) also compare Atkinson and Boore (1995) with Frankel et al. (1996) and find that Frankel et al. (1996) predicts greater amplitudes at almost all frequencies. From the comparisons made between Atkinson and Boore (1995) and the ground motion attenuation relations given for California by Boore et al. (1993), they conclude that ground motion relationships for the CEUS cannot be simply scaled for use in the Western United States (WUS).

Atkinson and Boore (1995) estimate the aleatory uncertainty, which captures the random variability of the ground motions, to increase from a value of 0.55 (in *ln* units) at 1 Hz to 0.62 at 10Hz for Eastern North America.

Frankel et al. (1996)

Frankel et al. (1996) provide tables of ground motion values as a function of earthquake magnitude and distance for firm-rock conditions (NEHRP B-C boundary). The tables provide the ground motion estimates for event magnitudes ranging from 5.0 M to 8.0 M and hypocentral distances ranging from 10 km to 1000 km. They use the single corner Brune source model to obtain their estimates. Frankel et al. (1996) use values of 0.75, 0.75, 0.75 and 0.8 for the natural logarithms of the standard deviation of the PGA, 0.2-, 0.3-, and 1.0-sec spectral responses respectively. These values are similar to the aleatory standard deviations reported in SSHAC (1996).

Toro et al. (1997)

Toro et al. (1997) propose attenuation relationships for the CEUS, using a stochastic point source model (Brune model). They develop response spectra for a frequency range of 1 Hz to 35 Hz and PGA. The relationships are for earthquakes of magnitudes 5M to 8 M and epicentral distances from 1 km to 500 km. They propose separate attenuation relations for two crustal regions found to be typical of the eastern North America-mid continent and the gulf crustal regions. The estimates of the ground motion can be directly applied to hard rock conditions (NEHRP site class A). Toro et al. (1997) also provide a

comprehensive study of the uncertainties in model parameters for eastern North America and propagate these uncertainties to their final ground motion estimates. They compare the estimates from their model with the existing CEUS ground motion data and conclude that model predictions are generally consistent with available data. The only discrepancy is with the data from the 1988 Saguenay (5.8 M) earthquake. The observed 10 Hz amplitudes are on an average 2 standard deviations above the median.

In the development of the National Seismic Hazard maps, when using the Toro et al. (1996) attenuation relation, Frankel et al. (1996) use values of 0.75, 0.75, 0.75 and 0.8 for the natural logarithm of the standard deviation of PGA, 0.2-, 0.3-, and 1.0-sec spectral responses, respectively.

Comparison of attenuation relations

Figure 3-3 to Figure 3-5 compare the median PGA values given by Atkinson and Boore (1995), Toro (1997) and Frankel et al. (1996) for hard rock conditions (NEHRP site class A). For M = 8.0, the median values in Toro et al. (1997) are close to those of Atkinson and Boore (1995). Estimates from Frankel et al. (1996) for M = 8.0 are much higher than those given by the other two relations. For M = 7.0 and M = 6.0, the PGA median values given in Frankel et al. (1996) and Atkinson and Boore (1995) are close to one another. The values given by Toro et al. (1997) are slightly lower than the values given by the other two data sources. Figure 3-6 to Figure 3-8 compare the 5% damped spectral acceleration at 1-sec period for M = 8.0, 7.0 and 6.0 respectively. The ground motion estimates by Atkinson and Boore (1995) are lower than those from the other two models for all the three magnitudes considered. The relatively low Sa (1sec) estimates by Atkinson and Boore (1995) are attributed mainly to the fact that they use a source model with two corner frequencies compared to the single corner frequency models used by Frankel et al. (1996) and Toro et al. (1997).

A focal depth of 10 km is assumed for the above comparisons. The quadratic form of the attenuation given in Atkinson and Boore (1995) is used for M = 7.0 and M = 8.0 in the above comparisons. For M = 6.0, the median estimates given in the tabular form are used.

The attenuation relation of Toro (1997) that is used for the comparisons is a modified version of the original relation obtained from HAZUS (2000). The modified version has an adjusted hypocentral distance term to model the saturation effect of extended ruptures on near fault ground motions. The values given in Table 4.A of HAZUS (2000) for Frankel et al. (1996) are used. HAZUS (2000) caps the PGA values to 1.5g and the SA 0.3-sec values to 3.75g.

Comments

The above comparisons of alternative median attenuation relations for CEUS suggest a large epistemic uncertainty in the ground motion attenuation in the CEUS. Earlier earthquake risk assessment studies took into account this epistemic uncertainty by assigning weights to alternative median attenuation relationships. In the development of the national seismic hazard maps in 1996, equal weights were assigned to the median relations of Toro et al. (1997) and Frankel et al. (1996). In the seismic hazard analysis for the New Madrid Seismic Zone done by Cramer (2001), equal weights were given to the median attenuation relationships of Toro et al. (1996), Frankel et al. (1996) and Atkinson and Boore (1995). Based on these, we suggest equal weights to each of the above three attenuation relations for use in loss estimation studies in CEUS.

3.2.3 Soil amplification

Here, we describe three ground motion amplification studies and compare the associated amplification factors.

Hwang et al. (1997a)

Hwang et al. (1997a) employ a probabilistic approach to obtain the statistics of amplification factors for the 5 site categories (A, B, C, D and E) provided in the 1994 NEHRP Provisions, by using the expected ground motions in the eastern United States. By including uncertainty in seismic source, path attenuation and local site conditions, they perform 250 runs for each site category. Using the simulated data, they perform regression analyses to obtain the site coefficients for different site categories. Hwang et al. (1997a) compare their estimates with those in the 1994 NEHRP provisions. For site

classes A and B, the amplification factors of Hwang et al. (1997a) are same as those proposed by the NEHRP provisions. For site class C, the amplification factors are independent of the ground shaking, implying a linear soil behavior. The amplification factors for site class C are close to those in the NEHRP provisions. However, for site classes D and E, the amplification factors are somewhat larger than those given in the NEHRP provisions. Also, according to Hwang et al. (1997a), for site classes D and E, the long period site coefficients, F_v, increase with ground shaking intensity. This is in contrast to the NEHRP provisions, where the amplification factors decrease with increase in the ground shaking intensity. Hwang et al. (1997a) comment that this difference could be attributed to the fact that the site coefficients in their study have been derived for the ground motions that are expected to occur in the eastern United States, whereas the site coefficients in the NEHRP provisions are primarily based on ground motion data from the Western United States.

Borcherdt et al. (2002)

Borcherdt et al. (2002) use the 17 January 1994, Northridge earthquake data and recent geotechnical data to develop empirical estimates of the amplification factors for site classes C and D. They find that their estimates at ground shaking levels of 0.3g or greater are consistent at the 95 percent confidence level with those provided in the codes. However, they find for ground motions of 0.1g and 0.2g that the code values are below their lower confidence bounds by up to 13%. Their amplification factors decrease with increasing intensity of ground shaking, which is consistent with the codes. Borcherdt et al. (2002) observe that the short period amplification factors given in their study are consistent with those in Grouse and McGuire (1996), Rodriguez-Marek et al. (1999), and Silva et al. (2000) and greater than those in the codes for site classes C and D. Hence they suggest that the corresponding factors in the codes may have to be increased. They also comment that mid- and long-period amplification factors given in the codes for site class C might have to be increased as the corresponding estimates given in Borcherdt et al. (2002), Crouse and McGuire(1996) and Silva et al. (2000) are higher. In addition, they say that an increase in the mid- and long- period amplification factors for site class D

might be appropriate based on their estimates and those of Silva et al. (2000) and the results in Joyner and Boore (2000) for Sa at 1sec.

Dobry et al. (2000)

The site coefficients given in Dobry et al. (2000) are the same as those given in the recent code provisions for buildings and other structures (1997 NEHRP Provisions, 1997 Uniform Building Code). These are also the site coefficients used by HAZUS (2000). These coefficients are derived based on empirical studies for motions up to 0.1g and on theoretical and laboratory tests for more intense motions. The empirical studies included the recordings from Loma Prieta earthquake and other earthquakes.

Comparison of the amplification factors

Table 3-3 and Table 3-4, and Figure 3-9 to Figure 3-12 list the short period and long-period amplification factors (denoted by F_a and F_v respectively) given in the above three studies for site classes C and D. It can be seen that the median estimates of Dobry et al. (2000) are consistently lower than those of the other two studies, except in the case of F_v site class C, for which they are slightly higher than the predictions by Hwang et al. (1997a) at lower ground motions. The median estimates from Hwang et al. (1997a) are lower than or equal to those by Borcherdt et al. (2002) except for the case of F_v for site class D.

Comments

To take into account the epistemic uncertainty in the amplification factors, it is suggested that weights of 0.4, 0.4 and 0.20 be given to the estimates in Hwang et al. (1997a), Borcherdt et al. (2002) and Dobry et al. (2000) respectively. Less weight is given to the estimates from Dobry et al. (2000) because they may be on a lower side, as was commented by Borcherdt et al. (2002).

3.3 Building Fragility

A fragility model is used to estimate the state of damage of the building infrastructure immediately following an earthquake. The first part of this section describes a model in

terms of engineering ground motion intensity parameters such as Peak Ground Acceleration (PGA) and 5% damped Spectral Acceleration (SA). The second part describes a model in terms of Modified Mercalli Intensity (MMI).

3.3.1 Fragility models (engineering approach)

The building fragility model consists of three components:

- Structural fragility model: This model is used to estimate structural damage.
- Non-structural acceleration-sensitive fragility model: This model is used to estimate the damage to acceleration-sensitive nonstructural components (e.g., mechanical and electrical equipment).
- Non-structural drift-sensitive fragility model: This model is used to estimate the damage to nonstructural components that are sensitive to inter-story drift (e.g., partition walls).

The structural fragility model is described next.

Structural Fragility Model

The Damage Factor (*DF*), which is the ratio of the dollar loss to the replacement value, is often used as an indicator of the level of damage to structural components of a building. It varies between 0 (no damage) and 1 (complete damage). Fragility curves are used to estimate *DF* as a function of some ground motion parameter (e.g.: spectral acceleration), for different seismic vulnerability classes.

Next we describe the fragility model of HAZUS (2000), followed by a description of a model proposed here and fitted to data in HAZUS (2000).

HAZUS (2000)

The structural damage estimation in HAZUS (2000) involves the following steps: (1) estimation of the peak building response to a specified level of ground shaking, (2) given the peak building response, estimation of the probability of being in or exceeding each of the four damage states (slight, moderate, extensive and complete) by using the structural fragility curves. Next we elaborate the above two steps.

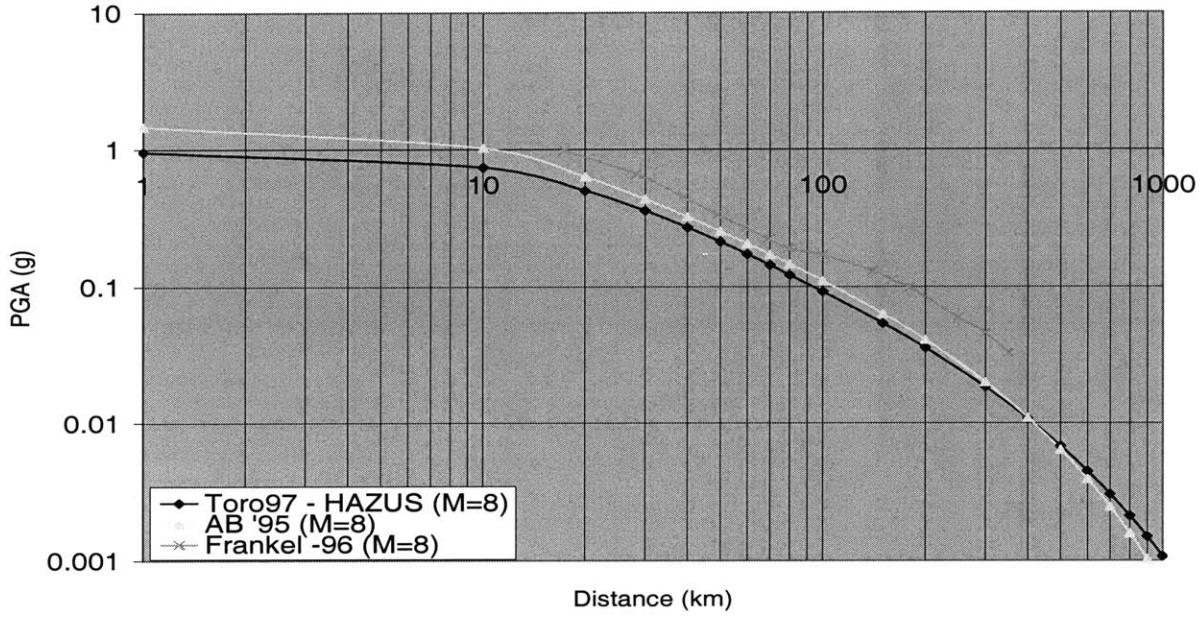

Figure 3-3: Attenuation of PGA at M=8.0 for CEUS hard rock (NEHRP site class A)

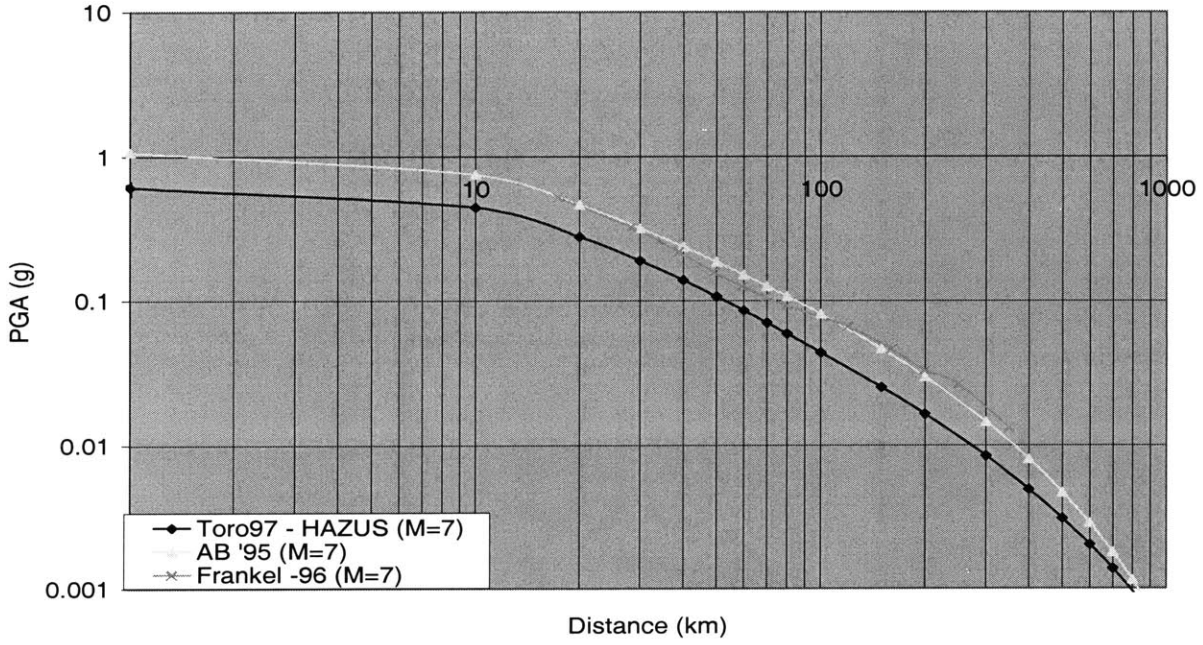

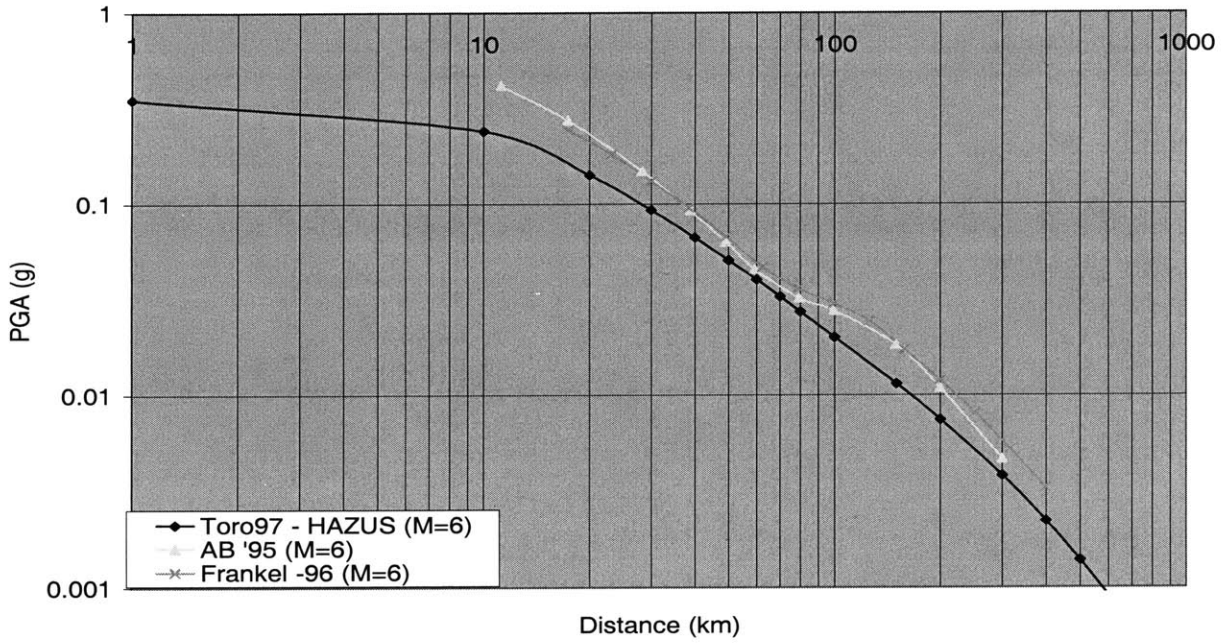

Figure 3-5: Attenuation of PGA at M=6.0 for CEUS hard rock (NEHRP site class A)

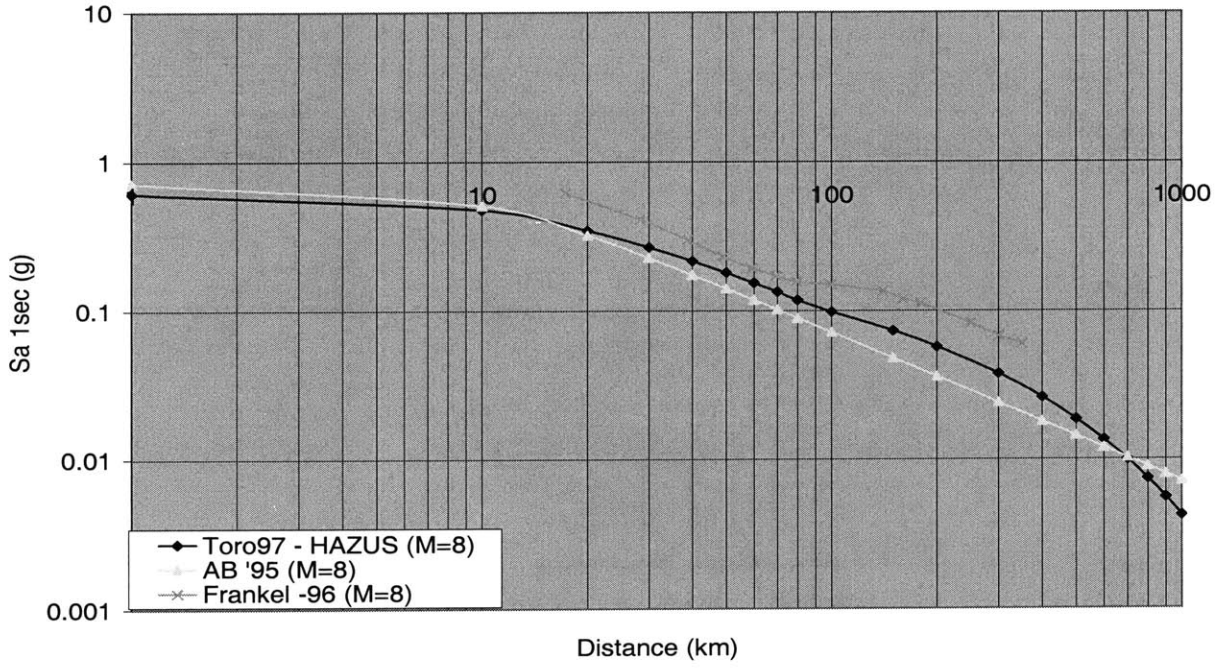

Figure 3-6: Attenuation of Sa (1sec) at M=8.0 for CEUS hard rock (NEHRP site class A)

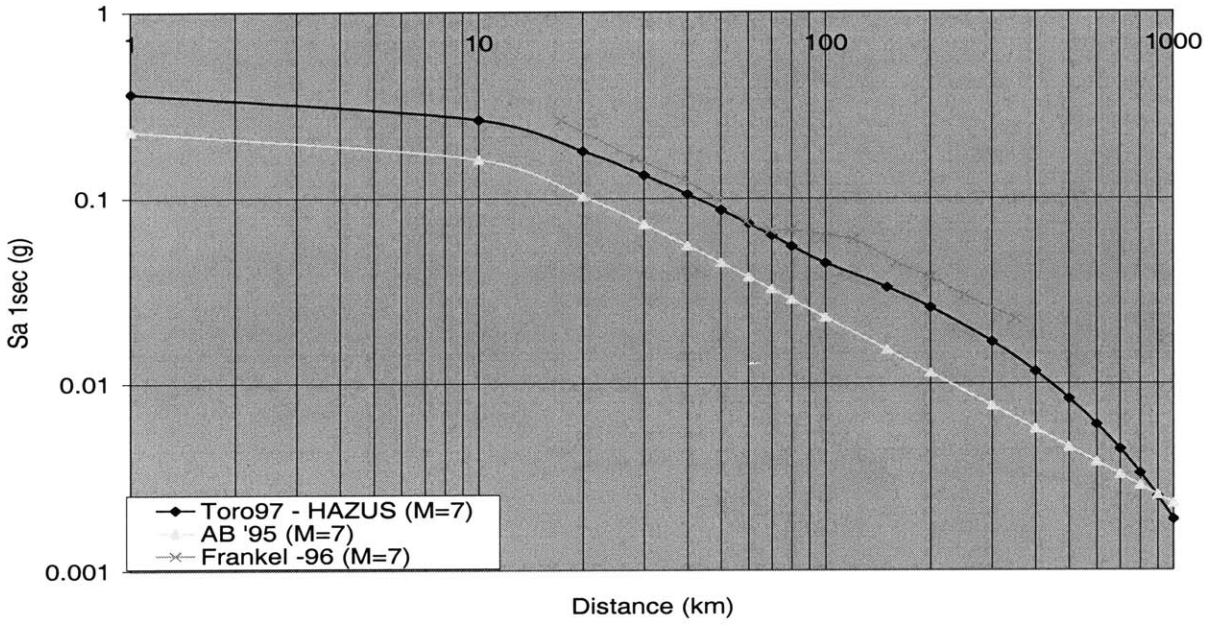

Figure 3-7: Attenuation of Sa (1sec) at M=7.0 for CEUS hard rock (NEHRP site class A)

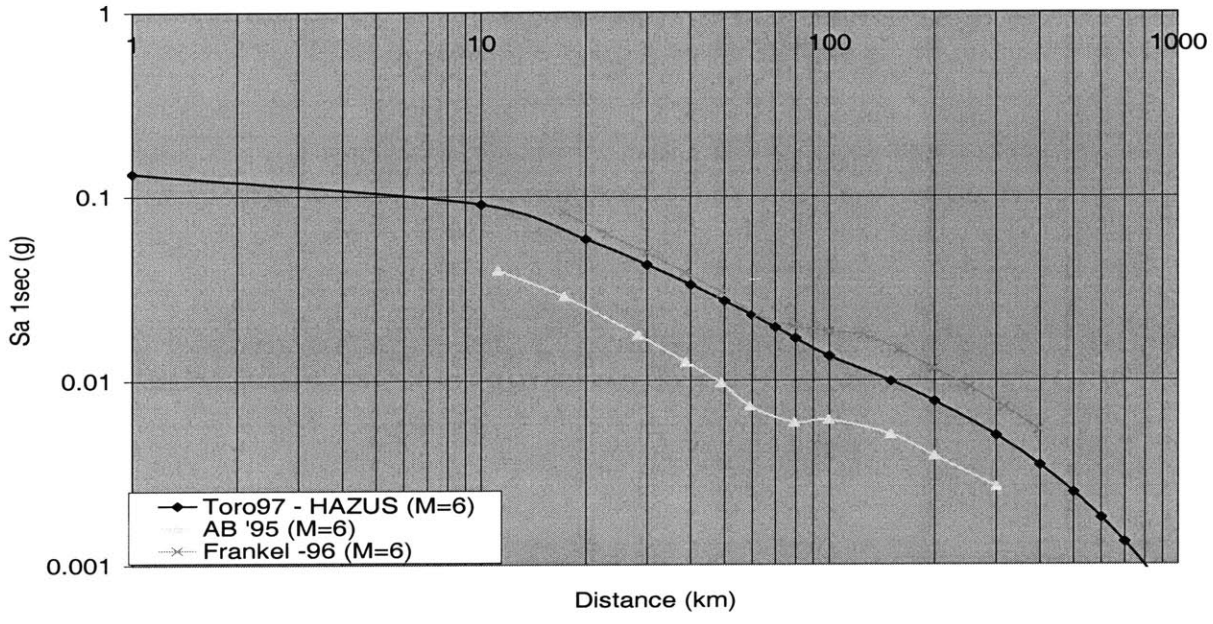

Figure 3-8: Attenuation of Sa (1sec) at M=6.0 for CEUS hard rock (NEHRP site class A)

Site Class		S_{AS}<0.25	S_{AS} =0.50	S_{AS} =0.75	S_{AS} =1.00	S_{AS} >1.25
C	Dobry (2000)	1.2	1.2	1.1	1.0	1.0
	Hwang (1997)-Median	1.4	1.4	1.4	1.4	1.4
	Hwang (1997)-95% confidence Interval	(1.0,1.8)	(1.0,1.9)	(1.0,1.9)	(1.0,1.9)	(1.0,1.9)
	Borcherdt (2002)-Median	1.6	1.5	1.5	1.4	1.3
	Borcherdt (2002)- 95% confidence Interval	(1.4,1.9)	(1.3,1.8)	(1.1,1.8)	(0.9,1.9)	(0.6,2.0)
D	Dobry (2000)	1.6	1.4	1.2	1.1	1.0
	Hwang (1997)	2.0	1.7	1.5	1.3	1.1
	Hwang (1997)-95% confidence Interval	(1.0,3.5)	(0.8,3.1)	(0.7,2.7)	(0.6,2.3)	(0.6,2.0)
	Borcherdt (2002)	2.06	1.88	1.71	1.54	1.36
	Borcherdt (2002)- 95% confidence Interval	(1.7,2.4)	(1.5,2.2)	(1.1,2.3)	(0.7,2.4)	(0.2,2.5)

Table 3-3: Comparison of short period amplification factor, F_a (using site class B as reference)

Site Class		S_{A1}<0.1	S_{A1} =0.2	S_{A1} =0.3	S_{A1} =0.4	S_{A1} >0.5
C	Dobry (2000)	1.7	1.6	1.5	1.4	1.3
	Hwang (1997)-Median	1.4	1.4	1.4	1.4	1.4
	Hwang (1997)-95% confidence Interval	(1.1,1.7)	(1.1,1.7)	(1.1,1.7)	(1.1,1.8)	(1.1,1.8)
	Borcherdt (2002)-Median	2.0	1.9	1.8	1.7	1.6
	Borcherdt (2002)- 95% confidence Interval	(1.6,2.3)	(1.6,2.1)	(1.4,2.1)	(1.1,2.2)	(0.8,2.3)
D	Dobry (2000)	2.4	2.0	1.8	1.6	1.5
	Hwang (1997)	2.6	2.6	2.7	2.8	2.8
	Hwang (1997)-95% confidence Interval	(1.4,3.4)	(1.4,3.5)	(1.4,3.6)	(1.5,3.6)	(1.5,3.7)
	Borcherdt (2002)	2.6	2.4	2.2	2.0	1.8
	Borcherdt (2002)- 95% confidence Interval	(2.3,3.0)	(2.0,2.8)	(1.6,2.9)	(1.1,3.0)	(0.6,3.1)

Table 3-4: Comparison of the long period amplification factor, F_v (using site class B as reference)

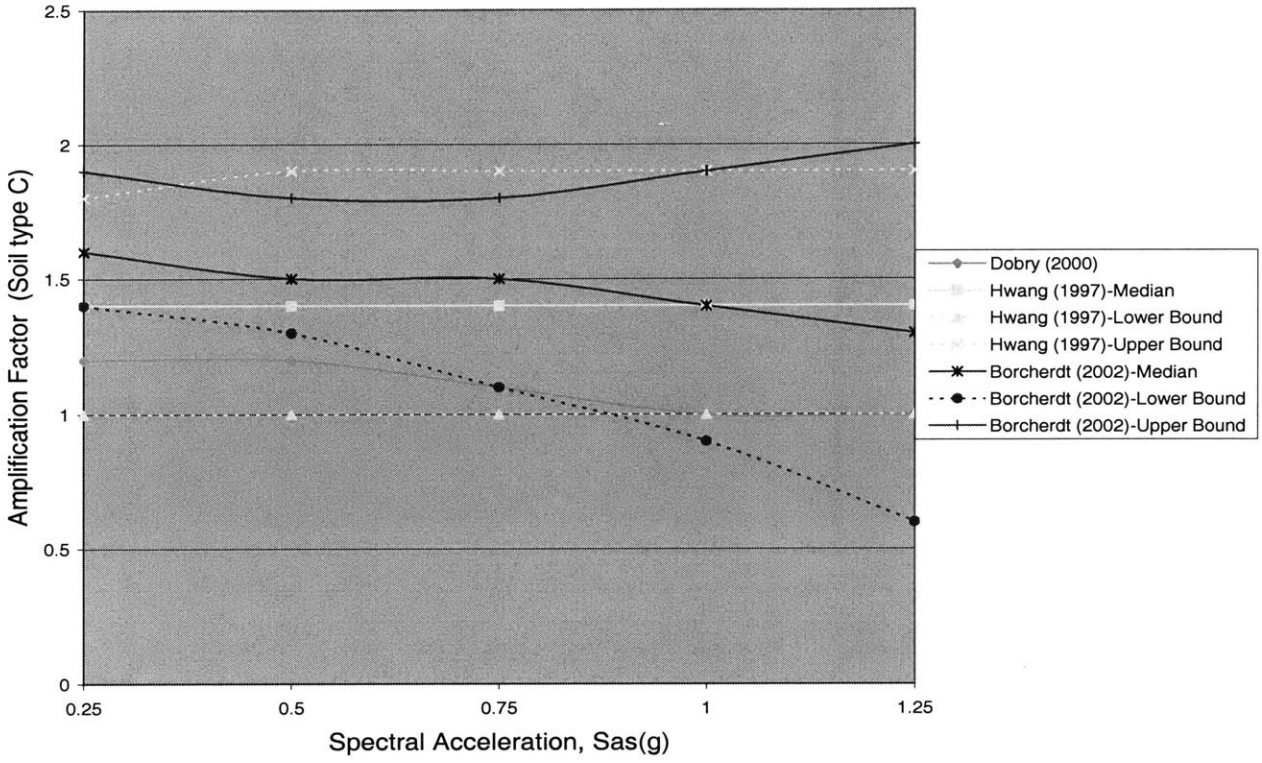

Figure 3-9: Comparison of short period amplification factors, F_a, for soil class C

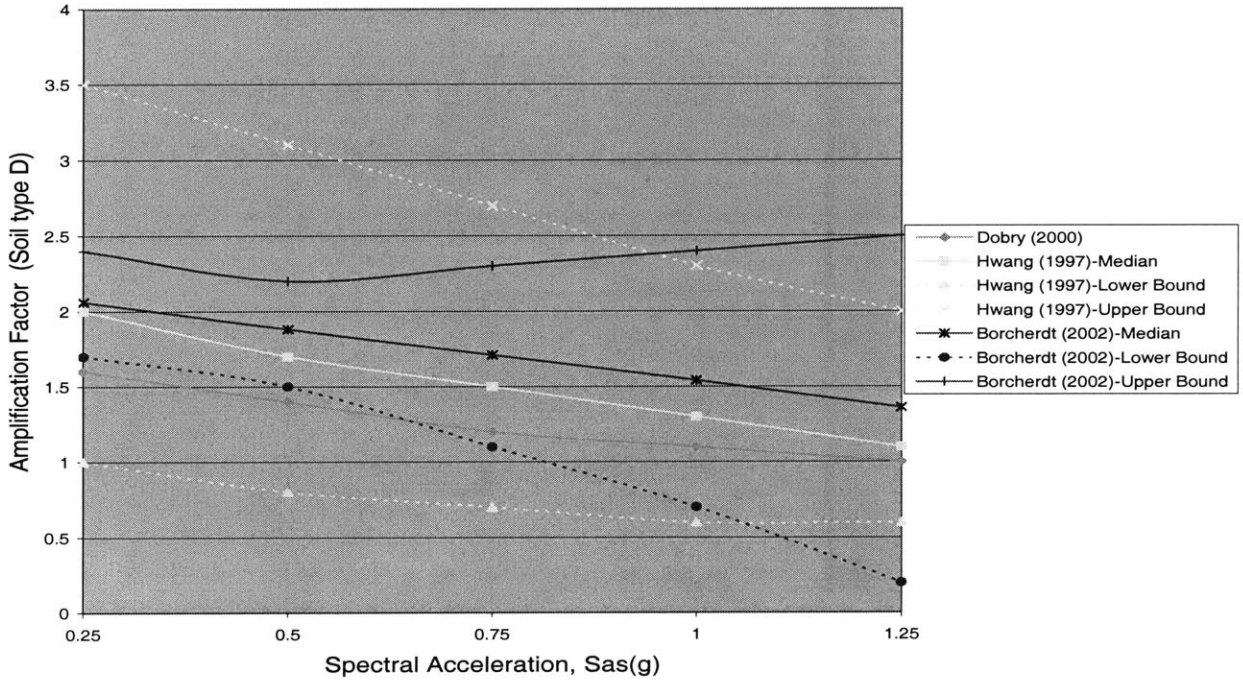

Figure 3-10: Comparison of short period amplification factors, F_a, for soil class D

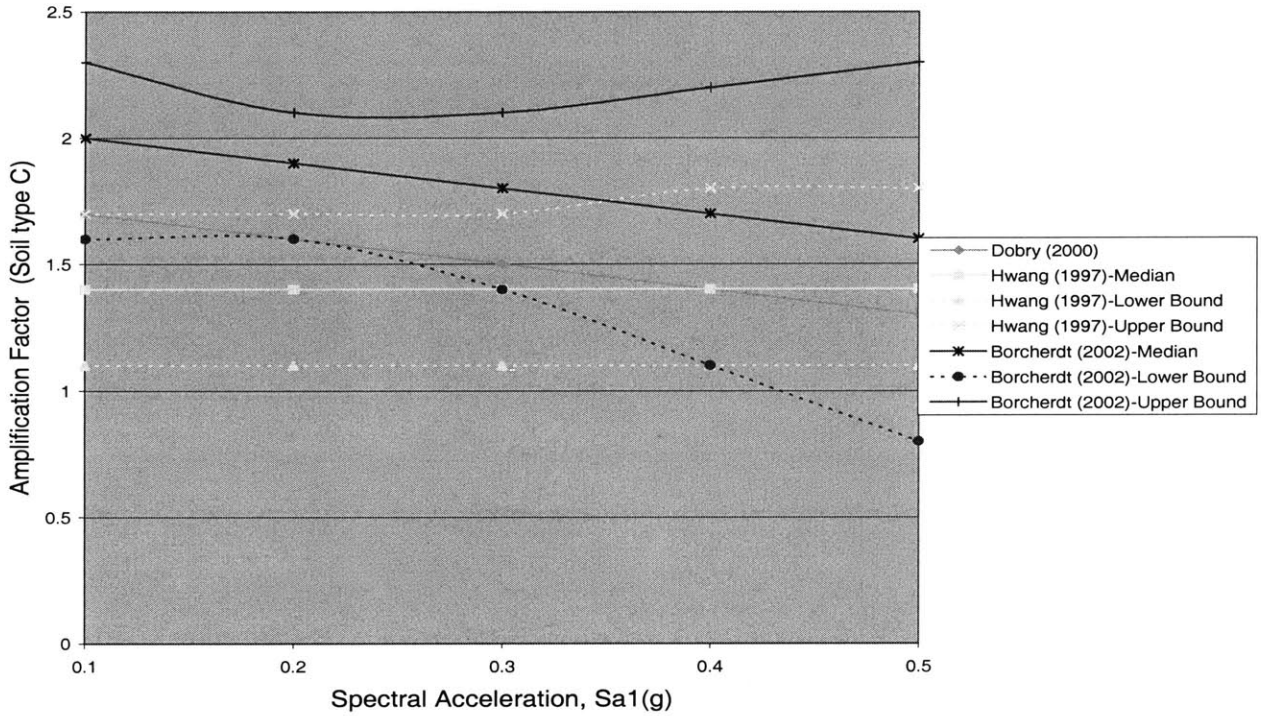

Figure 3-11: Comparison of long period amplification factors, F_v, for soil class C

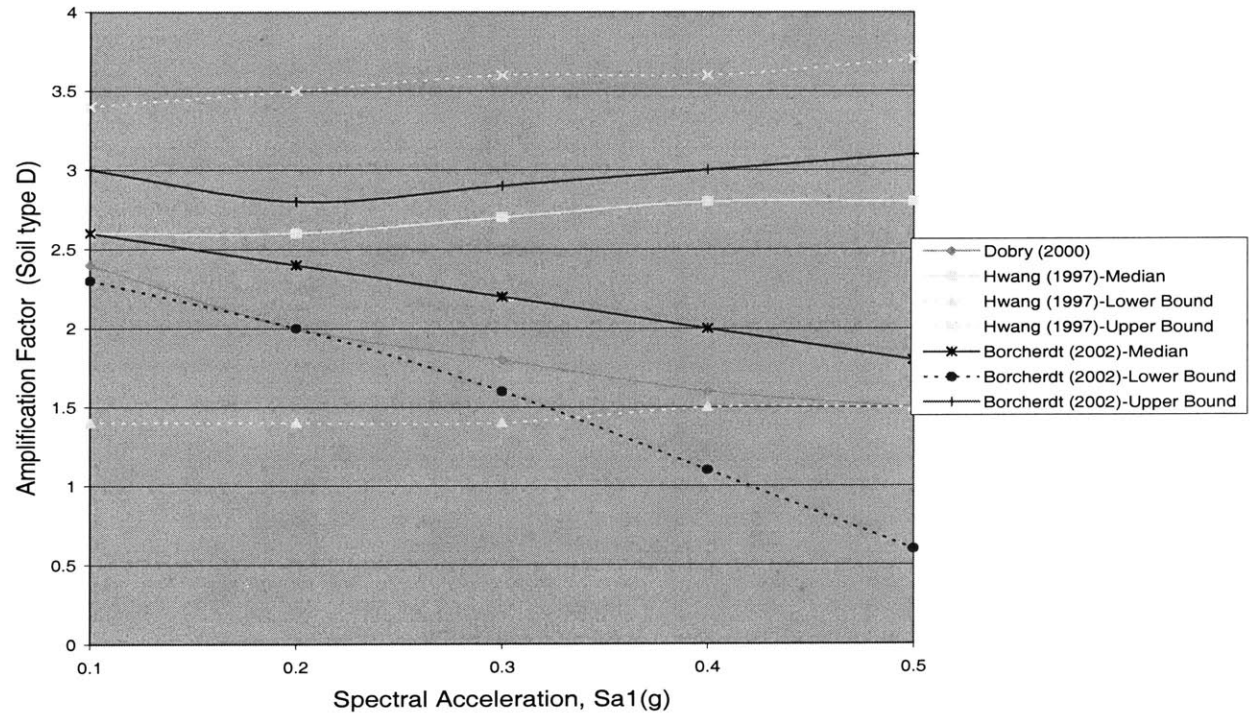

Figure 3-12: Comparison of long period amplification factors, F_v, for soil class D

Calculation of peak building response

HAZUS (2000) estimates the peak building response from the intersection of the demand spectrum and the building capacity curve. Demand spectrum is the 5%-damped response spectrum at the building's site, reduced for higher levels of effective damping. Building capacity curve describes the building's lateral load resistance as a function of the characteristic lateral displacement. It is derived from the plot of the building's roof displacement with the static-equivalent base shear. In order to permit the direct comparison with the demand spectrum, the base-shear axis is transformed to spectral acceleration and the roof displacement axis is transformed to spectral displacement. Figure 3-13 shows the typical building capacity curve and the demand spectrum in HAZUS (2000) along with the associated peak building response. As can be seen, the capacity curve intersects the demand spectrum at a peak response displacement of D inches, and acceleration of A (in g's). Next, we give a description of the structural damage functions in HAZUS (2000).

Fragility relations and damage calculation

Structural fragilities in HAZUS (2000) are lognormal curves, for each vulnerability class, that relate the probability of being in or exceeding a given structural damage state for different values of spectral displacement. For a description of the seismic vulnerability classes in HAZUS (2000), see Section 3.1. Four damage states are considered: slight, moderate, extensive and complete. Each fragility curve is defined by a median value of the spectral displacement that produces the given damage state and the dispersion about that median value. The spectral displacement Sd, that produces a particular damage state ds, is given by

$$Sd = \overline{Sd}_{ds} \cdot \varepsilon_{ds} \qquad \textbf{(3-3)}$$

where

$\overline{Sd}_{ds}$ is the median value of spectral displacement for damage state ds.

ε_{ds} is a lognormal random variable with unit median and logarithmic standard deviation of β_{ds}.

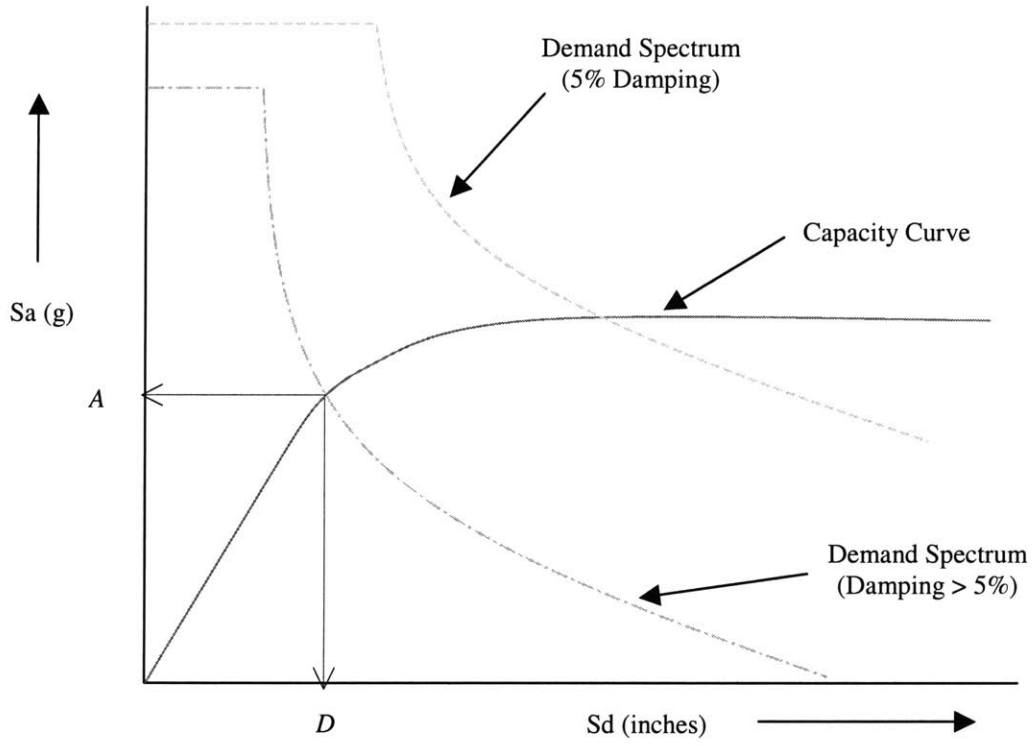

Figure 3-13: Example building capacity curve and demand spectrum in HAZUS (2000)

From equation (3-3) , given the spectral displacement *Sd*, one obtains the conditional probability that the damage factor is greater than or equal to the damage factor D_{ds} corresponding to a damage state *ds*, as

$$\mathrm{P}\left(DF > D_{ds} \middle| Sd\right) = \Phi\left(\frac{\ln(Sd) - \ln(\overline{Sd}_{ds})}{\beta_{ds}}\right) \tag{3-4}$$

The total variability for each damage state, β_{ds}, is contributed by three sources: (1) variability associated with the building capacity curve, (2) variability associated with the seismic demand, and (3) variability associated with the response threshold for each damage state. Each of these three contributors to the damage uncertainty is assumed to be a log-normally distributed random variable and β_{ds} is obtained as

$$\beta_{ds} = \sqrt{(CONV[\beta_C, \beta_D])^2 + (\beta_{M(ds)})^2} \tag{3-5}$$

where

β_C is the logarithmic standard deviation parameter that describes the variability of the building capacity curve.

β_D is the logarithmic standard deviation parameter that describes the variability of the demand spectrum. We assume that this parameter incorporates uncertainty associated with the ground motion estimates from attenuation relations and the building damping parameters.

$\beta_{M(ds)}$ is the logarithmic standard deviation parameter that describes the uncertainty in the estimate of the median value of the threshold of the damage state *ds*. For example, the spectral displacement at which the slight damage state (corresponding to a damage factor of 0.02) in structural class W1 is exceeded is given to be 0.5 inches in HAZUS (2000). However, a 2% structural loss could be incurred at spectral displacements lesser or greater than 0.5 inches.

The function "*CONV*" in equation (3-5) denotes a convolution of the probability distributions of the building capacity and the demand. This convolution process involves the following steps:

(1) A suite of capacity curves, which represent the capacity curve variability, are drawn in the spectral acceleration-spectral displacement domain.

(2) A suite of demand curves, representing the variability in the demand spectrum, are overlaid on the curves representing the capacity curve variability. Let D_i be the spectral displacement corresponding to the intersection of the median demand spectrum and median capacity curve.

(3) The probabilities of the points of intersection of the suite of demand and capacity curves are ascertained. Using these probabilities, the conditional probability of being in or exceeding a given damage state (given $\beta_{M(ds)} = 0$) is obtained for the median peak spectral displacement D_i.

(4) Steps 2 and 3 are repeated for different levels of ground shaking (i.e., different values of D_i), to obtain a set of values describing the probability of being in or exceeding a particular damage state (given $\beta_{M(ds)} = 0$).

(5) A lognormal function is fit to these data points, to obtain an estimate of the lognormal standard deviation of the combined effect of capacity and demand variability on structural fragility.

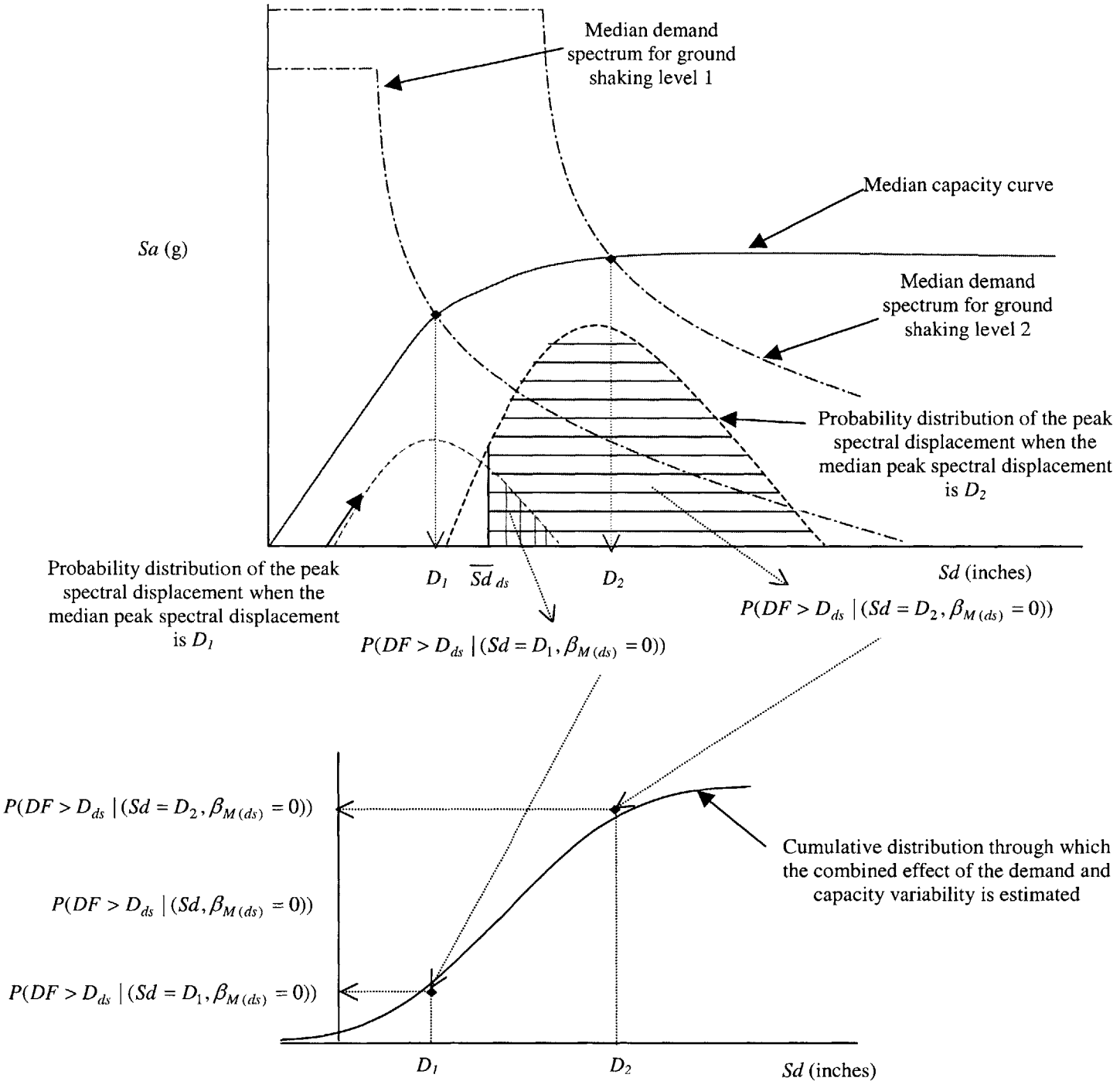

Figure 3-14: Illustration of the convolution process

Figure 3-14 illustrates this convolution process. The lognormal standard deviation parameter, $CONV[\beta_C, \beta_D]$, representing the combined effects of demand and capacity variability is added to $\beta_{M(ds)}$, which is assumed to be independent of capacity and demand, by using the square-root-of-sum-of-squares (SRSS) rule to obtain the total variability of the damage state ds, β_{ds} . For further details of the theory behind equation (3-5), see Kircher et al. (1997).

HAZUS (2000) estimates the mean damage factor $\overline{D(Sd)}_{HAZUS}$, at a given spectral displacement Sd, as the weighted average of the damage factors corresponding to the slight, moderate, extensive and complete damage states. The weights used in the mean damage factor calculation are the probabilities of being *in* the corresponding damage states, which are obtained by differencing the exceedance probabilities of successive damage states ,i.e.,

$$\overline{D(Sd)}_{HAZUS} = \begin{matrix} P(Slight \mid Sd) * 0.02 + P(Moderate \mid Sd) * 0.1 + \\ P(Extensive \mid Sd) * 0.5 + P(Complete \mid Sd) \end{matrix} \quad \textbf{(3-6)}$$

where

$$P(Slight \mid Sd) = P(df > D_{slight} \mid Sd) - P(df > D_{moderate} \mid Sd) \quad \textbf{(3-7)}$$

$$P(Moderate \mid Sd) = P(df > D_{moderate} \mid Sd) - P(df > D_{extensive} \mid Sd) \quad \textbf{(3-8)}$$

$$P(Extensive \mid Sd) = P(df > D_{extensive} \mid Sd) - P(df > D_{complete} \mid Sd) \quad \textbf{(3-9)}$$

$$P(Complete \mid Sd) = P(df > D_{complete} \mid Sd) \quad \textbf{(3-10)}$$

Next we describe a structural fragility model that we derived, the parameters of which are based on data in HAZUS (2000)

Our Model

Our fragility model is based on a simplifying assumption that the fragility curve of a generic building in a seismic vulnerability class has a deterministic functional form and that one of its parameters is uncertain. We assume that the fragility curve of a generic building in the seismic vulnerability class i, is a cumulative distribution function of a Gaussian random variable $R \mid M$,whose mean M , is uncertain. Through the uncertainty in the mean of the fragility curve, we model the variability in damage from building to

building in the vulnerability class. The mean of the fragility curve M, is assumed to be a Gaussian random variable with deterministic parameters. Figure 3-15 and Figure 3-16 illustrate the fragility model of HAZUS (2000) and our fragility model respectively. The seismic vulnerability classes in our model are the same as in HAZUS (2000).

Damage calculation

For a given spectral displacement *Sd*, we obtain the average damage $\overline{D^i(Sd)}$ as

$$\overline{D^i(Sd)} = \int_{m=-\infty}^{\infty} D^i(Sd,m) f_{M^i}(m) dm \tag{3-11}$$

where

$D^i(Sd,m)$ is the damage factor of class i for a given mean of the fragility curve m and spectral displacement Sd. It is calculated as

$$D^i(Sd,m) = \int_{r=-\infty}^{\ln(Sd)} f_{R^i|M^i}(r,m) dr = \Phi\left(\frac{\ln(Sd) - m}{\sigma_{\varepsilon^i}}\right) \tag{3-12}$$

$f_{M^i}(m)$ is the probability distribution function of the mean of the fragility curve of class i.

M^i is a Gaussian random variable with mean $E(M^i)$ and standard deviation σ_{M^i}.

$(R^i \mid M^i = m)$ is a Gaussian random variable with mean m and standard deviation σ_{ε^i}.

Equation (3-11) is written as

$$\overline{D^i(Sd)} = \int_{m=-\infty}^{\infty} \int_{r=-\infty}^{\ln(Sd)} f_{R^i|M^i}(r,m) f_{M^i}(m) dr dm \tag{3-13}$$

$$\Rightarrow \overline{D^i(Sd)} = \int_{r=-\infty}^{\ln(Sd)} f_{R^i}(r) dr \tag{3-14}$$

$$\Rightarrow \overline{D^i(Sd)} = \Phi\left(\frac{\ln(Sd) - E(R^i)}{\sigma_{R^i}}\right) \tag{3-15}$$

where

R^i is a Gaussian random variable with mean $E(R^i)$ and standard deviation σ_{R^i}.

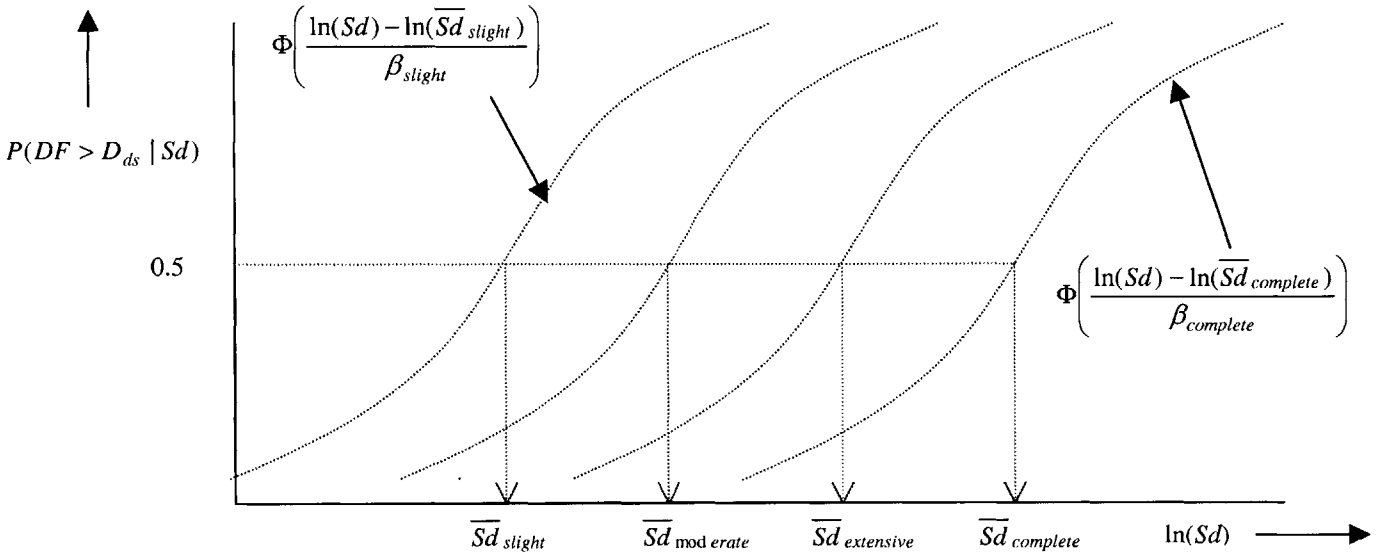

Figure 3-15: Representation of fragility model of HAZUS (2000)

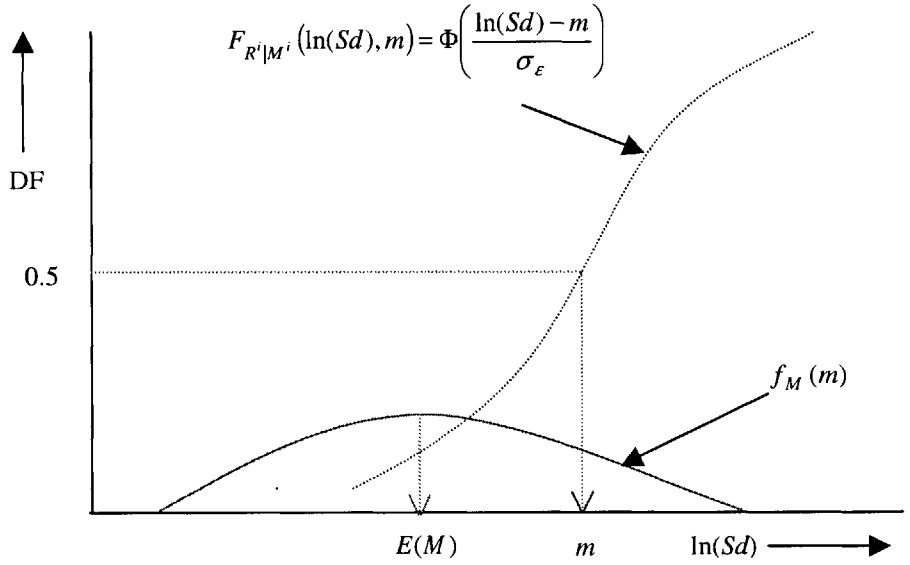

Figure 3-16: Representation of our fragility model

Next we express σ_{R^i} and $E(R^i)$ in terms of $E(M^i), \sigma_{M^i}$ and σ_{ε^i}. This is done in the following manner:

1. $E(R^i)$ is given by

$$E(R^i) = \int_{m=-\infty}^{\infty} E(R^i \mid M^i = m) f_{M^i}(m) dm \tag{3-16}$$

However, $E(R^i \mid M^i = m) = m$. Therefore,

$$E(R^i) = \int_{m=-\infty}^{\infty} m f_{M^i}(m) dm = E(M^i) \tag{3-17}$$

2. Here we express σ_{R^i} in terms of σ_{M^i} and σ_{ε^i}. Here we use the property that if X_1 and X_2 are two Gaussian random variables, then the conditional variable $(X_1|X_2 = x_2)$ is a Gaussian random variable with mean $E(X_1) + \rho \frac{\sigma_{X_1}}{\sigma_{X_2}}(x_2 - E(X_2))$ and standard deviation $\sigma_{X_1}\sqrt{(1-\rho^2)}$, where ρ is the correlation coefficient.

$E(R^i \mid M^i = m)$ can be written as

$$E(R^i \mid M^i = m) = E(R^i) + \rho \frac{\sigma_{R^i}}{\sigma_{M^i}}(m - E(M^i)) \tag{3-18}$$

$$\Rightarrow m = E(M^i) + \rho \frac{\sigma_{R^i}}{\sigma_{M^i}}(m - E(M^i)) \tag{3-19}$$

$$\Rightarrow (m - E(M^i))(\rho \frac{\sigma_{R^i}}{\sigma_{M^i}} - 1) = 0 \tag{3-20}$$

$$\Rightarrow \rho = \frac{\sigma_{M^i}}{\sigma_{R^i}} \tag{3-21}$$

Since σ_{ε^i} is the standard deviation of $(R^i \mid M^i = m)$, we write σ_{ε^i} as

$$\sigma_{\varepsilon^i} = \sigma_{R^i}\sqrt{(1-\rho^2)} \tag{3-22}$$

$$\sigma_{\varepsilon^i} = \sigma_{R^i}\sqrt{(1-(\frac{\sigma_{M^i}}{\sigma_{R^i}})^2)} \tag{3-23}$$

$$\sigma_{R^i}^2 = \sigma_{M^i}^2 + \sigma_{\varepsilon^i}^2 \tag{3-24}$$

By using equations (3-17) and (3-24), equation (3-15) is simplified to

$$\overline{D^i(Sd)} = \Phi\left(\frac{\ln(Sd) - E(M^i)}{\sqrt{(\sigma_{M^i})^2 + (\sigma_{\varepsilon^i})^2}}\right) \tag{3-25}$$

Next we describe the procedure used to estimate the three parameters $E(M^i), \sigma_{M^i}$ and σ_{ε^i} in (3-25) by calibration to the fragility data given in HAZUS (2000).

Parameter estimation

HAZUS (2000) gives the probability of being in or exceeding the damage factor corresponding to damage state *ds*, as a function of the spectral displacement *Sd*. Let $\mathrm{P}(DF > D_{ds} | Sd)^i_{HAZUS}$ be a data point given in HAZUS (2000) for seismic vulnerability class *i*. The unknown parameters of our fragility model, $E(M^i), \sigma_{M^i}$ and σ_{ε^i}, are estimated by matching the values of $\mathrm{P}(DF > D_{ds} | Sd)^i$ given in HAZUS (2000) with those given by our model. Following are the steps involved in the parameter estimation:

(1) We find the value of the mean of the fragility curve, which results in a damage factor of D_{ds}. If m' represents the unknown mean that results in D_{ds}, then using equation (3-12) we write D_{ds} as

$$D_{ds} = \Phi\left(\frac{\ln(Sd) - m'}{\sigma_{\varepsilon^i}}\right) \tag{3-26}$$

$$\Rightarrow m' = \ln(Sd) - \sigma_{\varepsilon^i}\Phi^{-1}(D_{ds}) \tag{3-27}$$

(2) Since m' results in a damage factor D_{ds} at a given spectral displacement *Sd*, whenever the mean of the fragility curve M^i, is lesser than m', the damage factor would be greater than D_{ds}. Therefore,

$$P(DF > D_{ds} \mid Sd)^i_{derived} = P(M^i < m') \tag{3-28}$$

$$\Rightarrow P(DF > D_{ds} \mid Sd)^i_{derived} = \Phi\left(\frac{m' - E(M^i)}{\sigma_{M^i}}\right) \tag{3-29}$$

By using equation (3-27), we simplify the above relation to

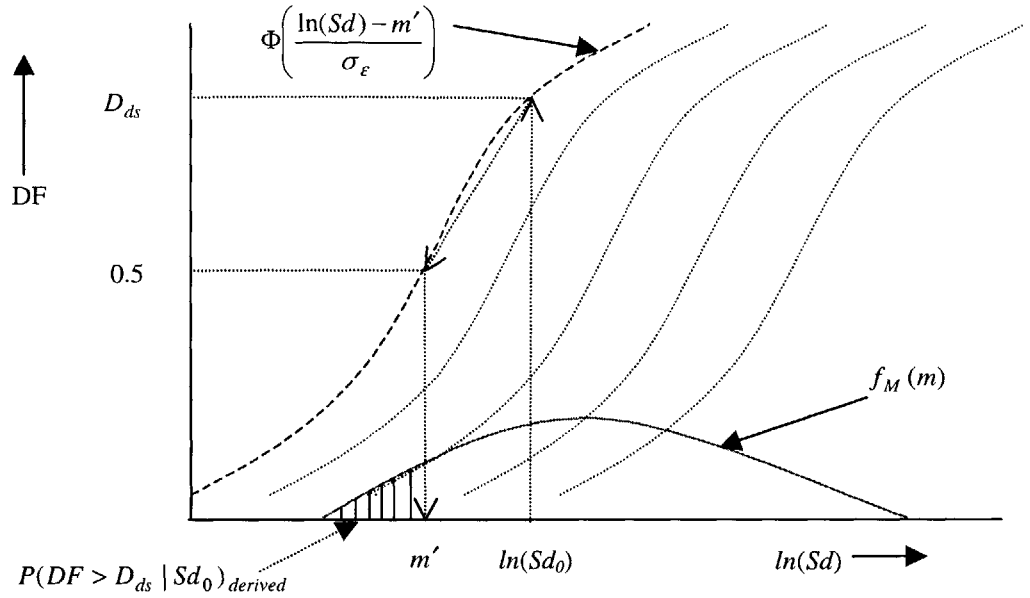

Figure 3-17: Illustration of the procedure for parameter estimation

$$P(DF > D_{ds} \mid Sd)^i_{derived} = \Phi\left(\frac{\ln(Sd) - \sigma_{\varepsilon^i}\Phi^{-1}(D_{ds}) - E(M^i)}{\sigma_{M^i}}\right) \quad \textbf{(3-30)}$$

Figure 3-17 illustrates the procedure used to obtain $\mathrm{P}\left(DF > D_{ds} \middle| Sd\right)^i$ using our model.

(3) Since we aim to match the predictions of $\mathrm{P}\left(DF > D_{ds} \middle| Sd\right)^i$ from our model with those in HAZUS (2000), we write

$$P(DF > D_{ds} \mid Sd)^i_{derived} = P(df > D_{ds} \mid Sd)^i_{HAZUS} \quad \textbf{(3-31)}$$

By using equation (3-30) and (3-4), we rewrite the above equation as

$$\Phi\left(\frac{\ln(Sd) - \sigma_{\varepsilon^i}\Phi^{-1}(D_{ds}) - E(M^i)}{\sigma_{M^i}}\right) = \Phi\left(\frac{\ln(Sd) - \ln(\overline{Sd}_{ds})}{\beta^i_{ds}}\right) \quad \textbf{(3-32)}$$

Since $\Phi(\cdot)$ is a monotonically increasing function, we equate the arguments on both sides of equation (3-32) to get

$$(\ln(Sd) - \sigma_{\varepsilon^i}\Phi^{-1}(D_{ds}) - E(M^i))\beta^i_{ds} = (\ln(Sd) - \ln(\overline{Sd}_{ds}))\sigma_{M^i} \quad \textbf{(3-33)}$$

(4) We obtain the parameter σ_{M^i} in this step. We write equation (3-33) at $Sd = \overline{Sd}_{ds}$ to get

$$\sigma_{\varepsilon^i}\Phi^{-1}(D_{ds}) + E(M^i) = \ln(\overline{Sd}_{ds}) \tag{3-34}$$

By substituting the value of $\ln(\overline{Sd}_{ds})$ from the above relation in equation (3-33), we get

$$(\ln(Sd) - \ln(\overline{Sd}_{ds}))\beta_{ds}^i = (\ln(Sd) - \ln(\overline{Sd}_{ds}))\sigma_{M^i} \tag{3-35}$$

Therefore,

$$\sigma_{M^i} = \beta_{ds}^i \tag{3-36}$$

This means that for the predictions made by our model to exactly match those from HAZUS (2000) for the damage state *ds*, the standard deviation of the mean of the fragility curve in our model needs to be equal to the logarithmic standard deviation of spectral displacement for damage state *ds* in HAZUS (2000). However, the β 's given in HAZUS (2000) for different damage states are not always equal. In such cases, we estimate σ_{M^i} to be the average of the β's associated with the slight, moderate and extensive damage states.

(5) In this step, we estimate $E(M^i)$ and σ_{ε^i}. We write equations similar to (3-34) at the median values of the spectral displacement for slight, moderate and extensive damage states. By simultaneously solving the three resulting equations, we obtain averaged values of the parameters $E(M^i)$ and σ_{ε^i}. However, as the damage factor corresponding to complete damage, $D_{complete}$, is close to 1.0, the corresponding term $\Phi^{-1}(D_{complete})$ in equation (3-34) diverges. Therefore, for the derivation of $E(M^i)$ and σ_{ε^i}, we do not consider the fragility information for the complete damage state given in HAZUS (2000).

An example is given next to further explain the above procedure.

Example

The seismic vulnerability class considered here is the *Low-rise Low-code Concrete moment frame ($C1L_{lowcode}$)*. The fragility parameters of the damage function of this structural class that are given in HAZUS (2000) are given in Table 3-5.

Slight		Moderate		Extensive		Complete	
Median	Beta	Median	Beta	Median	Beta	Median	Beta
0.9	0.95	1.44	0.91	3.60	0.85	9.00	0.97

Table 3-5: Parameters given in HAZUS (2000) for $C1L_{lowcode}$ class

From the table,

$\overline{Sd}_{slight} = 0.9$ inches

$\overline{Sd}_{moderate} = 1.44$ inches

$\overline{Sd}_{extensive} = 3.60$ inches

Similar to equation (3-34), for the slight, moderate and extensive damage states, we write

$$\ln(\overline{Sd}_{slight}) - \sigma_{\varepsilon^i}^{i}\Phi^{-1}(0.02) - E(M^i) = 0.0 \quad \textbf{(3-37)}$$

$$\ln(\overline{Sd}_{moderate}) - \sigma_{\varepsilon^i}^{i}\Phi^{-1}(0.10) - E(M^i) = 0.0 \quad \textbf{(3-38)}$$

$$\ln(\overline{Sd}_{extensive}) - \sigma_{\varepsilon^i}^{i}\Phi^{-1}(0.50) - E(M^i) = 0.0 \quad \textbf{(3-39)}$$

where 0.02, 0.10 and 0.50 are the damage factors corresponding to slight, moderate and extensive damage states respectively. By solving equations (3-37),(3-38) and (3-39) simultaneously, the following values of parameters are obtained:

$E(M^{C1L_{lowcode}}) = 1.235$

$\sigma_{\varepsilon^{C1L_{lowcode}}} = 0.666$

The parameter $\sigma_{M^{C1L_{lowcode}}}$ is obtained by averaging the beta values for the slight, moderate and extensive damage states. It is estimated as 0.903.

Parameter validation

The validity of the estimated parameters can be checked by comparing $P(df > D_{ds} \mid Sd)^i_{derived}$ with $P(df > D_{ds} \mid Sd)^i_{HAZUS}$. $P(df > D_{ds} \mid Sd)^i_{derived}$ is obtained by

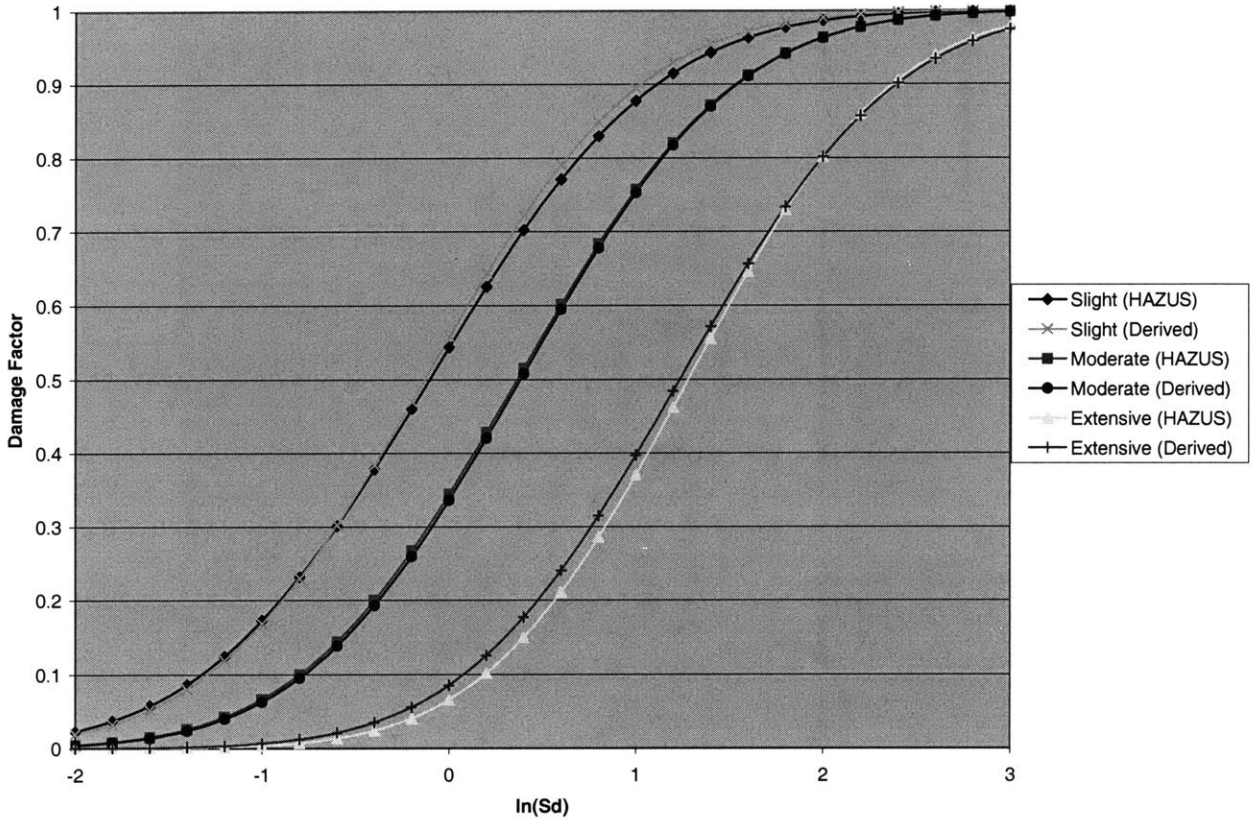

Figure 3-18: Comparison of the damage functions in HAZUS (2000) and the derived damage functions, for $C1L_{lowcode}$ seismic vulnerability class

using equation (3-30). Figure 3-18 shows the actual damage functions given in HAZUS (2000) and those derived by using our fragility model. As can be seen, the derived values match very well those in HAZUS (2000).

Next we compare the mean damage predictions obtained by using the fragility model in HAZUS (2000) and those from our model.

Comparison of mean damage factor predictions

Figure 3-19 compares the mean damage predictions made by the model in HAZUS (2000) and those predicted by the model proposed here. For a given spectral displacement, the mean damage factor from our model, at a given spectral displacement, is calculated by using equation (3-25). From the model given in HAZUS (2000), the same is calculated by using equation (3-6). As can be seen in Figure 3-19, the mean damage

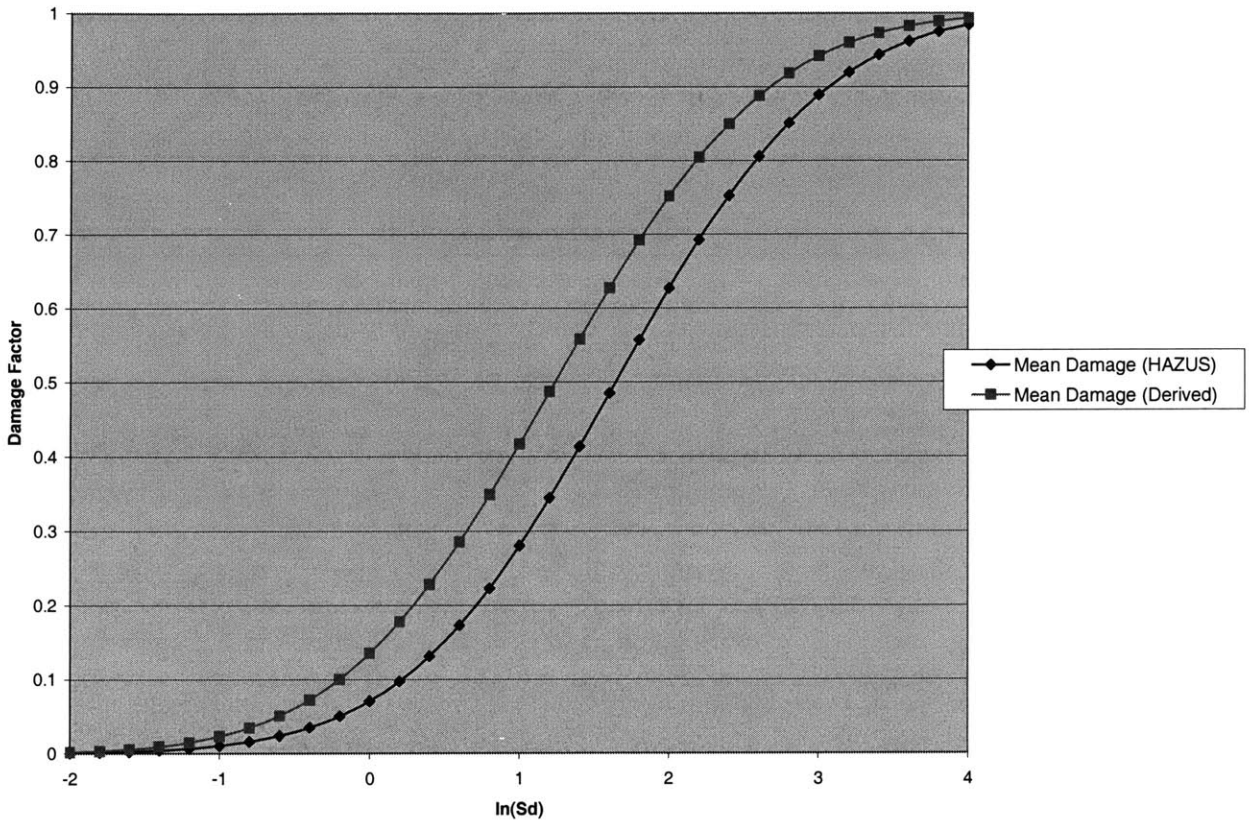

Figure 3-19: Comparison of the mean damage factors predicted by the model in HAZUS (2000) and by the derived model, for $C1L_{lowcode}$ seismic vulnerability class

predictions by the derived model are higher (to maximum of about 0.15 units) than those obtained directly from HAZUS (2000). The main reason for this difference is that in the derivation of the parameters of our fragility model from HAZUS (2000), we do not consider the damage function given in HAZUS (2000) for the complete damage state.

3.3.2 Fragility models (macroseismic approach)

Here we consider fragility models for building damage in terms of Modified Mercalli Intensity (MMI). MMI is a subjective measure of ground motion intensity based in part on the level of damage to various infrastructure components. Specifically, we describe a fragility model for the CEUS and a procedure to obtain its parameters using information in ATC-13 and FEMA (1990).

The proposed model describes uncertainty in the damage factor of the generic building in a given seismic vulnerability class. The model assumes that the fragility curve has the

form of the cumulative distribution of a Gaussian random variable. The mean of the fragility curve is uncertain and varies from building to building within the vulnerability class, whereas the standard deviation is deterministically known. The mean value of the fragility curve is in turn assumed to be a Gaussian random variable with deterministic parameters.

The main difference between this model and the engineering fragility model that we derived in Section 3.3.1 is in the vulnerability classification that is used. Here, we use the classification of HAZUS (2000) (except for the mobile homes category), which has 35 classes as shown in Table 3-1. We do not further classify the 35 classes into sub-classes (Pre-Code, Low-Code, etc.) based on the quality of construction. For example, in the engineering fragility model the Low-rise Concrete moment frame (C1L) buildings were sub-divided into $C1L_{precode}$, $C1L_{lowcode}$, $C1L_{moderatecode}$, $C1L_{highcode}$ buildings. The overall losses to the C1L buildings were calculated by adding the losses to buildings in each of the code-levels, by using the fragility information for these code-levels. However, in the macroseismic approach, disaggregation of the buildings into different code-levels is not done primarily due to the fact that existing literature lacks information regarding the fragility of the sub-classes with in the C1L class. Here we use two parameters, $\sigma_{\overline{M}}^{i}$ and σ_{M}^{i} , to characterize the variability in the mean seismic resistance of a generic building in seismic vulnerability class *i*. $\sigma_{\overline{M}}^{i}$ is the variability in the mean seismic resistance of different sub-classes within the structural class *i* and σ_{M}^{i} is the variability in the mean seismic resistance of different buildings within a sub-class within the structural class *i*.

The mean damage factor $\overline{D(I)^i}$ corresponding to a seismic vulnerability class *i*, at a ground shaking intensity I (in MMI), is calculated by incorporating the variability in the damage of various buildings in the vulnerability class as

$$\overline{D(I)^i} = \int_{m=-\infty}^{\infty} D(I,m)^i f_{M^i}(m)dm \qquad \textbf{(3-40)}$$

where

$D(I,m)^i$ is the damage factor corresponding to an intensity I when the mean of the fragility curve takes a value m. It is expressed as

$$D(I,m)^i = \Phi\left(\frac{I-m}{\sigma_\varepsilon^i}\right) \tag{3-41}$$

where

$f_{M^i}(m)$ is the probability distribution function of the mean of the fragility curve of class i.

M^i is a Gaussian random variable with mean $E(M)^i$ and standard deviation $\sqrt{(\sigma_M^i)^2+(\sigma_{\overline{M}}^i)^2}$.

σ_ε^i represents the slope of the fragility curve. It is assumed to be independent of the value taken by the mean of the fragility curve.

By using a procedure similar to the one given in the description of our engineering fragility model in Section 3.3.1, equation (3-40) is simplified to

$$\overline{D(I)^i} = \Phi\left(\frac{I-E(M)^i}{\sqrt{(\sigma_M^i)^2+(\sigma_{\overline{M}}^i)^2+(\sigma_\varepsilon^i)^2}}\right) \tag{3-42}$$

Equation (3-42) gives the average damage factor associated with the vulnerability class i given the ground shaking intensity I, in terms of the parameters $E(M)^i$, σ_M^i, $\sigma_{\overline{M}}^i$ and σ_ε^i.

Next we describe the procedure used to estimate these four parameters by using the fragility data in ATC-13 and FEMA (1990).

Parameter estimation

The characteristics of the fragility data in ATC-13 and FEMA (1990) are:

- ATC-13 and FEMA (1990) give the probability distribution of the damage factor at integral values of earthquake intensity. ATC-13 gives fragility estimates for MMI in the range 6-12. FEMA (1990) gives fragilities for MMI in the range 6-9. Figure 3-20 shows the typical form of the fragility data in ATC-13 and FEMA (1990). For example, $f_{DF}(df/I=6)$ is the probability density function of the damage factor for MMI 6.

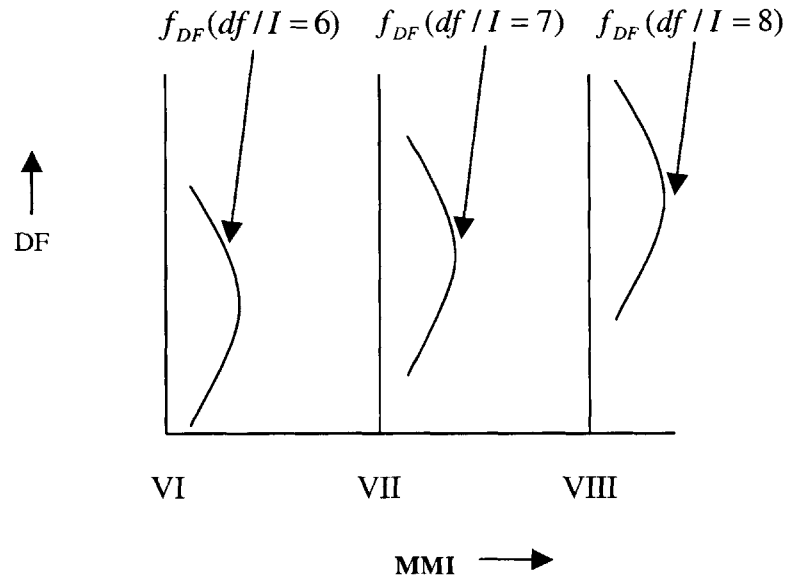

Figure 3-20: Typical format of the fragility data, as given in ATC-13 and FEMA

- Both ATC-13 and FEMA (1990) do not consider the damage to structural and non-structural components separately. Rather, they give an aggregate measure of the building damage factor.

We interpret that the damage factor distribution in ATC-13 gives only the variability in the mean seismic resistance of different sub-classes within a seismic vulnerability class. Therefore, we use ATC-13 to estimate the parameters $E(M)^i$ and $\sigma_{\overline{M}}^i$. We interpret that the damage factor distribution in FEMA (1990) represents the variability in the seismic resistance of buildings in each sub-class of a seismic vulnerability class. Hence, we use FEMA (1990) to estimate the parameters $E(M)^i$, σ_M^i and σ_ε^i.

Next we give a description of the procedure used to estimate parameters $E(M)_{FEMA}^i$, $\sigma_{M,FEMA}^i$ and $\sigma_{\varepsilon,FEMA}^i$ based on the data in FEMA (1990). The procedure used here is somewhat similar to that used to derive the parameters of our engineering fragility model. The required parameters are estimated by matching the estimates of $P(DF \le df \mid I)$ made by our model and those by FEMA (1990). Following are the steps involved in the parameter estimation:

1. We find the value of the mean of the of our fragility curve that results in a damage factor *df*, at a given intensity level I. If m' is unknown mean, using equation (3-41), we get

$$df = \Phi\left(\frac{I - m'}{\sigma^i_{\varepsilon,FEMA}}\right) \tag{3-43}$$

$$\Rightarrow m' = I - \Phi^{-1}(df)\sigma^i_{\varepsilon,FEMA} \tag{3-44}$$

2. When the mean of the fragility curve is greater than m', the damage factor would be less than df. Therefore,

$$P(DF \le df \mid I)^i_{derived} = P(M^i \ge m') \tag{3-45}$$

By substituting the value of m' in the RHS of the above relation, we get

$$P(DF \le df \mid I)^i_{derived} = P(M^i \ge I - \Phi^{-1}(df)\sigma^i_{\varepsilon,FEMA}) \tag{3-46}$$

$$\Rightarrow P(DF \le df \mid I)^i_{derived} = \Phi\left(\frac{\Phi^{-1}(df)\sigma^i_{\varepsilon,FEMA} - (I - E(M)^i_{FEMA})}{\sigma^i_{M,FEMA}}\right) \tag{3-47}$$

3. Here we equate the $P(DF \le df \mid I)$ values from our model with those given in FEMA (1990), i.e.,

$$P(DF \le df \mid I)^i_{derived} = P(DF \le df \mid I)^i_{FEMA} \tag{3-48}$$

$$\Rightarrow \Phi\left(\frac{\Phi^{-1}(df)\sigma^i_{\varepsilon,FEMA} - (I - E(M)^i_{FEMA})}{\sigma^i_{M,FEMA}}\right) = P(DF \le df \mid I)^i_{FEMA} \tag{3-49}$$

$$\Rightarrow \sigma^i_{M,FEMA}\Phi^{-1}(P(DF \le df \mid I)^i_{FEMA}) - \Phi^{-1}(df)\sigma^i_{\varepsilon,FEMA} + I - E(M)^i_{FEMA} = 0 \tag{3-50}$$

Equation (3-50) relates the known $P(DF \le df \mid I)^i_{FEMA}$, df and I to the unknown parameters $E(M)^i_{FEMA}$, $\sigma^i_{M,FEMA}$ and $\sigma^i_{\varepsilon,FEMA}$. These unknown parameters are estimated by using an optimization procedure, wherein the sum of the square of the LHS of equation (3-50), for different combinations of I and df is minimized.

Table 3-6 shows the parameters of the fragility model that have been derived by using the data given in FEMA (1990) for 11 structural classes. Table 3-7 shows the parameters of the fragility model derived from ATC-13, using a similar procedure. Even though ATC-13 provides fragility data for intensities greater than 9MMI, the ATC-13 parameters

Structural Class	$E(M)_{FEMA}$	$\sigma_{M,FEMA}$	$\sigma_{\varepsilon,FEMA}$
Timber	11.26	1.32	1.75
Low-rise URM	9.16	1.04	1.23
Low-rise RM	11.25	1.36	1.79
Low-rise RC Shear Wall	11.82	1.67	1.71
Mid-rise RC Shear Wall	10.84	1.57	1.72
High RC Wall	10.64	1.39	1.93
Low-rise RC Pre-stressed	9.17	0.85	1.14
High-rise Steel	12.09	1.15	1.90
Light Metal	11.51	1.88	1.87
Low-rise RC Frame	11.82	1.67	1.71
Mid-rise RC Frame	10.84	1.57	1.72

Table 3-6: Parameters of the fragility model derived by using the data given in FEMA (1990)

shown in Table 3-7 are derived using the data given for MMI < 10, as the fragility data in ATC-13 for higher intensities may not be very reliable.

The fragility parameters derived for the 11 structural classes in FEMA (1990) are extended to the 35 structural classes considered in HAZUS (2000) by using the parameters that are derived from the fragility data in ATC-13. As the nomenclature used for the structural classes in FEMA (1990) is not exactly same as that used by ATC-13 or HAZUS (2000), we map the FEMA (1990) structural classes to those in HAZUS (2000) and ATC-13. Table 3-8 shows the mapping that has been judgmentally assumed. Next, we give an example to illustrate the method adopted to extend the parameters for 11 classes in FEMA (1990) to 35 classes in ATC-13, by using the parameters derived from ATC-13.

Example

As can be seen in Table 3-8, the High rise Steel structural class in FEMA (1990) has been mapped to High rise Moment Resisting Steel Frame (Perimeter Frame), in ATC-13 and S1H in HAZUS (2000). The fragility parameters of S1H structural class obtained from FEMA (1990), as shown in Table 3-6 are:

$E(M)_{FEMA}^{S1H} = 12.09$

$\sigma_{M,FEMA}^{S1H} = 1.15$

$\sigma_{\varepsilon,FEMA}^{S1H} = 1.9$

Referring to Table 3-7, the fragility parameters of the Moment Resisting Steel Frame structural class obtained from ATC-13 are:

$E(M)^{S1H}_{ATC-13} = 11.40$

$E(M)^{S1M}_{ATC-13} = 12.83$

$E(M)^{S1L}_{ATC-13} = 13.61$

The parameters $E(M)^{S1M}_{FEMA}$ and $E(M)^{S1L}_{FEMA}$ are unknown because of the unavailability of data in FEMA regarding the fragilities of these two structural classes. In our fragility model, the values of the unknown parameters are estimated in the following manner:

$$E(M)^{S1L}_{FEMA} = E(M)^{S1H}_{FEMA} + E(M)^{S1L}_{ATC-13} - E(M)^{S1H}_{ATC-13}$$

$$\Rightarrow E(M)^{S1L}_{FEMA} = 12.09 + 13.61 - 11.40$$

$$\Rightarrow E(M)^{S1L}_{FEMA} = 14.30$$

Similarly, $E(M)^{S1M}_{FEMA}$ is estimated to be 13.51.

The unknown values of $\sigma^{S1M}_{M,FEMA}$, $\sigma^{S1L}_{M,FEMA}$, $\sigma^{S1M}_{\varepsilon,FEMA}$ and $\sigma^{S1L}_{\varepsilon,FEMA}$ are assumed to be equal to the corresponding values of the S1H structural class, i.e.,

$$\sigma^{S1M}_{M,FEMA} = \sigma^{S1L}_{M,FEMA} = \sigma^{S1H}_{M,FEMA}$$

$$\sigma^{S1M}_{\varepsilon,FEMA} = \sigma^{S1L}_{\varepsilon,FEMA} = \sigma^{S1H}_{\varepsilon,FEMA}$$

Table 3-9 shows the values of the parameters that are used in the fragility model, derived from the fragility data given in ATC-13 and FEMA (1990).

Comments

The required parameters of the fragility model, $E(M)^i$, σ^i_M, $\sigma^i_{\overline{M}}$ and σ^i_ε for structural class *i* are determined by using the following relations:

$$E(M)^i = 0.6 * E(M)^i_{FEMA} + 0.4 * E(M)^i_{ATC-13} \quad \textbf{(3-51)}$$

$$\sigma^i_M = \sigma^i_{M,FEMA} \quad \textbf{(3-52)}$$

$$\sigma^i_{\overline{M}} = \sigma^i_{M,ATC-13} \quad \textbf{(3-53)}$$

$$\sigma^i_\varepsilon = \sigma^i_{\varepsilon,FEMA} \quad \textbf{(3-54)}$$

A weight of 0.4 is given to the expected mean value of the fragility curve obtained by using the fragility information in ATC-13 and a weight of 0.6 is given to the expected mean value obtained by using FEMA (1990). Less weight is given to the expected mean

obtained from ATC-13 mainly because the fragility data in ATC-13 are primarily for California not CEUS construction.

Structural Class (ID)	Structural Class (Description)	$E(M)_{ATC\text{-}13}$	$\sigma_{M,ATC-13}$	$\sigma_{\varepsilon,ATC-13}$
W1	Timber	12.67	0.71	2.66
S1L	Low rise Moment Resisting Steel Frame (Perimeter Frame)	13.61	0.57	3.05
S1M	Mid rise Moment Resisting Steel Frame (Perimeter Frame)	12.83	0.68	2.73
S1H	High rise Moment Resisting Steel Frame (Perimeter Frame)	11.40	0.60	2.14
S2L	Low rise Braced Steel Frame	12.12	0.74	2.37
S2M	Mid rise Braced Steel Frame	11.51	0.82	2.18
S2H	High rise Braced Steel Frame	10.87	0.57	2.07
S3	Light Metal	13.84	0.72	2.90
S4L	Low rise Reinforced Concrete Shear Wall, with Moment Resisting Frame	12.52	0.56	2.55
S4M	Mid rise Reinforced Concrete Shear Wall, with Moment Resisting Frame	11.20	0.48	1.99
S4H	High rise Reinforced Concrete Shear Wall, with Moment Resisting Frame	11.27	0.51	2.14
S5L	Low rise Un-reinforced Masonry, with Load Bearing Frame	10.03	0.67	1.71
S5M	Mid rise Un-reinforced Masonry, with Load Bearing Frame	9.83	0.73	1.91
S5H	High rise Un-reinforced Masonry, with Load Bearing Frame	9.37	0.71	1.80
C1L	Low rise Moment Resisting Ductile Concrete Frame	11.95	0.43	2.20
C1M	Mid rise Moment Resisting Ductile Concrete Frame	12.87	0.73	3.01
C1H	High rise Moment Resisting Ductile Concrete Frame	12.61	0.83	3.08
C2L	Low rise Reinforced Concrete Shear Wall, without Moment Resisting Frame	11.52	0.54	2.20
C2M	Mid rise Reinforced Concrete Shear Wall, without Moment Resisting Frame	11.02	0.61	2.10
C2H	High rise Reinforced Concrete Shear Wall, without Moment Resisting Frame	10.34	0.55	1.89
C3L	Low rise Moment Resisting Non-Ductile Concrete Frame	10.52	0.47	1.96
C3M	Mid rise Moment Resisting Non-Ductile Concrete Frame	10.33	0.49	1.96
C3H	High rise Moment Resisting Non-Ductile Concrete Frame	10.44	0.61	2.04
PC2L	Low rise Pre-Cast Concrete, other than Tilt-up	10.36	0.49	1.70
PC2M	Mid rise Pre-Cast Concrete, other than Tilt-up	10.36	0.54	1.73
PC2H	High rise Pre-Cast Concrete, other than Tilt-up	10.14	0.56	1.65
RM1L	Low rise Reinforced Masonry Shear Wall, without Moment Resisting Frame	11.55	0.61	2.26
RM1M	Mid rise Reinforced Masonry Shear Wall, without Moment Resisting Frame	10.83	0.55	2.05
RM2L	Low rise Reinforced Masonry Shear Wall, with Moment Resisting Frame	12.30	0.62	2.50
RM2M	Mid rise Reinforced Masonry Shear Wall, with Moment Resisting Frame	12.11	0.67	2.61
RM2H	High rise Reinforced Masonry Shear Wall, with Moment Resisting Frame	11.49	0.52	2.44
URML	Low rise Un-Reinforced masonry Bearing Wall	9.37	0.59	1.66
URMM	Mid rise Un-Reinforced masonry Bearing Wall	8.96	0.60	1.56

Table 3-7: Parameters of the fragility model derived by using the data given in ATC-13

Facility No. (ATC 13)	ATC-13 Class	HAZUS (2000) Class ID	FEMA Class No.	FEMA Class
1	Timber	W1,W2	14	Wood Frame Buildings
17	High rise Moment Resisting Steel Frame (Perimeter Frame)	S1H	10	High Rise Steel Buildings(>13 Stories)
14	Braced Steel Frame	S2H	10	High Rise Steel Buildings(>13 Stories)
2	Light Metal	S3	11	Light Metal Buildings
3	Low rise Reinforced Concrete Shear Wall, with Moment Resisting Frame	S4L	5	R/C Low rise Shear Wall Buildings(1-5 Stories)
4	Mid rise Reinforced Concrete Shear Wall, with Moment Resisting Frame	S4M	6	R/C Mid rise Shear Wall Buildings(6-13 Stories)
5	High rise Reinforced Concrete Shear Wall, with Moment Resisting Frame	S4H	7	R/C High rise Shear Wall Buildings(>13 Stories)
18	Low rise Moment Resisting Ductile Concrete Frame	C1L	30	R/C Frame Building (1 to 5 Stories)
19	Mid rise Moment Resisting Ductile Concrete Frame	C1M	31	R/C Frame Building (6 to 13 Stories)
6	Low rise Reinforced Concrete Shear Wall, without Moment Resisting Frame	C2L	5	R/C Low rise Shear Wall Buildings(1-5 Stories)
7	Mid rise Reinforced Concrete Shear Wall, without Moment Resisting Frame	C2M	6	R/C Mid rise Shear Wall Buildings(6-13 Stories)
8	High rise Reinforced Concrete Shear Wall, without Moment Resisting Frame	C2H	7	R/C High rise Shear Wall Buildings(>13 Stories)
87	Low rise Moment Resisting Non-Ductile Concrete Frame	C3L	8	Low rise pre-stressed R/C framed structures
81	Low rise Pre-Cast Concrete, other than Tilt-up	PC2L	5	R/C Low rise Shear Wall Buildings(1-5 Stories)
82	Mid rise Pre-Cast Concrete, other than Tilt-up	PC2M	6	R/C Mid rise Shear Wall Buildings(6-13 Stories)
83	High rise Pre-Cast Concrete, other than Tilt-up	PC2H	7	R/C High rise Shear Wall Buildings(>13 Stories)
9	Low rise Reinforced Masonry Shear Wall, without Moment Resisting Frame	RM1L	4	Low rise RM buildings

Table 3-8: Mapping between the FEMA(1990), HAZUS (2000) and ATC-13 structural classes

Structural Class (ID)	$E(M)_{ATC\text{-}13}$	$E(M)_{FEMA}$	$\sigma_M = \sigma_{M,FEMA}$	$\sigma_{\overline{M}} = \sigma_{M,ATC-13}$	$\sigma_\varepsilon = \sigma_{\varepsilon,FEMA}$
W1	12.67	11.26	1.32	0.71	1.75
W2	12.67	11.26	1.32	0.71	1.75
S1L	13.61	14.30	1.15	0.57	1.90
S1M	12.83	13.51	1.15	0.68	1.90
S1H	11.40	12.09	1.15	0.60	1.90
S2L	12.12	13.34	1.15	0.74	1.90
S2M	11.51	12.73	1.15	0.82	1.90
S2H	10.87	12.09	1.15	0.57	1.90
S3	13.84	11.51	1.88	0.72	1.87
S4L	12.52	11.82	1.67	0.56	1.71
S4M	11.20	10.84	1.57	0.48	1.72
S4H	11.27	10.64	1.39	0.51	1.93
S5L	10.03	9.66	1.04	0.67	1.72
S5M	9.83	9.46	1.04	0.73	1.72
S5H	9.37	9.00	1.04	0.71	1.72
C1L	11.95	11.82	1.67	0.43	1.71
C1M	12.87	10.84	1.57	0.73	1.72
C1H	12.61	10.57	1.57	0.83	1.72
C2L	11.52	11.82	1.67	0.54	1.71
C2M	11.02	10.84	1.57	0.61	1.72
C2H	10.34	10.64	1.39	0.55	1.93
C3L	10.52	9.17	0.85	0.47	1.14
C3M	10.33	8.97	0.85	0.49	1.14
C3H	10.44	9.09	0.85	0.61	1.14
PC1	11.05	11.05	1.16	0.50	1.63
PC2L	10.36	11.82	1.67	0.49	1.71
PC2M	10.36	10.84	1.57	0.54	1.72
PC2H	10.14	10.64	1.39	0.56	1.93
RM1L	11.55	11.25	1.36	0.61	1.79
RM1M	10.83	10.52	1.36	0.55	1.79
RM2L	12.30	11.99	1.36	0.62	1.79
RM2M	12.11	11.80	1.36	0.67	1.79
RM2H	11.49	11.18	1.36	0.52	1.79
URML	9.37	9.16	1.04	0.59	1.23
URMM	8.96	8.75	1.04	0.60	1.23

Table 3-9: Parameters used in the macroseismic fragility model

3.4 'Structural-Occupancy mapping' model

The 'structural-occupancy mapping' model enables the estimation of the damage to the social function (occupancy) classes from the damage to the structural classes. This mapping gives the fraction of each structural class in a specific occupancy class. Large uncertainties exist in this mapping. The following section describes these uncertainties by comparing four data sources, which are considered relevant to CEUS.

3.4.1 Review of data sources

Jones et al. (1996)

Jones et al. (1996) obtain estimates of the distribution of each structural type, by number and square footage, in different occupancy classes for Memphis-Shelby County. They obtain this information based mainly on the indirect methods for rapid building stock estimation developed by Jones (1994). They compare these indirect estimates to the direct estimates of the Memphis stock obtained by using the Shelby County Tax Assessor's records supplemented with information from many other sources. Comparisons are also made between the estimates for Memphis with the estimates obtained in an earlier study for Wichita-Sedgwick County, Kansas, for 1982.

Jones et al. (1996) find similarities in the structural-occupancy distribution estimates for Memphis and Wichita, even though there are major differences in the two metropolitan areas in terms of population, size, location and other characteristics. Wood Frame construction predominates in both regions, accounting for 85% of the total number of buildings and 55% to 60% of the total area. About 90% to 95% of the residential buildings, both by area and number are of wood frame. They also find that approximately 15% of the total building area is comprised of engineered structures. Figure 3-21 shows the structural-occupancy mapping as given in Jones et al. (1996) for Memphis.

French et al. (2000)

French et al. (2000) study the characteristics of the inventory of essential facilities such as hospitals, police and fire stations, and schools in a total of 93 counties in mid-America, in the states of Arkansas, Illinois, Indiana, Kentucky, Mississippi, Missouri and

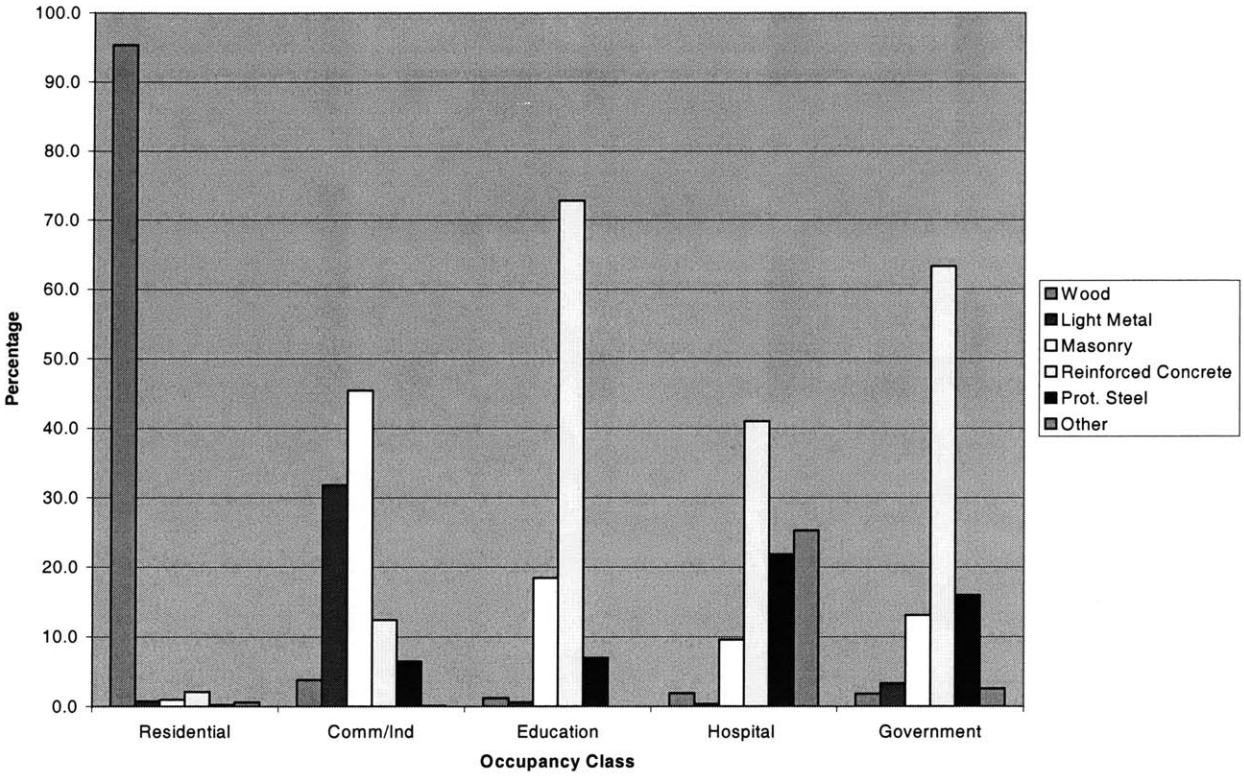

Figure 3-21: Structural – occupancy mapping in Jones et al. (1996) for Memphis

Tennessee. The data were gathered mainly through telephone surveys. The survey data includes the number of floors, square footage, age, frame type and structural system of each inventoried building.

French et al. (2000) find that un-reinforced masonry comprised one-third of the total inventory surveyed. 20% of the inventory is found to be either reinforced masonry or concrete. Steel frame structures of all types comprise nearly 27% of the inventory. Wood frame, precast concrete and mobile homes account for only a small percentage of the total. French et al. (2000) also provide the distribution of the structural classes for different essential facility types.

Hwang et al. (1997b)

This study was conducted to evaluate the seismic performance of fire stations in Shelby County, Tennessee. Data relevant to 71 fire stations were collected from various government agencies. In addition, architectural and structural drawings were reviewed

and field inspections were performed to determine the structural types of fire stations. They found that most of the fire stations in Shelby county were unreinforced masonry (URM) buildings. Some of the fire stations were of the type S5L (Steel frame with URM infill walls).

HAZUS (2000)

HAZUS (2000) considers 28 specific occupancy classes as shown in Table 3-10. Default mapping schemes for specific occupancy classes to model building (structure) types by floor area percentage are provided. The default estimates are based on expert opinion, propriety insurance data and tax assessors' records. HAZUS (2000) provides the mapping as a function of building height. For example, default mapping for low-rise construction in Tennessee is shown in Table 3-11. Referring to Table 3-11, out of a 100 sq ft. of the low-rise single family dwellings in the mid-west, 90 sq ft. are contributed by the wood light frame and 10 sq ft. by unreinforced masonry construction.

3.4.2 Comparisons of data sources

Here we compare the structural-occupancy mapping according to different sources for two occupancy classes, viz., residential and emergency response. The residential sector is considered mainly because it is the most predominant sector in the building inventory in the CEUS. We consider the emergency response sector because French et al. (2000), Hwang et al. (1997b) and HAZUS (2000) give estimates of the structural class distribution for this sector.

HAZUS (2000) is the source that gives data regarding the distribution of structural classes in other commercial and industrial sectors as well. It gives distributions for different height categories and for different sub-classes within the commercial and industrial sectors. Even though Jones et al. (1996) give estimates for commercial and industrial sector, the data is more aggregated, i.e., they neither give the distribution among the different height categories nor among different sub-classes for these sectors. Therefore, we do not compare the data in HAZUS (2000) with the data in Jones et al. (1996) for the commercial and industrial sectors.

Label	Occupancy Class	Example Descriptions
	Residential	
RES1	Single Family Dwelling	House
RES2	Mobile Home	Mobile Home
RES3	Multi Family Dwelling	Apartment/Condominium
RES4	Temporary Lodging	Hotel/Motel
RES5	Institutional Dormitory	Group Housing (military, college), Jails
RES6	Nursing Home	
	Commercial	
COM1	Retail Trade	Store
COM2	Wholesale Trade	Warehouse
COM3	Personal and Repair Services	Service Station/Shop
COM4	Professional/Technical Services	Offices
COM5	Banks	
COM6	Hospital	
COM7	Medical Office/Clinic	
COM8	Entertainment & Recreation	Restaurants/Bars
COM9	Theaters	Theaters
COM10	Parking	Garages
	Industrial	
IND1	Heavy	Factory
IND2	Light	Factory
IND3	Food/Drugs/Chemicals	Factory
IND4	Metals/Minerals Processing	Factory
IND5	High Technology	Factory
IND6	Construction	Office
	Agriculture	
AGR1	Agriculture	
	Religion/Non/Profit	
REL1	Church/Non-Profit	
	Government	
GOV1	General Services	Office
GOV2	Emergency Response	Police/Fire Station/EOC
	Education	
EDU1	Grade Schools	
EDU2	Colleges/Universities	Does not include group housing

Table 3-10: Occupancy classes that are used in HAZUS (2000) - *Source HAZUS (2000)*

No.	Specific Occup. Class	Model Building Type															
		1	2	3	6	9	10	13	16	19	22	25	26	29	31	34	36
		W1	W2	S1L	S2L	S3	S4L	S5L	C1L	C2L	C3L	PC1	PC2L	RM1L	RM2L	URML	MH
1	RES1	90														10	
2	RES2																100
3	RES3	75												2		23	
4	RES4	50												3	2	45	
5	RES5	20							4	13	2	22	4	2		33	
6	RES6	90														10	
7	COM1		30	2	4	11	6	7		5		5		2		28	
8	COM2		10	2	4	11	6	7	2	10	2	14	2	2		28	
9	COM3		30	2	4	11	6	7		5		5		2		28	
10	COM4		30	2	4	11	6	7		5		5		2		28	
11	COM5		30	2	4	11	6	7		5		5		2		28	
12	COM6				2	4	2	2	6	21	4	33	6	2		18	
13	COM7		30	2	4	11	6	7		5		5		2		28	
14	COM8		30	2	4	11	6	7		5		5		2		28	
15	COM9			2	6	14	8	10	4	13	2	22	4			15	
16	COM10			2	4	11	6	7	6	21	4	33	6				
17	IND1			5	10	25	13	17	2	7	2	12	2			5	
18	IND2		10	2	4	11	6	7	2	10	2	14	2	3		27	
19	IND3		10	2	4	11	6	7	2	10	2	14	2	3		27	
20	IND4			5	10	25	13	17	2	7	2	12	2			5	
21	IND5		10	2	4	11	6	7	2	10	2	14	2	2		28	
22	IND6		30	2	4	11	6	7		5		5		2		28	
23	AGR1		10	2	4	11	6	7	2	10	2	14	2	2		28	
24	REL1	30			3	5	3	4		5		5		2	2	41	
25	GOV1		15	14	21				7	6		4		3		30	
26	GOV2		14	7	17				4	12					3	43	
27	EDU1		10	5	12				5	7				11		50	
28	EDU2		14	6	12			2	8	11					10	37	

Table 3-11: Distribution Percentage of Floor Area for Model Building Types within Each Building Occupancy Class, Low Rise, Mid-West in HAZUS 2000 – *Source HAZUS (2000)*

Residential Occupancy Class

HAZUS (2000) subdivides the residential occupancy class into 6 sub-classes. While HAZUS (2000) gives separate structural-occupancy mappings for different height categories, the mapping of Jones et al. (1996) covers all the height categories and sub-sectors in the residential sector. In order to compare these two data sources, assumptions regarding the following quantities need to be made:

- The distribution of floor area among the residential sub-occupancy classes.
- The distribution of floor area among the low, mid and high-rise categories.

Table 3-12 and Table 3-13 are two mappings, denoted by R_1 and R_2 respectively that give the distribution of the sub-occupancy classes within the residential occupancy class.

	RES1	RES3	RES4	RES5	RES6
Low-rise	75	10	5	5	5
Mid-rise	0	50	25	25	0
High-rise	0	25	50	25	0

Table 3-12: Percentages assigned to the different sub-occupancy classes in the different height categories of the residential sector in mapping R_1

	RES1	RES3	RES4	RES5	RES6
Low-rise	95	2	1	1	1
Mid-rise	0	50	25	25	0
High-rise	0	25	50	25	0

Table 3-13: Percentages assigned to the different sub-occupancy classes in the different height categories of the residential sector in mapping R_2

Mapping	Low-Rise	Mid-Rise	High-Rise
H_1	80	15	5
H_2	95	4	1
H_3	99	0.7	0.3

Table 3-14: Percentages assigned to the different height categories in the Residential sector

Combination Mapping	Sub-Occupancy Mapping	Height Category Mapping
Case1	R_1	H_1
Case2	R_1	H_2
Case3	R_2	H_1
Case4	R_2	H_2
Case5	R_2	H_3

Table 3-15: Combinations considered for comparison of HAZUS (2000) with Jones et al. (1996)

These mappings are obtained from the information about the inventory of each residential sub-class that is given in HAZUS (2000). For example, in mapping R_1, it is assumed that 100sq ft. of the low-rise residential occupancy is made up of 75 sq ft. of single family dwellings (RES1), 10 sq ft. of multi-family dwellings (RES3) and 5 sq ft. each of RES4, RES5 and RES6. Table 3-14 shows three possible mappings H_1, H_2 and H_3 for the proportion of buildings of the residential sector within the three height categories low, mid and high-rise. For example, H_1 could be assumed to crudely represent an urban environment and H_3 a rural environment.

Table 3-15 shows the combination of R and H mappings that have been considered for comparison of HAZUS (2000) and Jones et al. (1996). Figure 3-22 shows the comparison of the distribution for the residential sector given by Jones et al. (1996) with that obtained by using the default mapping for Tennessee in HAZUS (2000) and the different combination mappings in Table 3-15. The percentage of the Wood-Frame in the residential sector, as given by HAZUS (2000) for cases 2, 4 and 5 is close to that by Jones et al. (1996). However, even in Case 5, where almost all of the residential construction is assumed to be low-rise RES1, there is discrepancy in the percentages of Wood-Frame and Masonry buildings. One possible explanation is that the default structural-occupancy mapping given in HAZUS (2000) represents the average mapping for the whole of Tennessee, whereas the mapping in Jones et al. (1996) is for Memphis alone.

Emergency Response Occupancy Class

Figure 3-23 compares the mappings in HAZUS (2000), French et al. (2000) and Hwang et al. (1997b) for the GOV2 sector, which corresponds to emergency response facilities like police and fire stations. It can be seen that HAZUS (2000) and French et al. (2000) agree rather well, except for the unreinforced masonry category. Even though the percentage of steel buildings as given by the three studies is almost identical, Hwang et al. (1997b) differs with the other two studies in the mapping of the other structural classes. Differences in the estimates provided by HAZUS (2000), French et al. (2000) with Hwang et al. (1997b) could be caused by the fact that the former two studies give

average values for the whole of mid-America, while the latter study is primarily for the Shelby County.

Comments

These comparisons for the residential sector and the emergency response sector indicate that large uncertainties exist in the structural-occupancy mappings used in earthquake loss estimation. Uncertainties in the damage estimates associated with this variability are expected to be large. For example, if one uses the occupancy mapping values of Hwang et al. (1997b) and estimates the damage to the GOV2 sector one might get much higher damage estimates than when using the mapping of HAZUS (2000), due to the large proportion of URM buildings and smaller proportion of wood frame buildings in Hwang et al. (1997b).

Alternative structural-occupancy mappings

For use in earthquake loss estimation studies in the CEUS, two alternative structural-occupancy mappings are proposed here. These are essentially based on the default structural-occupancy mapping that is given in HAZUS (2000) for the mid-west and the combination mappings corresponding to Case 1 and Case 4 that are given in Table 3-15. Table 3-16 and Table 3-17 show the alternative structural-occupancy mappings. Equal weights could be given to these mappings for earthquake loss estimation studies that are applicable to CEUS.

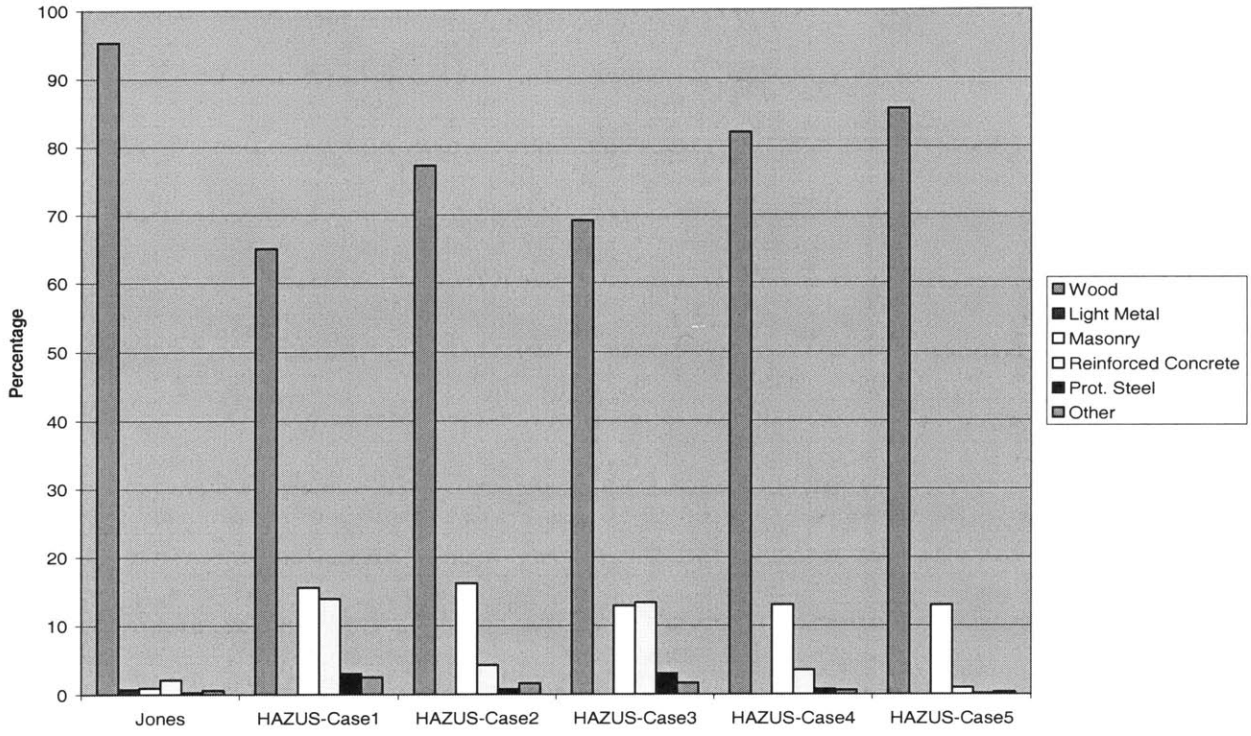

Figure 3-22: Comparison of Structural-Occupancy mapping in Jones et al. (1996) and HAZUS for the Residential Sector

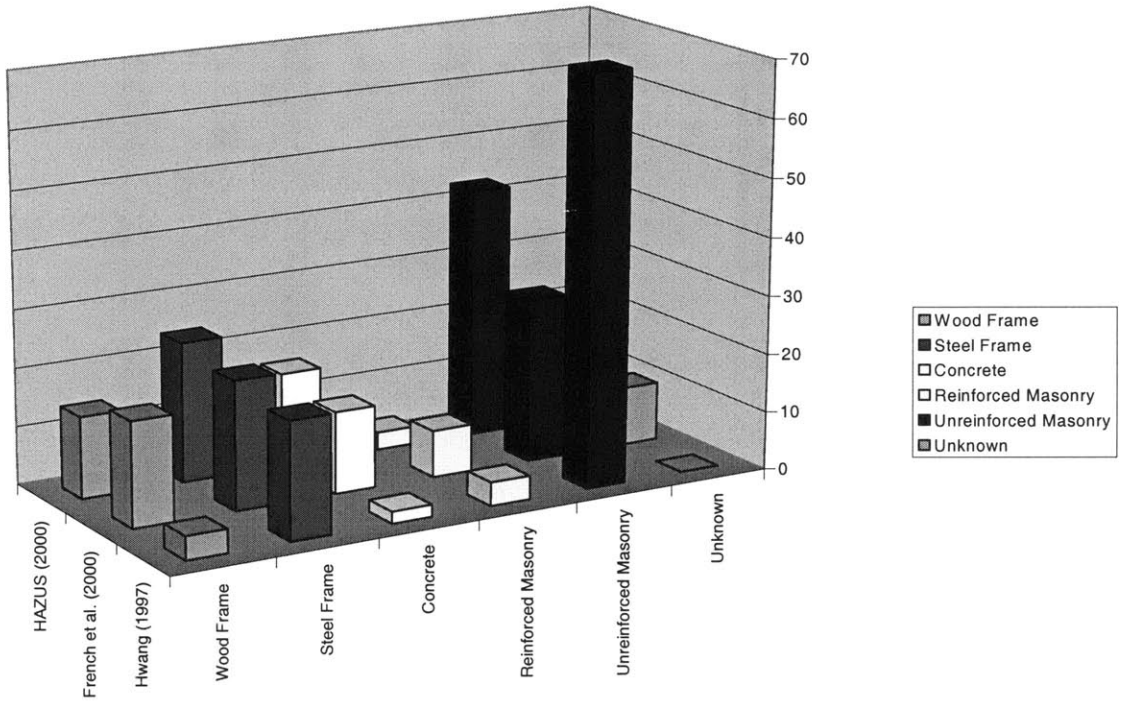

Figure 3-23: Comparison of the structural-occupancy mapping for the GOV2 sector

Structural Class	Residential	Commercial	Heavy Industry	Light Industry	Hi tech	Food & Drug	Chemical
W1	65	0	0	0	0	0	0
W2	0	18	0	9	9	9	9
S1L	0	3	5	2	2	2	2
S1M	0	1	0	0	0	0	0
S1H	0	0	0	0	0	0	0
S2L	0	5	10	4	4	4	4
S2M	1	3	0	1	1	1	1
S2H	0	1	0	0	0	0	0
S3	0	7	25	10	10	10	10
S4L	0	4	13	5	5	5	5
S4M	1	2	0	0	0	0	0
S4H	0	0	0	0	0	0	0
S5L	0	4	17	6	6	6	6
S5M	0	1	0	0	0	0	0
S5H	0	0	0	0	0	0	0
C1L	0	1	2	2	2	2	2
C1M	3	2	0	1	1	1	1
C1H	1	1	0	0	0	0	0
C2L	1	6	7	9	9	9	9
C2M	7	4	0	4	4	4	4
C2H	3	2	0	0	0	0	0
C3L	0	1	2	2	2	2	2
C3M	0	0	0	0	0	0	0
C3H	0	0	0	0	0	0	0
PC1	1	7	12	13	13	13	13
PC2L	0	1	2	2	2	2	2
PC2M	1	1	0	1	1	1	1
PC2H	0	0	0	0	0	0	0
RM1L	0	2	0	3	2	3	3
RM1M	0	0	0	0	0	0	0
RM2L	0	0	0	0	0	0	0
RM2M	0	0	0	0	0	0	0
RM2H	0	0	0	0	0	0	0
URML	13	22	5	24	25	24	24
URMM	2	2	0	3	3	3	3

Table 3-16: Proposed mapping for mid-America based on combined mapping of Case 1

Structural Class	Residential	Commercial	Heavy Industry	Light Industry	Hi tech	Food & Drug	Chemical
W1	82	0	0	0	0	0	0
W2	0	21	0	9	9	9	9
S1L	0	3	5	2	2	2	2
S1M	0	0	0	0	0	0	0
S1H	0	0	0	0	0	0	0
S2L	0	6	10	4	4	4	4
S2M	0	1	0	1	1	1	1
S2H	0	0	0	0	0	0	0
S3	0	8	25	10	10	10	10
S4L	0	5	13	5	5	5	5
S4M	0	0	0	0	0	0	0
S4H	0	0	0	0	0	0	0
S5L	0	5	17	6	6	6	6
S5M	0	0	0	0	0	0	0
S5H	0	0	0	0	0	0	0
C1L	0	2	2	2	2	2	2
C1M	1	0	0	1	1	1	1
C1H	0	0	0	0	0	0	0
C2L	0	7	7	9	9	9	9
C2M	2	1	0	4	4	4	4
C2H	1	0	0	0	0	0	0
C3L	0	1	2	2	2	2	2
C3M	0	0	0	0	0	0	0
C3H	0	0	0	0	0	0	0
PC1	0	9	12	13	13	13	13
PC2L	0	1	2	2	2	2	2
PC2M	0	0	0	1	1	1	1
PC2H	0	0	0	0	0	0	0
RM1L	0	2	0	3	2	3	3
RM1M	0	0	0	0	0	0	0
RM2L	0	0	0	0	0	0	0
RM2M	0	0	0	0	0	0	0
RM2H	0	0	0	0	0	0	0
URML	12	26	5	24	25	24	24
URMM	1	1	0	3	3	3	3

Table 3-17: Proposed mapping for mid-America based on combined mapping of Case 4

3.5 Bridge Fragility

Bridge fragility model is used to estimate the damage factor of bridges. Uncertainties exist in the bridge damage estimates given by the fragility models proposed in different data sources. The first part of this section has a description of the fragility models in three relevant studies and the second part has comparisons of the damage factors estimated by alternative bridge fragility models.

3.5.1 Review of data sources

The following section has a description of three references on bridge fragilities.

DesRoches (2002)

Fragility information for 6 bridge types is given by DesRoches (2002). Probability of exceedance of four damage states, viz., slight, moderate, extensive and complete, are given as a function of the Peak Ground Acceleration (PGA). Six bridge classes are considered based on the number of spans, the continuity at supports and the superstructure type material. Table 3-18 shows the different classes for which bridge fragility information is given by DesRoches (2002).

Hwang et al. (2000a)

Hwang et al. (2000a) provide fragility information for highway bridges in Shelby County, Tennessee. They use a bridge classification that is primarily based on the National Bridge Inventory classification. They also include the pier (bent) information of each bridge in their classification. The NBI/FHWA recording and coding guide classifies the superstructure type and material using a three digit code. For example, "202" refers to a

Class Identifier	Description of the bridge class
MSSS-S	Multi-span simply supported Steel
MSSS-C	Multi-span simply supported Concrete
MSC-S	Multi-span continuous Steel
MSC-C	Multi-span continuous Concrete
SS-S	Single Span Steel
SS-C	Single Span Concrete

Table 3-18: Description of the bridge classes used in DesRoches (2002)

multiple span continuous concrete girders. Hwang et al. (2000a), in addition, use a two digit code to identify the bent material. For example, according to them a bridge type 202-11 corresponds to a bridge with multiple span continuous concrete girders (202) supported by concrete multi column bents (11).

HAZUS (2000)

HAZUS (2000) provides fragility information for 28 bridge types, classified based on NBI category, location (California or outside California), year built and the maximum span. They provide damage functions separately for ground shaking and ground failure. The fragility curves for ground shaking are based on the probability of exceedance of four damage states viz., slight, moderate, extensive and complete. These are given as a function of Sa-1sec. Table 3-19 shows the nomenclature used in HAZUS and the corresponding NBI categories for non-California bridges.

NBI Material Class	Length	Conventional(<1990)	Seismic(>1990)
1		HWB5	HWB7
2		HWB10	HWB11
3	>20m	HWB12	HWB14
4	>20m	HWB15	HWB16
5		HWB17	HWB19
6		HWB22	HWB23
3	<20m	HWB24	
4	<20m	HWB26	

Table 3-19: Bridge Classification used in HAZUS (2000) for non-California bridges

3.5.2 Comparison of bridge fragility models

In order to compare the bridge damages predicted by different studies, a mapping needs to be made between the classifications used therein. This is done by using the NBI classification as a reference. Table 3-20 shows our mapping of the NBI material class to the classes used in different studies.

NBI Bridge Material Class	Description of the Bridge type	DesRoches' Class	Hwang's Class	HAZUS Bridge Class
1	Multi-span simply supported Concrete	MSSS-C	4	HWB5,HWB7
2	Multi-span continuous Concrete	MSC-C	5	HWB10,HWB11
3	Multi-span simply supported Steel	MSSS-S	1	HWB12,HWB14
4	Multi-span continuous Steel	MSC-S	3	HWB15,HWB16, HWB26
5	Multi-span simply supported Prestressed Concrete	MSSS-C	4	HWB17,HWB19
6	Multi-span continuous Prestressed Concrete	MSC-C	5	HWB22,HWB23

Table 3-20: Mapping to relate the NBI material classes with the classes used in different studies

Since the fragility information in DesRoches (2002) and Hwang et al. (2000a) is in terms of PGA and that in HAZUS (2000) is in terms of Sa-1sec, comparisons between the bridge fragilities given in the different data sources is done in the following manner. Bridges of a certain class (based on the NBI material classification) are assumed to be located at certain distances from the epicenter on a site which corresponds to the NEHRP site class A. By using the PGA and Sa-1sec values predicted by the attenuation relationship of Toro and Silva (2001), damage to each bridge is estimated as a function of the distance from the epicenter, for an earthquake magnitude of $8m_b$. Figure 3-24 shows the comparison of the estimated damage as a function of the distance for NBI bridge material class 2 and Figure 3-25 shows similar comparisons for a NBI bridge material class 3. It can be seen that there are large differences in the damage estimates given by different studies. Damage estimates from HAZUS (2000) are much below the estimates by Hwang et al. (2000a) and DesRoches (2002).

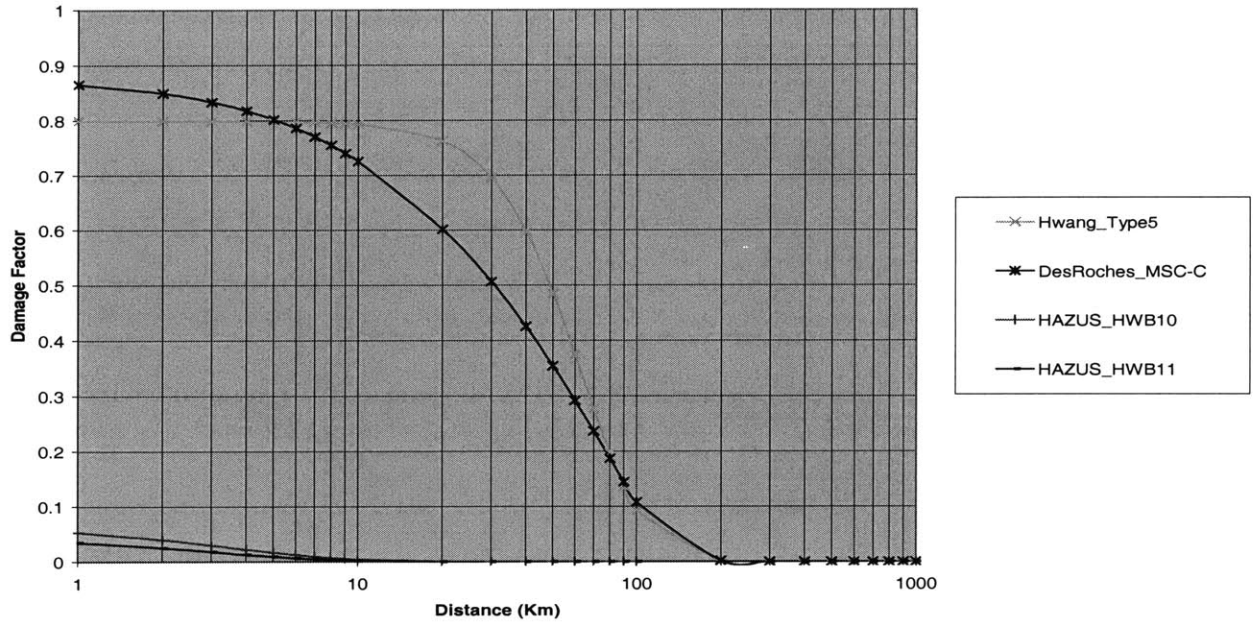

Figure 3-24: Comparison of the attenuation of damage of a bridge of NBI material class 2

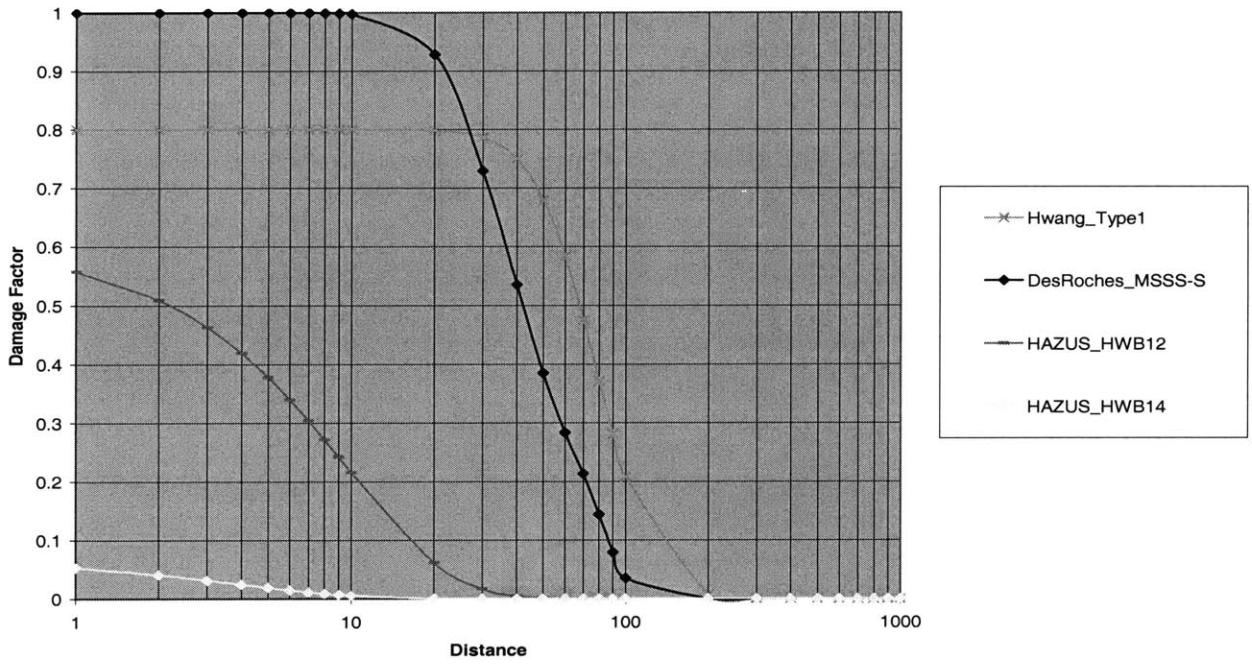

Figure 3-25: Comparison of the attenuation of damage of a bridge of NBI material class 3

Comments

A similar trend has been found from comparisons made to other bridge categories (Karaca (2002)) and by using alternative attenuation relationships. To account for the epistemic uncertainty, we assign weights of 0.4, 0.4, 0.2 to the fragility data given in Hwang et al. (2000a), DesRoches (2002) and HAZUS (2000) respectively, for use in earthquake loss estimation studies for CEUS. HAZUS (2000) provides fragility information for non-California bridges, but does not provide bridge fragility data explicitly for the CEUS. Therefore, we give a lower weight to HAZUS (2000).

3.6 Loss of Functionality and Recovery

Due to earthquake damage, a facility may lose all or part of its functionality. The extent of this loss depends on the amount of structural, non-structural and contents damage. Indirect causes of loss of functionality are the damage to lifelines serving the facility and casualties. As time progresses, the initial functionality is recovered as the facility is repaired. The rate at which functionality is restored may further depend on the rate of recovery of the lifelines serving the facility and the availability of human resources on which the operation of the facility depends.

For the estimation of losses from business interruption, also referred to as Time Element (*TE*) losses, one needs to accurately model the initial loss of functionality and the recovery process. Unfortunately, there is much uncertainty on these processes, due to the lack of statistical data from past earthquakes.

Next we present the loss of functionality and recovery-interaction models that have been given in the literature.

3.6.1 Review of data sources

ATC-13, RMS (1994) and Kunnumkal (2001) have proposed models for loss of function and recovery as a function of initial damage and social function class. A brief description of these models is given below.

ATC-13

This study gives the time to 30%, 60% and 100% recovery of functionality for different social function classes as a function of 7 damage states after an earthquake. These estimates have been obtained based on expert opinion. ATC-13 gives the minimum, mean, maximum and standard deviation of the time to recover to 30%, 60% and 100% functionality. These times are denoted respectively by TE_{30}, TE_{60} and TE_{100}. The estimates are based on the assumption that the reconstruction and repair follow non-emergency schedules and that unlimited resources are available for reconstruction.

In addition to the TE losses, ATC-13 provides models and parameters for the dependence of the functionalities of various occupancy classes on the functionalities of various lifelines. ATC-13 does so by giving "importance" factors that indicate the dependence of the social function class on 11 different lifelines. The lifelines considered are water supply, waste water, electric power, natural gas, petroleum fuel, highway transportation, railway transportation, air transportation, sea/water transportation, telephone, radio & T.V.

In ATC-13, the functionality of a social function class i at time t, $F^{i}_{actual}(t)$, is expressed as

$$F^{i}_{actual}(t) = F^{i}_{physical}(t) * F^{lifelines}_{actual}(t) \tag{3-55}$$

where

$$F^{lifelines}_{actual}(t) = \frac{F^{main}_{actual}(t) + F^{distribution}_{actual}(t)}{2} \tag{3-56}$$

$$F^{main}_{actual}(t) = \frac{\sum_{j} IF_{i}^{j,main} * F^{j,main}_{actual}(t)}{n_{main}} \tag{3-57}$$

where

$F^{i}_{physical}(t)$ - Functionality of facility class i at time t, based exclusively on its damage level.

$F^{i}_{actual}(t)$ - Actual functionality of the facility class i at time t.

$F_{actual}^{lifelines}(t)$ - Average functionality of the "main" and "distribution" lifelines affecting the facility at time t. In case of electric power lifeline systems, for example, the "main" components include the generating facilities and the "distribution" components include the distribution lines and distribution sub-stations.

$F_{actual}^{main}(t)$ - Average functionality of the "main" lifelines that affect a social function class at time t.

$IF_i^{j,main}$ - Importance factor of j^{th} main lifeline for social function class i.

$F_{actual}^{j,main}(t)$ - Actual functionality of the j^{th} main component lifeline at time t.

$F_{actual}^{distribution}(t)$ - Average functionality of the "distribution" lifelines that affect a social function class at time t, calculated in a similar manner as $F_{actual}^{main}(t)$.

n_{main} –Number of "main" lifelines that affect the social function class.

One drawback of equations (3-55), (3-56) and (3-57) is the dependence on the importance factors, *IF*. An importance factor of 1 would mean that the social function class is fully dependent on the lifeline and a value of 0 would mean that the functionality of the social class is independent of the functionality of the lifeline. If none of the lifelines affect a social function class, then $F_{actual}^{distribution}(t)$ and $F_{actual}^{main}(t)$ would be zero, resulting in $F_{actual}^{i}(t)$ to be zero, irrespective of the physical functionality of the social function class. This is a contradiction. Moreover, the definition of n_{main} that is used in equation (3-57) is unclear. For instance, if there are 10 'main' lifelines that affect the functionality of a function class and the importance factors associated with 9 of these lifelines are 0.0001 each, and the importance factor associated with the 10th lifeline is 0.99, ambiguity arises regarding the value of n_{main} that needs to be used in equation (3-57) (n_{main} could be either 10 or 1).

RMS (1994)

RMS (1994) estimates the *TE* losses for four damage states. This study distinguishes between the time needed for building re-construction and clean-up, *BCT(DF)*, and the time for business recovery, *TE(DF)*. The business recovery time, *TE(DF)*, is the time period during which the business is not operational. It is estimated to be shorter than the

time needed to repair and reconstruct the damaged facility. The reason is that, after a moderate earthquake, businesses can relocate or find temporary means of operation. RMS (1994) provides the median repair times, but does not provide a measure of uncertainty on these repair times. Specifically, the business recovery time, *TE(DF)*, is expressed as a function of the business clean up time, *BCT(DF)*, as

$$TE(DF)=BCT(DF)*MF \tag{3-58}$$

where

MF is a modification factor between 0 and 1.

Figure 3-26 compares the time element (TE) losses as a function of initial damage as predicted by ATC-13 and RMS (1994). The RMS (1994) values shown in the figure do not consider the modification factors. The TE losses for ATC-13 are calculated as

$$\overline{TE} = 0.375\overline{TE}_{30} + 0.35\overline{TE}_{60} + 0.2\overline{TE}_{100} \tag{3-59}$$

The above relation assumes that no restoration occurs before $\overline{TE}_{30}/2$ and that at any point of time, the percentage of restoration is given through linear interpolation between the points (0,0%), ($\overline{TE}_{30}/2$,0%), ($\overline{TE}_{30}$,30%),($\overline{TE}_{60}$,60%) and ($\overline{TE}_{100}$,100%). Figure 3-26 shows that the TE losses in the two studies are generally consistent (if one excludes the modification factor in the RMS model).

Kunnumkal (2001)

Kunnumkal (2001) developed models to estimate the loss of functionality and recovery of various social function (occupancy) classes. The models are mainly based on ATC-13, augmented with data from RMS (1994).

The model for recovery of functionality (without considering interactions with other social function classes) has the form

$$F_{physical}(t) = at^b + c(D) \qquad 0 \le F_{physical}(t) \le 1 \tag{3-60}$$

where

$F_{physical}(t)$ is the functionality of a facility as a function of time, t, after the earthquake, based only on its current damage state.

a ,b are parameters, which control the rate of recovery of a function class.

$c(D)$ is a parameter that depends on the initial structural damage, D, as

$$c(D) = c_0 * D + c_1 + c_2 / D \tag{3-61}$$

The parameters a, b, c_0, c_1 and c_2 are estimated from data in ATC-13, except for conventional bridges, for which estimates in Hwang et al. (2000b) are used.

Kunnumkal (2001) also estimates uncertainties in the initial loss of functionality and recovery parameters. The variance of TE for each occupancy class is calculated as

$$VAR(TE) = \begin{array}{l}(0.375)^2 VAR(TE_{30}) + (0.35)^2 VAR(TE_{60}) + (0.2)^2 VAR(TE_{100}) + \\ 2(0.375)(0.35)\rho_{30,60} + 2(0.35)(0.2)\rho_{60,100} + 2(0.375)(0.2)\rho_{30,100}\end{array} \tag{3-62}$$

where

$VAR(TE_{30})$, $VAR(TE_{60})$, $VAR(TE_{100})$ are the variances of the times to 30%, 60% and 100% functionalities respectively, which are given in ATC-13 for each damage state and occupancy class. The correlation coefficients $\rho_{30,60}$, $\rho_{60,100}$ and $\rho_{30,100}$ are estimated by using the times to 30%, 60% and 100% functionality of different damage states. These correlation coefficients are found to be within a range of 0.9 to 1.

By assuming that a in equation (3-60) is the only uncertain parameter, Kunnumkal (2001) uses the variance of TE in equation (3-62) to calculate the variance of a. Table 3-21 shows best estimates of the parameters and the standard deviation of a.

Kunnumkal (2001) calculates the initial functionality by assuming that this quantity depends only on structural damage and not also on non-structural and contents damage. In reality, even if the structural damage is small, damage to the non-structural components or contents could cause significant loss in functionality. The existing literature lacks information on the relative importance of the different types of damage. Thus uncertainty exists in how to consider structural, non-structural and contents damage to assess the total functionality of a facility. A sensitivity analysis using different weights will be provided in Chapter 4.

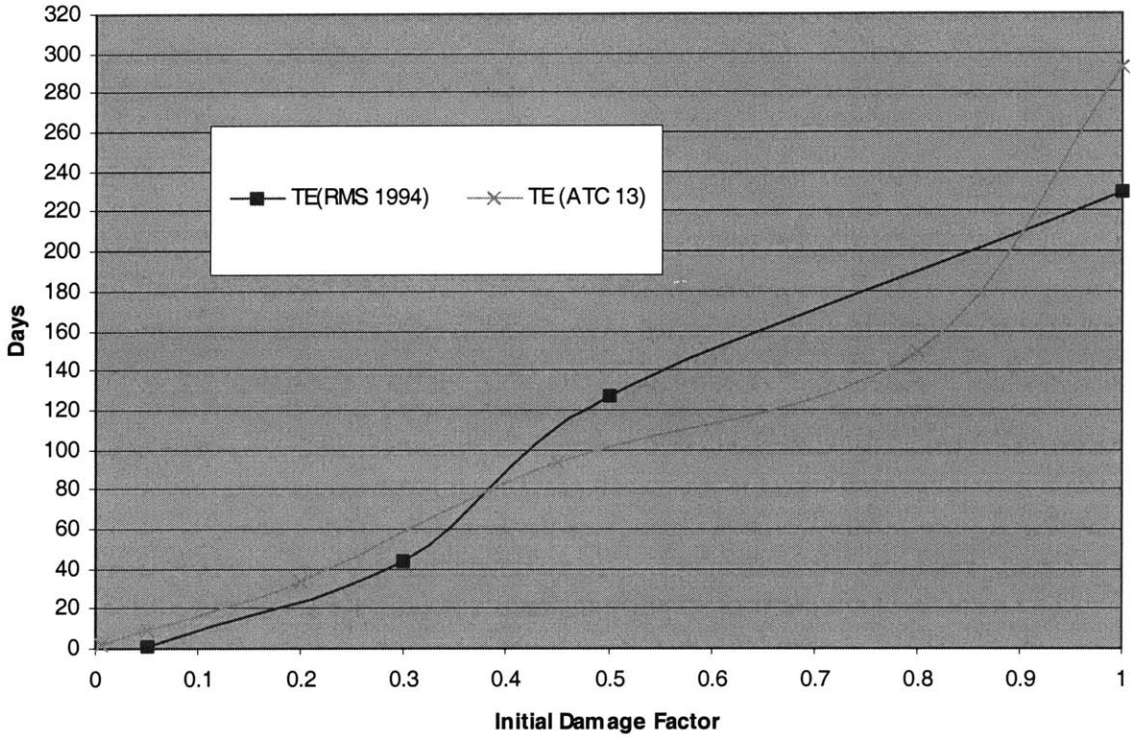

Figure 3-26: Comparison of the Time Element Losses, as given by ATC-13 and RMS (1994)

Function Class	a	b	c0	c1	c2	SD(a)*
Residential	1.3	0.2	-0.707	-2.88	0.173	0.062
Commercial	4	0.1	-2.055	-4.694	0.252	0.09
Heavy Industry	0.6	0.25	-0.881	-1.293	0.079	0.036
Light Industry	0.6	0.25	-0.881	-1.293	0.079	0.036
High Technology	1	0.25	-1.793	-2.488	0.066	0.059
Food and Drug	0.55	0.3	-1.415	-1.374	0.061	0.039
Chemical	1.27	0.2	-1.39	-2.362	0.067	0.06
Lifelines	4.5	0.1	-1.05	-5.562	0.086	0.11
Highway pavement	5.5	0.1	-2.416	-6.886	0.05	0.13
Major-Bridges	0.32	0.4	-1.836	-1.816	0.005	0.016
Conventional-Bridges	1.6	0.22	-2.013	-1.991	0.005	0.08

* Standard Deviation of the parameter 'a'

Table 3-21: Recovery and Loss of functionality parameters given by Kunnumkal (2001)

Kunnumkal (2001) also provides models for how the functionality of a social function class depends on the functionality of lifelines and the residential sector. He considers two alternative forms of the functionality interaction model, a linear/additive model and a non-linear multiplicative model. The linear model is a modified version of the ATC-13 model. Kunnumkal (2001) compares the two formulations and concludes that non-linear model is superior to the linear model. The two models are reviewed next.

Linear/Additive Model

The linear/additive model of Kunnumkal (2001) is a modified version of the interaction model given in ATC-13. Following are the conceptual differences between the linear model in Kunnumkal (2001) and the one given in ATC-13:

- Both the functionality and the recovery rate of a social function class are assumed to be influenced by the functionality of the lifelines in Kunnumkal (2001). ATC-13, on the other hand, does not explicitly model the dependence of the recovery rate of a social function class on the functionality of the lifelines.
- In ATC-13, if a social function class does not depend on any of the lifelines, the actual functionality of the function class goes to zero, even though the facility may have a non-zero physical functionality (as was discussed earlier). This deficiency is corrected by Kunnumkal (2001).

In the linear/additive model of Kunnumkal (2001), the functionality of a social function class is calculated as

$$F^i_{actual}(t) = F^i_{physical}(t) * RF^i_1(t) \tag{3-63}$$

$$\frac{dF^i_{physical}(t)}{dt} = g_i(F^i_{physical}(t))\Big|_{\max, F^i_{physical}(t)} * RF^i_2(t) \tag{3-64}$$

$$RF^i_1(t) = 1 - \frac{\sum_{j \neq i} \gamma_{ji\_sum}(1 - F^j_{actual}(t))}{n} \tag{3-65}$$

$$RF^i_2(t) = 1 - \frac{\sum_{j \neq i} \beta_{ji\_sum}(1 - F^j_{actual}(t))}{n} \tag{3-66}$$

where

$g_i(F^i_{physical}(t))$ - The maximum possible recovery rate of social function class i when the physical functionality (the functionality based exclusively on the current damage state) is $F^i_{physical}(t)$.

$\frac{dF^i_{physical}(t)}{dt}$ - The rate of recovery of class i taking into account the functionality of other classes at time t.

$RF^i_1(t)$ - A factor that reflects the effect of the functionality of other classes on the functionality of class i at time t.

$RF^i_2(t)$ - A factor that reflects the effect of the functionality of other classes on the recovery of class i at time t.

γ_{ji_sum} - An interaction coefficient that gives the effect of the functionality of class j on the functionality of class i.

β_{ji_sum} - An interaction coefficient that gives the effect of the functionality of class j on the recovery rate of class i.

n - The number of interacting classes.

In equation (3-65), if $\gamma_{ji\_sum} = 0$ for all the occupancy classes, then $RF^i_1(t) = 1$. In this case, the actual functionality of class i equals its physical functionality. Greater values of γ_{ji_sum} mean greater interaction among the classes, resulting in a greater decrease in functionality.

The linear model in equations (3-63) to (3-66) underestimates the indirect economic losses, because of its averaging effect. For example, assume that a certain economic sector is completely dependent on electric power and the intra-nodal transportation network, i.e., the γ coefficients corresponding to these two lifelines are equal to 1. Suppose the electric power is fully disrupted, but no loss of functionality is incurred by the transportation system. Then, $RF_1 = 1 - \frac{1*(1-0)+1*(1-1)}{1+1} = 1/2$, when in reality one expects RF_1 to be zero because the economic sector is fully dysfunctional without electric

power. Similarly, if there are many sectors with a small influence on the sector of interest, then the additive model grossly under-predicts the reduction in functionality. For example, suppose that there are three lifelines that affect the functionality of an industrial sector. Let γ's corresponding to lifeline1 and lifeline2 be both equal to 0.001 and that for lifeline3 is 1. Hence the industrial sector is fully dependent on lifeline3, but is very little dependent on lifeline1 and lifeline2. Let the functionalities of lifeline1 and lifeline2 be 50% and that of lifeline3 be 1%. Then

$$RF_1 = 1 - \frac{0.01*(1-0.5)+0.01*(1-0.5)+1*(1-0.01)}{1+1+1} = 1-(1/3) \approx 0.66$$

In reality, RF_1 should be close to 0 because of the greater dependence on lifeline3 than on the other two lifelines. These deficiencies of the linear model are corrected by using the following non-linear model.

Non-Linear/Multiplicative Model

In this model, the actual functionality and the rate of recovery are modeled by equations (3-63) and (3-64), but the reduction factors are modeled as

$$RF_1^i(t) = \prod_j (F_{actual}^j(t))^{\gamma_{ji\_prod}} \quad \textbf{(3-67)}$$

$$RF_2^i(t) = \prod_j (F_{actual}^j(t))^{\beta_{ji\_prod}} \quad \textbf{(3-68)}$$

where

γ_{ji_prod} - An interaction coefficient that gives the effect of the functionality of class j on the functionality of class i.

β_{ji_prod} - An interaction coefficient that gives the effect of the functionality of class j on the recovery rate of class i.

The nonlinear model calculates the reduction factors as the product of the functionalities of the affecting lifelines, raised to different powers. This means that if any of the interacting lifelines of an economic sector have zero functionality, then the sector's functionality drops down to zero. In this way, the non-linear model behaves as a series system. Unlike the additive model, the multiplicative model represents correctly the case

of a large number of sectors that influence a given sector in a very small manner. In the example with three lifelines that was considered earlier, the value of RF_1 in the non-linear model is $RF_1 = (0.5)^{0.01}(0.5)^{0.01}(0.01)^1 \approx 0.01$. This value is much more reasonable than that predicted by the additive model.

3.6.2 Interaction coefficients

ATC-13 provides the importance factors, IF_i^j, for the dependence of the functionality of social function class i on functionality of lifeline j. Importance factors for the transportation and electric power are reproduced in Table 3-22.

The interaction coefficients, γ_{ji_sum}, β_{ji_sum}, γ_{ji_prod}, β_{ji_prod}, used in the revised linear and nonlinear models of Kunnumkal (2001), are judgmentally set to values shown in Table 3-23 and Table 3-24. These values are primarily based on the importance factors given in ATC-13. The basis for assigning these values is that the functionality of the utilities should have a greater effect on the functionalities of the social function classes than on their recovery rates. The opposite should be true for the transportation system. This is reflected in the higher values of β compared to γ in the case of transportation. Since the residential sector is expected to affect both the functionality and the recovery rate, β and γ coefficients for the residential sector have similar values.

The following example shows the sensitivities of the recovery of an industrial sector to using Kunnumkal's (2001) linear or non-linear interaction models.

Example

Consider the recovery of the Heavy Industry (HI) sector after an earthquake that causes a 50% damage to the Heavy Industry, Residential, Transportation and Lifelines. Four different cases are considered with different combinations of the γ and β coefficients.

Case 1

Let the interaction coefficients be such that the functionality of the HI sector depends on the functionality of the Residential sector as well as Transportation and Utilities. The

corresponding γ's are given in Table 3-25. It is assumed that the rate of recovery of the HI sector is independent of the functionalities of other sectors, i.e., the corresponding β's are zeroes. Figure 3-27 shows the functionality recovery curve of the different sectors considered.

Comments

- As the utilities become almost fully functional by the time HI starts to recover from zero functionality, there is not much effect of the functionality of the lifelines on the actual functionality of the HI sector.
- After 240 days, when all of the three sectors on which the functionality of HI depends become fully functional, the physical and actual functionality curves for the HI sector merge.
- The linear/additive interaction model results in slightly higher functionalities than the nonlinear/multiplicative interaction model.

Case 2

Same as Case 1, but all the γ coefficients are 1. Figure 3-28 shows the associated functionality recovery curves.

Comments

- As the functionality of the HI sector is fully dependent on all the three remaining sectors, the TE losses are much larger than for Case 1.
- As in Case 1, the actual and physical functionalities are same after 240 days.

Case 3

We may assume the β coefficients shown in Table 3-26 and set all the γ coefficients to zero. Figure 3-29 shows the corresponding functionality recovery curves.

Case 4

In this final case, we let all the β coefficients to one and all the γ coefficients to zero. Figure 3-30 has the resulting curves.

Comments

- As the rate of recovery of the HI sector is fully dependent on the three remaining sectors, the TE losses in Case 4 are much larger than in Case 3.

	Power	Transportation
Residential	0.5	0.6
Commercial	0.45	0.85
Heavy Industry	1	0.9
Light Industry	1	1
Food and Drug	0.9	1
Chemical	0.9	1
High Technology	1	1

Table 3-22: Importance factors given in ATC-13 for electric power and transportation

	Residential Sector	Utilities (Electric Power)	Transportation
Residential		0.5	0.3
Commercial	0.6	0.45	0.4
Heavy Industry	0.3	1	0.3
Light Industry	0.3	1	0.3
Food and Drug	0.3	1	0.3
Chemical	0.3	0.9	0.3
High Technology	0.6	0.9	0.3

Table 3-23: γ 's – Effect of functionality of residential, utilities and transportation on the functionality of other classes, used in both the linear and nonlinear interaction models (Kunnumkal 2001)

	Residential Sector	Utilities (Electric Power)	Transportation
Residential		0.1	0.6
Commercial	0.5	0.3	0.9
Heavy Industry	0.5	0.3	0.9
Light Industry	0.5	0.3	1
Food and Drug	0.5	0.3	1
Chemical	0.5	0.3	1
High Technology	0.5	0.3	1

Table 3-24: β 's – Effect of functionality of residential, utilities and transportation on the rate of recovery of other classes, used in both the linear and nonlinear interaction models (Kunnumkal 2001)

	Residential	Utilities	Transportation
Heavy Industry	0.3	1	0.3

Table 3-25: γ 's for the dependence of the functionality of HI on the functionality of other classes

	Residential	Utilities	Transportation
Heavy Industry	0.3	1	0.3

Table 3-26: β 's for the dependence of the recovery rate of HI on the functionality of other classes

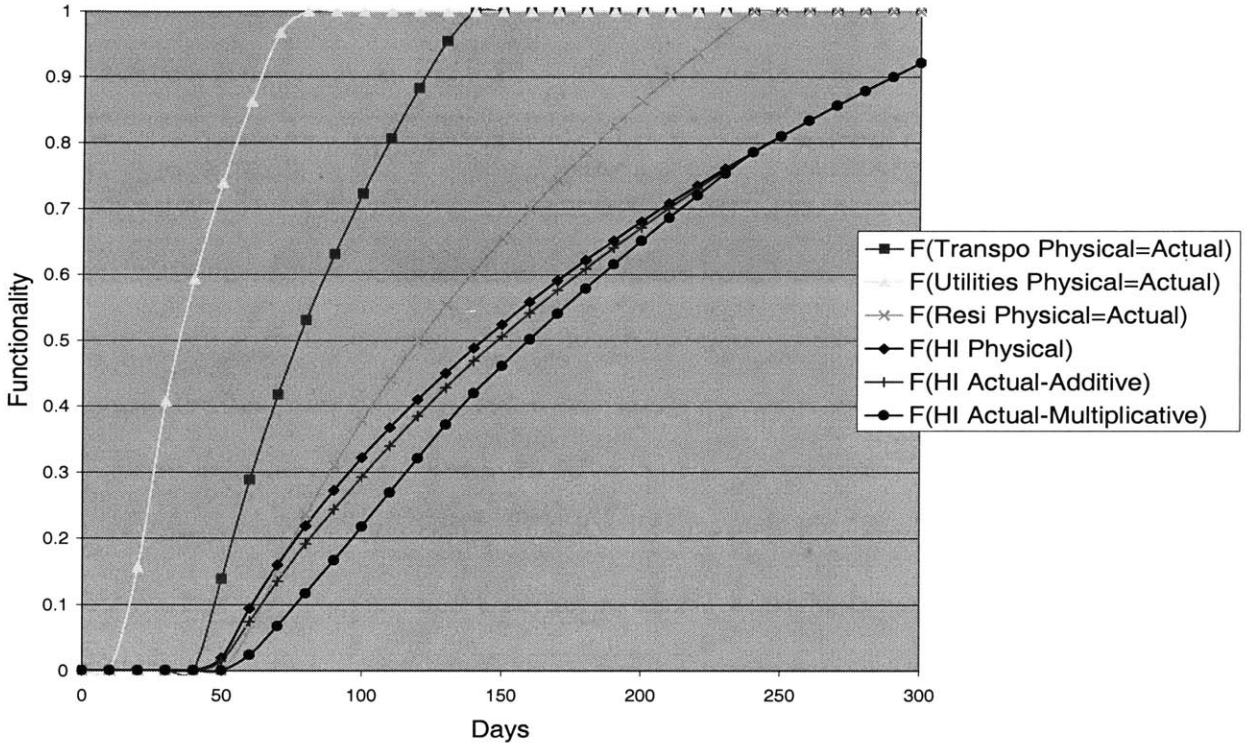

Figure 3-27: Functionality dependence of HI sector on lifelines and residential sector (assuming no dependence for the rate of recovery), Case 1

In Figure 3-27,

- **F(Transpo Physical =Actual)** is the physical functionality of the Transportation sector as a function of time, which is also the actual functionality as this sector does not depend on any other sector.
- **F(Utilities Physical =Actual), F(Resi Physical =Actual)** are the functionality curves for the Utilities (Electric Power) and Residential sectors respectively. As both these sectors do not depend on any other sectors, their actual functionalities are equal to their physical functionalities.
- **F(HI Physical)** is the physical functionality curve of the Heavy Industry sector as a function of the time after the earthquake.
- **F(HI Actual-Additive)** is the actual functionality curve of the Heavy Industry sector when the linear/additive interaction model is used.
- **F(HI Actual-Multiplicative)** is the actual functionality curve of the Heavy Industry sector when the multiplicative interaction model is used.

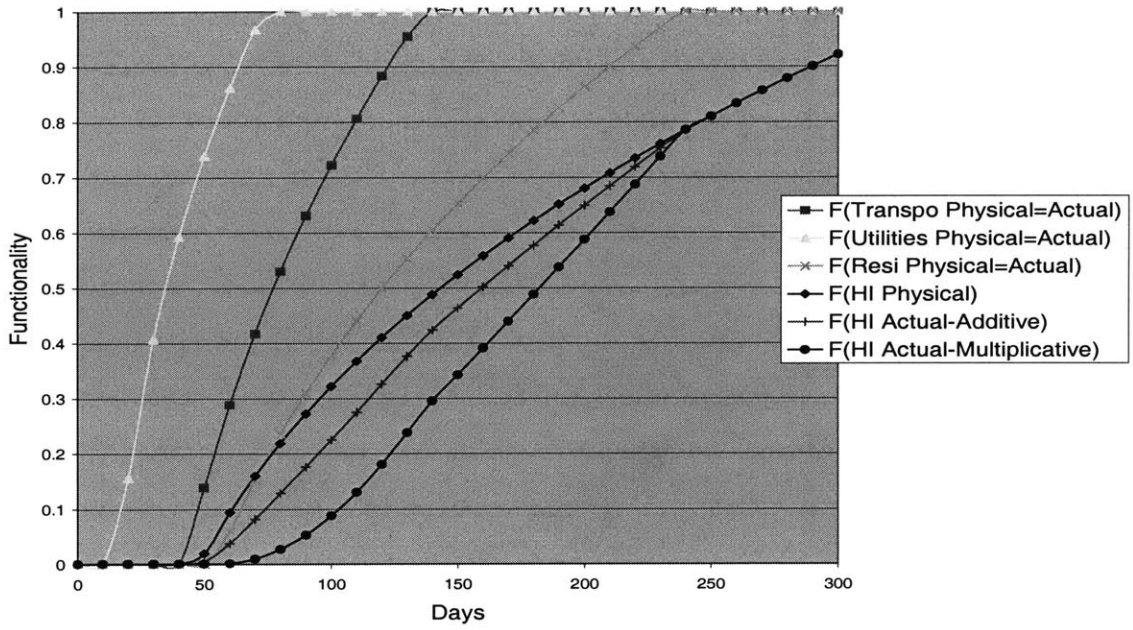

Figure 3-28: Functionality dependence of HI sector on lifelines and residential sector (assuming no dependence for the rate of recovery), Case 2

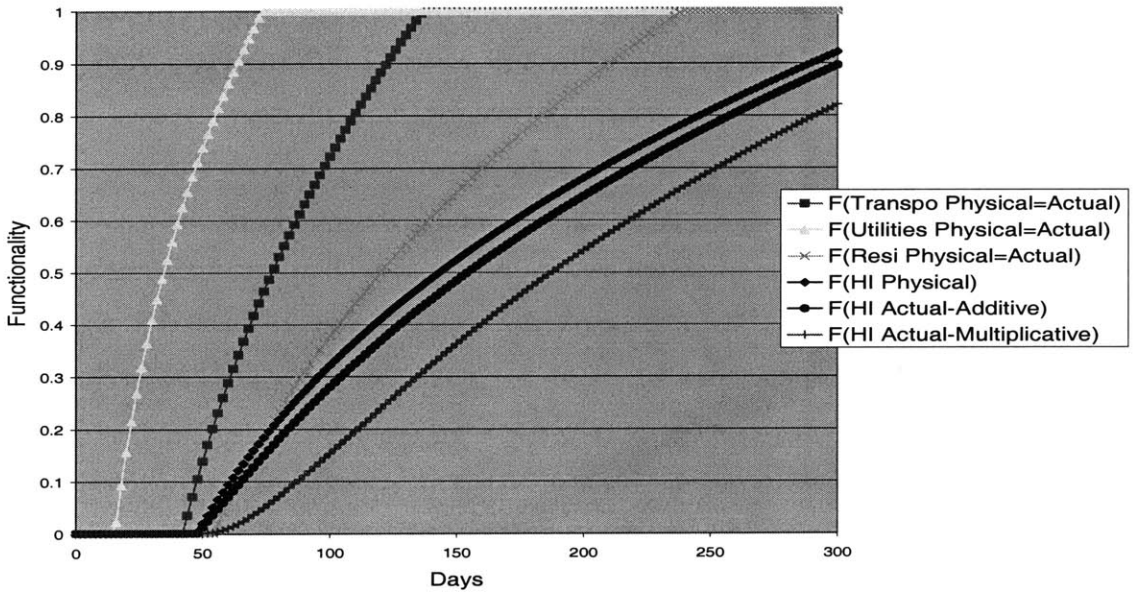

Figure 3-29: Recovery of HI sector with functionalities of other sectors affecting HI's rate of recovery alone (functionality is assumed to be independent), Case 3

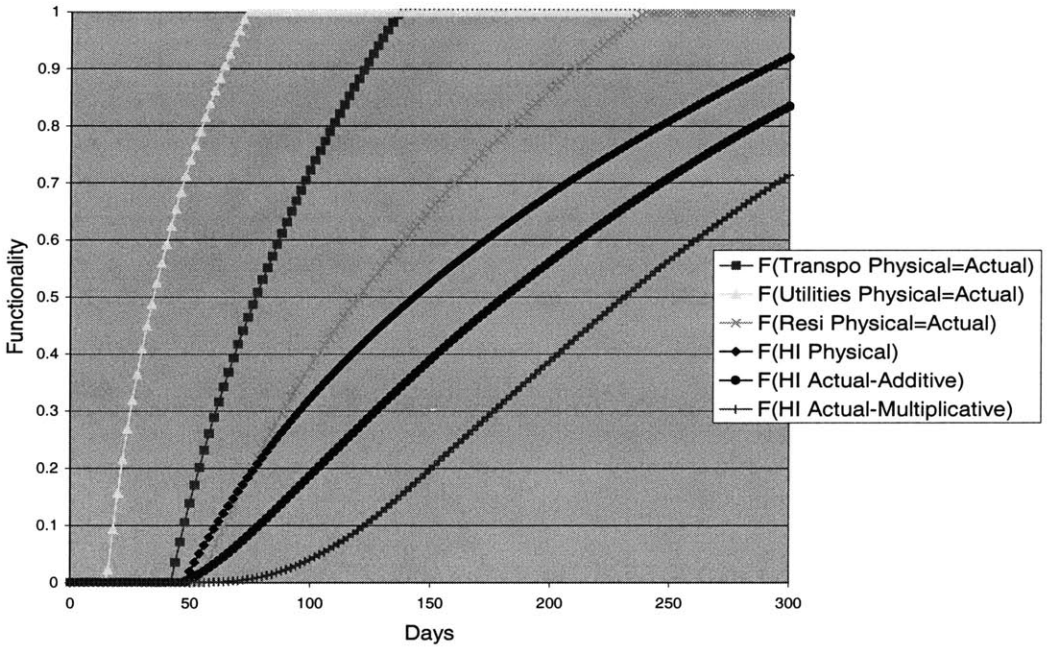

Figure 3-30: Recovery of HI sector with functionalities of other sectors affecting HI's rate of recovery alone (functionality is assumed to be independent), Case 4

- As in Case 3, the slope of the physical and actual functionality recovery curves in Case 4 remains the same after 240 days because all the sectors on which HI depends become fully functional.

In this chapter, we have assessed the uncertainties in the earthquake ground motion/intensity attenuation, site amplification, building inventory and fragility, bridge fragility and loss of function and recovery of occupancy classes. However, we did not consider uncertainties in transportation network flow parameters and economic parameters relevant for loss estimation. In the next chapter, we perform sensitivity analysis by including the uncertainties in the components discussed in this chapter and on some of the transportation network flow parameters and economic parameters.

4 Sensitivity Analysis

In this chapter, we look at the sensitivity of the losses obtained by using the methodology of Kunnumkal (2002) to alternative models and parameters in various components of loss estimation that were discussed in Chapter 3. In addition, we also look at the sensitivity of the losses to some of the highway network and economic parameters.

4.1 Framework for Sensitivity Analysis

In this section, we illustrate the methodology employed to perform the sensitivity analysis that would be discussed later.

The objectives here are to perform sensitivity studies to, (a) identify those factors that have the greatest impact on earthquake losses, (b) get some sense of the extent of uncertainty in the losses. We try to achieve these objectives by devising studies in the following manner:

- For some of the components of loss estimation, alternative models are proposed by various authors. We test the sensitivities of the losses by incorporating each of these models into the methodology. However, the alternative models considered are those that, we feel, are reasonably accurate for application, with our present state of knowledge, in the CEUS. For example, in order to study the sensitivity of the losses to the use of alternative ground motion attenuation relationships, we only consider the attenuation relations by Atkinson and Boore (1995), Toro et al. (1997) and Frankel et al. (1996), which are given non-zero weights (as shown in Section 3.2.2).
- We test the sensitivity to some of the uncertain parameters by comparing the losses at their average values with the losses when the parameters are increased or decreased by one standard deviation. This would give a sense of uncertainty on the final losses. For example, we compare the losses obtained when we increase the value of the expected mean resistance of all the seismic vulnerability classes by one standard deviation with the losses when using the nominal expected mean

resistance values (assuming that the fragilities of all the structural classes are positively correlated).

- For some of the parameters, the level of uncertainty may be so high that we may not be able to quantify the associated uncertainty (for example, we may not know the parameters of their probability distribution due to complete lack of statistical information). One such parameter is the re-routing parameter (ρ), used in Kunnumkal (2002) to model the effect of secondary roads in the transportation network. The influence of this parameter on the losses is tested by giving it a set of values that it can possibly take.
- Some of the sensitivity runs are made to rank the factors according to their influence on the losses. For example, (a) in order to understand the importance of the damage of various structural classes, we change the expected mean resistance of the structural classes, one at a time, by 5% (b) in order to identify the social function classes that influence the indirect losses the most, we change the times to recovery of the social function classes, one at a time, by 50%.
- In some cases, sensitivity of the losses to changing parameter p could depend on the value that another parameter, say q, takes. We also try to get a sense of such two-way interactions between some of the models and parameters. For example, the sensitivity to the re-routing parameter is tested at alternative conditions of the highway network damage.

Table 4-1 shows the parameters and models used for the sensitivity studies done in this chapter. In the table, items that are highlighted are used as default models/parameters.

Specifically, we do the following:

- We compare the losses given by the macroseismic and the engineering approaches. We do these comparisons for the following cases:
    - With 5% slack in production capacity, we employ alternative production loss evaluation methods, viz.,

        - *Production Loss Method 1*: The production loss calculation that does not include the increased productions due to the slack in the production capacity. This corresponds to equation (2-22).
        - *Production Loss Method 2*: The production loss evaluation that considers the increased productions due to the slack in the production capacity. This corresponds to equation (2-23).
    - No slack in production capacity.
- We study the sensitivities of the losses to alternative engineering attenuation relationships and site amplification models. These comparisons are made when using alternative production loss evaluation methods.
- For both the engineering and macroseismic approaches, we study
    - Sensitivity to alternative structural-occupancy mappings.
    - Sensitivity by changing the expected mean resistance of different building classes, considering one class at a time. For example, the sensitivity to a 5% change in the mean resistance of all buildings that are wood-frame.
    - Sensitivity by changing the fragility parameters (expected mean resistance and building to building variability in the mean resistance) of all building classes by a fixed amount. For example, the expected mean resistance of all the building classes is simultaneously changed by one standard deviation.
- When using the engineering approach, and with no slack in the production capacity, we study
    - Sensitivity of the losses to alternative bridge fragility models and when using alternative production loss evaluation methods.
    - Sensitivities to alternative highway functionality models (by changing the value of the rerouting parameter).
- We investigate the dependence of the losses on the functionality-interaction and recovery models/parameters by
    - Changing the values of the functionality-interaction parameters (γ and β coefficients, which were introduced in Section 3.6.2).

- Changing the functionality interaction model from multiplicative to additive.
- Changing the time to full recovery of the social function classes, one at a time, by a fixed percentage to obtain the relative influence of different sectors on the indirect losses.
- Changing the parameter *a* (which controls the physical recovery of the economic sectors-introduced in Section 3.6.1) associated with all economic sectors by one standard deviation.
- Increasing and decreasing the time to full recovery of the residential sector to understand whether the losses have a linear dependence on the time to recovery.

- We study the sensitivities of the losses to economic parameters such as: (a) maximum production capacity slack (in equation (2-5)), (b) coefficients C_2 and C_3 (in equation (2-13)).

	ENGINEERING APPROACH	MACRO-SEISMIC APPROACH
EARTHQUAKE MAGNITUDE	**8m_b**	**11.5MMI**
EPICENTER LOCATION	**(35.10 lat, -89.89 lon)** (35.40 lat, -90.14 lon) (35.79 lat, -89.9 lon)	**(35.10 lat, -89.89 lon)** --- ---
ATTENUATION RELATIONSHIP	**Atkinson and Boore (1995)** Frankel et al. (1996) Toro et al. (1997)	**Bollinger (1977)** --- ---
SITE AMPLIFICATION FACTORS	**Borcherdt et al. (2002)** Hwang et al. (1997a) Dobry et al. (2000)	--- --- ---
BUILDING FRAGILITY MODEL	**100% Pre-Code Construction** 100% Low-Code Construction 100% Moderate-Code Construction	**Parameters derived from ATC-13** Parameters derived from FEMA (1990) ---
BRIDGE FRAGILITY MODEL	**HAZUS (2000)** Hwang et al. (2000a) DesRoches (2002)	**HAZUS (2000)** --- ---
STRUCTURAL-OCCUPANCY MAPPING	**Mapping in Table 3-16** Mapping in Table 3-17	**Mapping in Table 3-16** Mapping in Table 3-17
INITIAL FUNCTIONALITY CALCULATION	**Considers damage to only the structural components** Weight of 0.85 to structural functionality and the remaining weight to the non-structural and content functionalities Weight of 0.50 to structural functionality and the remaining weight to the non-structural and content functionalities	**Considers damage to structural and non-structural components** --- ---

Table 4-1: Models and parameters considered for the sensitivity analysis (default models/parameters are highlighted)

	ENGINEERING APPROACH	MACRO-SEISMIC APPROACH
FUNCTIONALITY-INTERACTION MODEL	**Multiplicative, from Kunnumkal (2001)** Additive, from Kunnumkal (2001)	**Multiplicative, from Kunnumkal (2001)** ---
FUNCTIONALITY-INTERACTION PARAMETERS	**Nominal values in Kunnumkal (2001)** Correspond to no dependence on Residential sector Correspond to no dependence on utilities and intra-nodal transportation Correspond to no dependence on lifelines and Residential sector	**Nominal values in Kunnumkal (2001)** --- --- ---
RECOVERY PARAMETERS	**Kunnumkal (2001)**	**Kunnumkal (2001)**
HIGHWAY NETWORK REROUTING PARAMETER	**0.25** 0.001	**0.25** 0.001
AVAILABLE PRODUCTION SLACK	**5%** 0%	**5%** 0%
PRODUCTION LOSS METHOD	**Method in equation (2-22)** Method in equation (2-23)	**Method in equation (2-22)** Method in equation (2-23)

Table 4-1 (*Continued*): Models and parameters considered for the sensitivity analysis (default models/parameters are highlighted)

4.2 Comparison of losses from engineering and macroseismic approaches

In this section, we compare the loss estimates when using the engineering and macroseismic approaches and try to understand the reasons for the differences.

Table 4-2 summarizes the loss estimates when using Production Loss Method 1 (where the loss calculation does not include the increased productions due to the slack in the production capacity). The total direct losses (including buildings, links and bridges)

	Engineering Approach	Macroseismic Approach
Building Losses ($B)	51.23	70.18
Bridge Losses ($B)	1.33	1.08
Highway Link Losses ($B)	0.98	1.38
Production Losses ($B)	50.93	11.56
Consumption Losses ($B)	2.02	1.77

Table 4-2: Comparison of the macroseismic and engineering loss estimates, Production Loss Method 1

	Engineering Approach		Macroseismic Approach	
	<150 km	**>150 km**	**<150 km**	**>150 km**
Production Loss Method 1, Production Slack = 5%	48.09	2.84	9.31	2.13
Production Loss Method 2, Production Slack = 5%	47.86	-44.65	9.27	-6.46

Table 4-3: Sensitivity of production losses to the production loss method

estimated by the engineering approach are $53.54B and those estimated by the macroseimic approach are $72.64B. However, the total indirect losses (production and consumption losses) given by the engineering approach are greater than those given by the macroseismic approach by about $39B. Next we discuss the reason for these differences.

Figure 4-1 shows the mean damage factor of the residential sector as a function of distance from the epicenter. It can be seen that the engineering approach predicts a higher mean damage factor near the epicenter. However, the mean damage factor predicted by the engineering approach has a faster decay with distance. Figure 4-2 illustrates the differences in the direct building losses from the two approaches at various distance ranges. One can see that the bulk of the difference in the direct losses comes from the distance range 100 km-700 km. This difference in the building losses is mainly due to the slower decay of the mean damage factor in the macroseismic approach.

The recovery parameter 'CD', which affects the time to full recovery of a damaged sector, is shown in Figure 4-3 for the residential and commercial sectors. In both sectors, the engineering approach predicts smaller 'CD', implying a greater loss in functionality near the epicenter. Beyond 125 km, the macroseismic approach predicts slightly greater 'CD'. These differences in the 'CD' values are directly related to the differences in the damage factor estimated by the two approaches. Near the epicenter, the damage factor estimated by the engineering approach is greater. Therefore, the corresponding 'CD' is greater. However, the damage factor estimated by the macroseismic approach is greater beyond 150 km, resulting in a greater 'CD'. These differences in 'CD', especially near the epicenter, drastically affect the recovery of the economic sectors. For example, the macroseismic approach predicts that the commercial sector near the epicenter would recover in about 4 months, whereas the engineering approach predicts that the same sector near the epicenter would take about 2.0 years to fully recover. These differences in the recovery times are reflected in the differences in production losses near the epicenter, as shown in Figure 4-4.

Effect of production capacity slack and production loss evaluation method

Figure 4-5 compares the production losses obtained when using the macroseismic and engineering approaches with Production Loss Method 2 (where the loss calculation includes the increased productions due to the slack in the production capacity). It can be seen that for both the macroseimic and engineering approaches, the losses are almost same as those when using Production Loss Method 1 for distances less than 150 km. However, there are gains in productions beyond 150 km when using Production Loss Method 2. As can be seen in Table 4-3, beyond 150 km, the production gains are \$44.65B in case of the engineering approach and \$6.46B in the macroseismic approach. These differences in the gains are due to the differences in the damage estimates from the engineering and macroseismic approaches. Greater losses in functionality result in greater productions factors, f^k (factors by which the post-earthquake productions increase as a result of the available the slack in the production capacity; these factors are obtained from solving the LP problem of equation (2-3)). Greater production factors in turn result in greater post-earthquake productions in case of the engineering approach.

Figure 4-6 shows the distribution of the production losses when there is no available slack in production. By comparing Figure 4-6 and Figure 4-4, one can see that production losses with no production slack are very similar to those with Production Loss Method 1 for a maximum slack of 5%.

Summary

- While the engineering approach predicts greater damages near the epicenter, the macroseismic approach predicts greater damages in the 100-750 km distance range. As greater proportion of the building inventory is located in the 100-750 km range compared to that within an epicentral distance of 100 km, the macroseismic approach results in greater direct losses.
- When there is no production slack, production losses are mainly contributed by the epicentral region. As the engineering approach predicts greater damages and hence greater losses in functionality near the epicenter, the associated production losses are much greater than those from the macroseismic approach.
- In the case of a 5% slack in production capacity, production losses from the epicentral region in the engineering approach are much greater than those in the macroseismic approaches. However, the engineering approach gives much greater production gains from regions beyond 150 km compared to the macroseismic approach. As a result, the total production losses given by the two approaches are not very different.

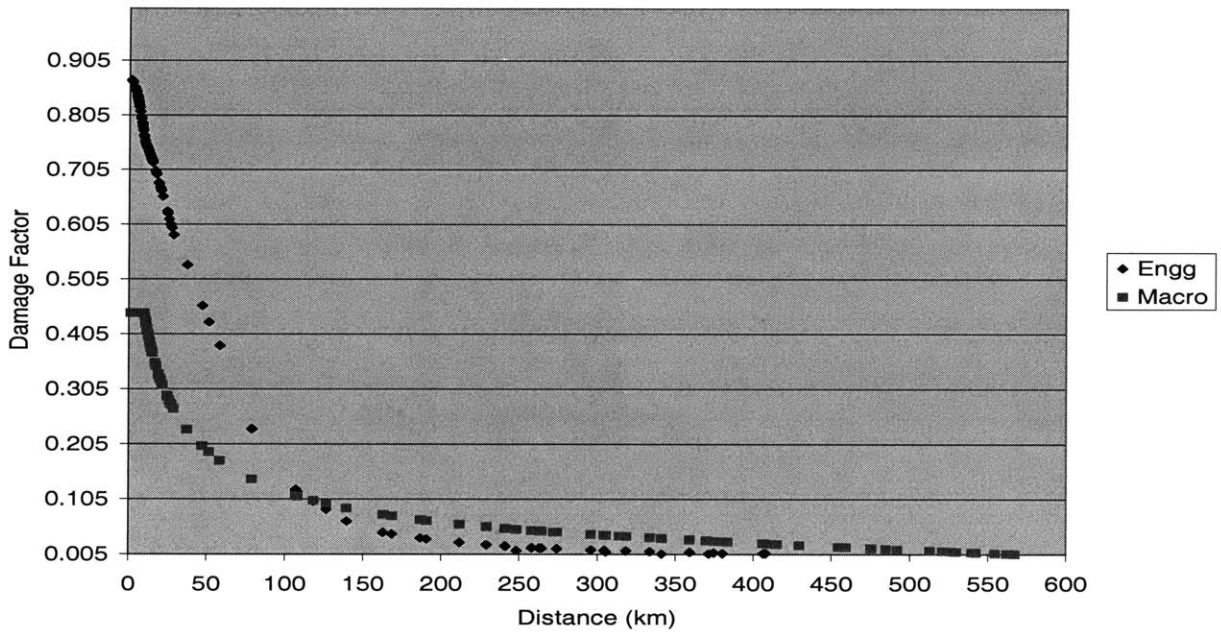

Figure 4-1: Comparison of the damage factor for the residential sector as a function of epicentral distance

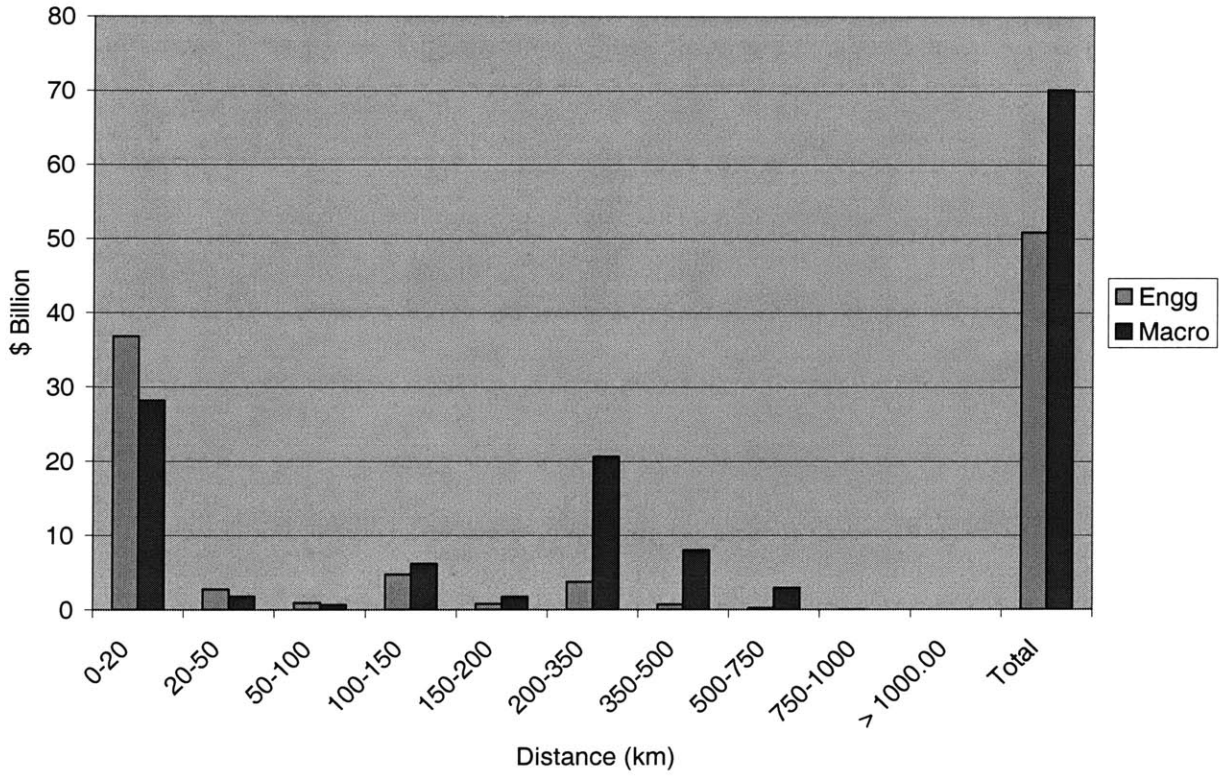

Figure 4-2: Comparison of building losses with distance in the 'macroseismic' and 'engineering' approach.

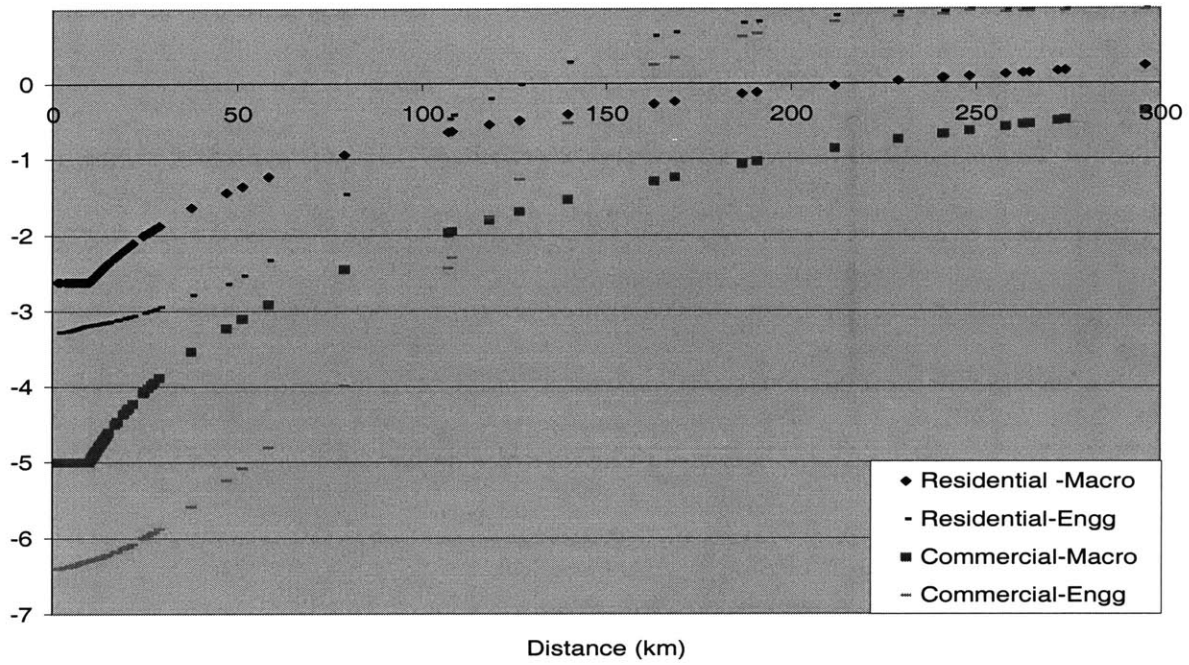

Figure 4-3: Comparison of the recovery parameter 'CD' with distance from the epicenter (for two economic sectors)

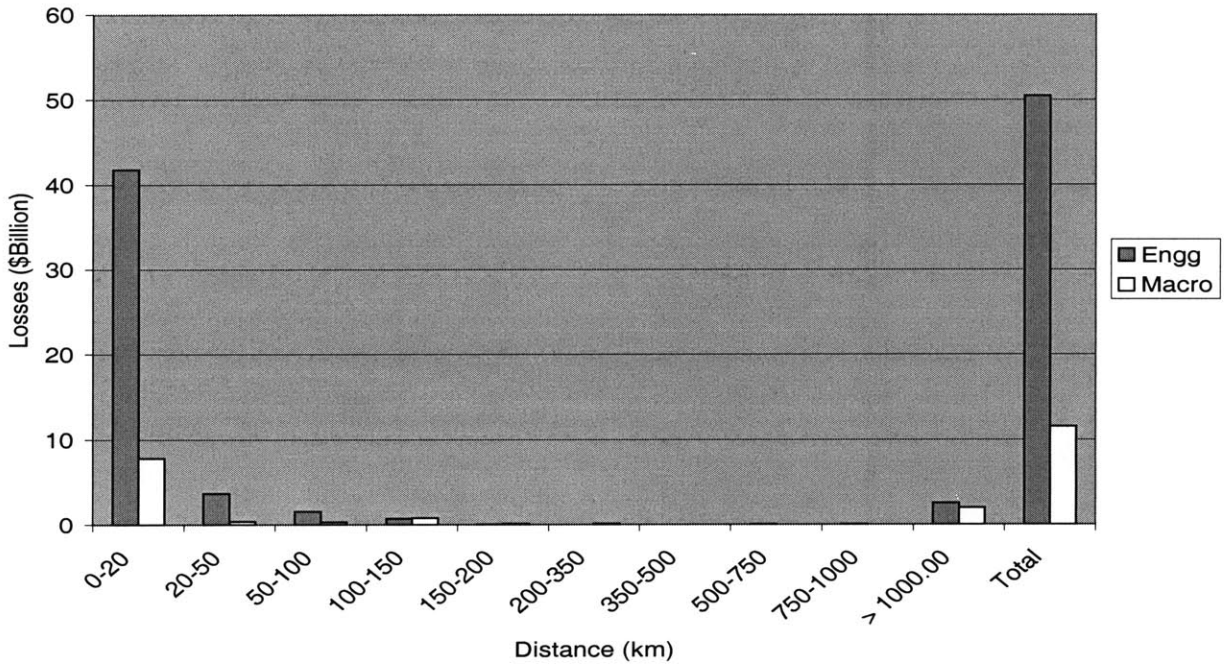

Figure 4-4: Comparison of production losses with distance in the macroseismic and engineering approach (Production Slack = 5% and Production Loss Method 1)

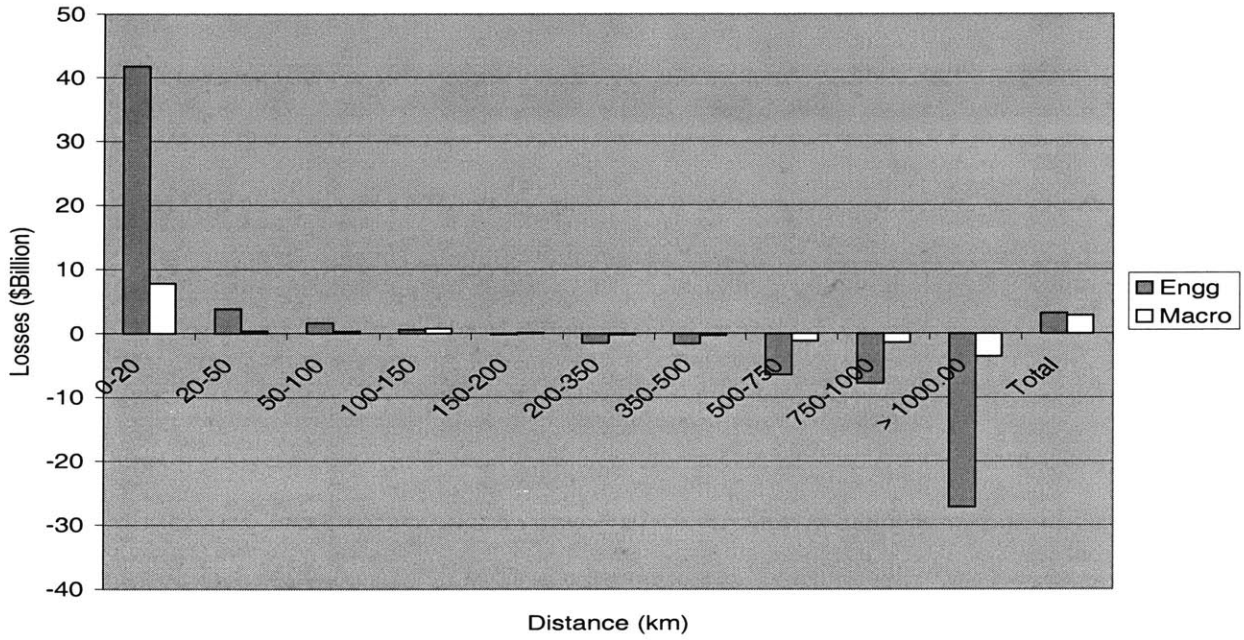

Figure 4-5: Comparison of production losses with distance in the 'macroseismic' and 'engineering' approach (Production Slack = 5% and Production Loss Method 2)

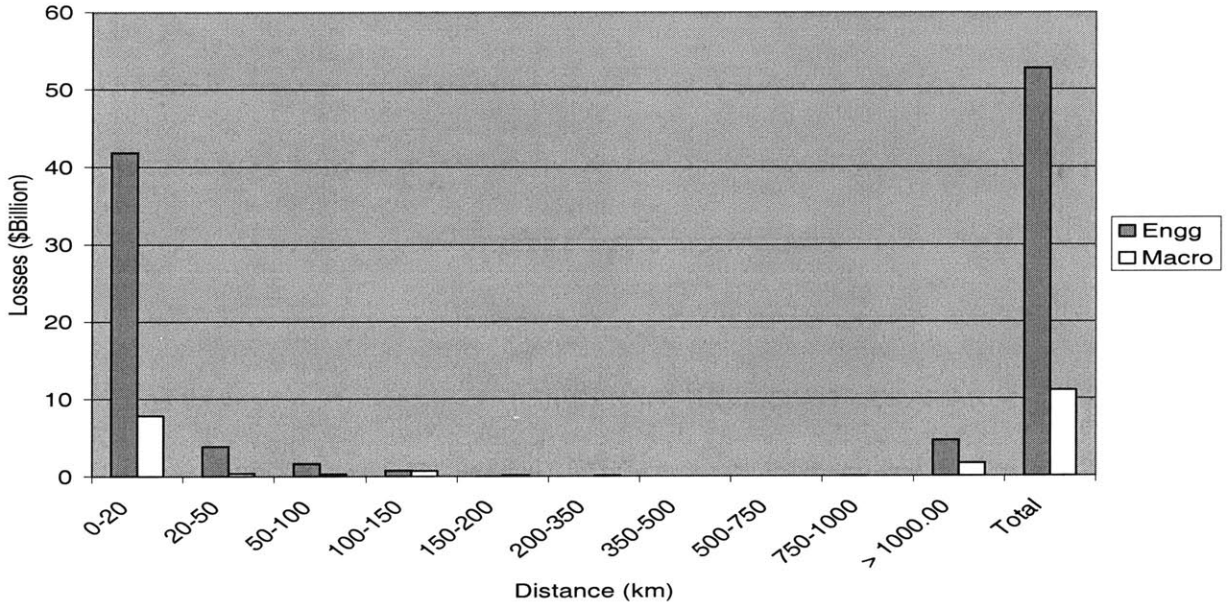

Figure 4-6: Comparison of production losses with distance in the 'macroseismic' and 'engineering' approach (No Production Slack)

4.3 Sensitivity to magnitude of ground shaking (engineering approach)

4.3.1 Sensitivity to epicenter location and ground motion attenuation

In this section, we study the sensitivity of earthquake losses to the three ground motion attenuation relations that are applicable to CEUS, given in Section 3.2.2. In addition, we study the loss sensitivity by varying the spatial distribution of property and economic activities around the epicenter. This is done by considering three hypothetical epicenters, A, B and C, as shown in Figure 4-7. The coordinates of the three epicenters are given in Table 4-4. Epicenter A is at the centroid of Shelby County. Epicenter B is about 35 km north-west of A and epicenter C is about 80 km north of A. A comparison of the building inventory and annual productions with distance for the three epicenters is shown in Figure 4-8 and Figure 4-9 respectively. As can be seen, epicenter A is located in a region with a large amount of property and economic activity. Epicenters B and C are relatively far-off from this region of large economic activity. The three epicenters have been chosen such that they are in/close to the active New Madrid Seismic Zone (NMSZ), given in Nuttli et al. (1984).

Figure 4-10 illustrates the sensitivity of the building losses as a function of the attenuation relation, when epicenter A is considered. It can be seen that the building loss estimates given by Frankel et al. (1996) are greater than those given by Atkinson and Boore (1995) by about $40B. This large difference in the loss estimates is mainly due to the higher ground motion estimates predicted by Frankel et al. (1996) at almost all epicentral distances. Loss estimates by Atkinson and Boore (1995) and Toro (1997) differ only by $0.3B due to the relatively consistent ground motion estimates. As the building loss estimates shown in Figure 4-10 are not normalized by the amount of building inventory within a distance range, even though the mean building damage factor in the 100-150 km range is less than that in the 50-100 km range, due to the larger inventory in the 100-150 km range, the loss estimates in the 100-150 km range are greater than those in the 50-100 km range. It can also be seen in Figure 4-10 that the building losses are almost zero beyond 500 km for all of the three attenuation relations.

Figure 4-11 shows the distribution of the production loss estimates with distance when the earthquake epicenter is at A and when using Production Loss Method 1 (where the production loss evaluation does not include the increased productions due to the slack in the production capacity). The production losses predicted by Frankel et al. (1996) are greater than those given by Atkinson and Boore (1995) by about $23B. The estimates of Atkinson and Boore (1995) are greater than those when using Toro et al. (1997) by $0.3B. Greater structural damage predicted by Frankel et al. (1996) results in greater loss of functionality of the economic sectors and hence higher production losses. It can also be seen in Figure 4-11 that the cumulative production losses from regions that are beyond 1000km from the epicenter are about $7B, when using Frankel (1996), and about $2.5B when using the other two attenuation relations. Even though there is no direct damage to the infrastructure beyond 1000km, production losses at these distances are mainly due to the interdependence of the economic sectors in the earthquake affected regions and those in far-off regions.

A summary of the loss estimates with epicenter A is given in Table 4-5. Figure 4-12 to Figure 4-15 compare loss estimates for epicenters B and C. It can be seen that both the direct (building) and indirect (production) loss estimates given by Frankel et al. (1996) are much greater than those estimated using the other two attenuation models. The percentage increase in the direct building losses when using Frankel et al. (1996), compared to those obtained when using Toro et al. (1997) is 89% and 140% when considering epicenters B and C respectively. This large difference in the direct losses is mainly due to the greater ground motion estimates given by Frankel et al. (1996) for all distances greater than 20km. The percentage change in the indirect loss estimates, when changing the attenuation relationship from Toro et al. (1997) to Frankel et al. (1996) is 104% and 148% for epicenters B and C respectively. This is due to the greater loss in functionality obtained when using Frankel et al. (1996) at epicentral distances greater than 20 km.

Figure 4-16 compares the production losses with epicenter A and when using the Production Loss Method 2 (where the production losses are evaluated by considering the

increased productions due to the slack in the production capacity). The cumulative production losses by Atkinson and Boore (1995), Frankel et al. (1996) and Toro et al. (1997) are $3.21B, $10.51B and $4.1B respectively.

Summary

- For an $8m_b$ earthquake, both the direct and indirect losses predicted by Frankel et al. (1996) are much greater than those predicted by Toro et al. (1997) and Atkinson and Boore (1995). However, the predictions by Toro et al. (1997) and Frankel et al. (1996) are reasonably consistent.
- The direct losses are almost zero beyond 500km from the epicenter, in case of all the three attenuation relations.
- The differences in the direct and indirect loss estimates given by Frankel et al. (1996) and those given by the other two relations are found to be considerably sensitive to the spatial distribution of the property around the epicenter. For example, in the case where a large proportion of the building inventory within an epicentral distance of 500 km is located in 50-350 km range, the direct losses from Frankel et al. (1996) are almost 2.5 times those predicted by the other two sources (this is the case with epicenter C). In the case when there is considerable inventory near the epicenter, the direct loss estimates from Frankel et al. (1996) are about 1.8 times those from Atkinson and Boore (1995) and Toro et al (1997) (corresponds to epicenter A).

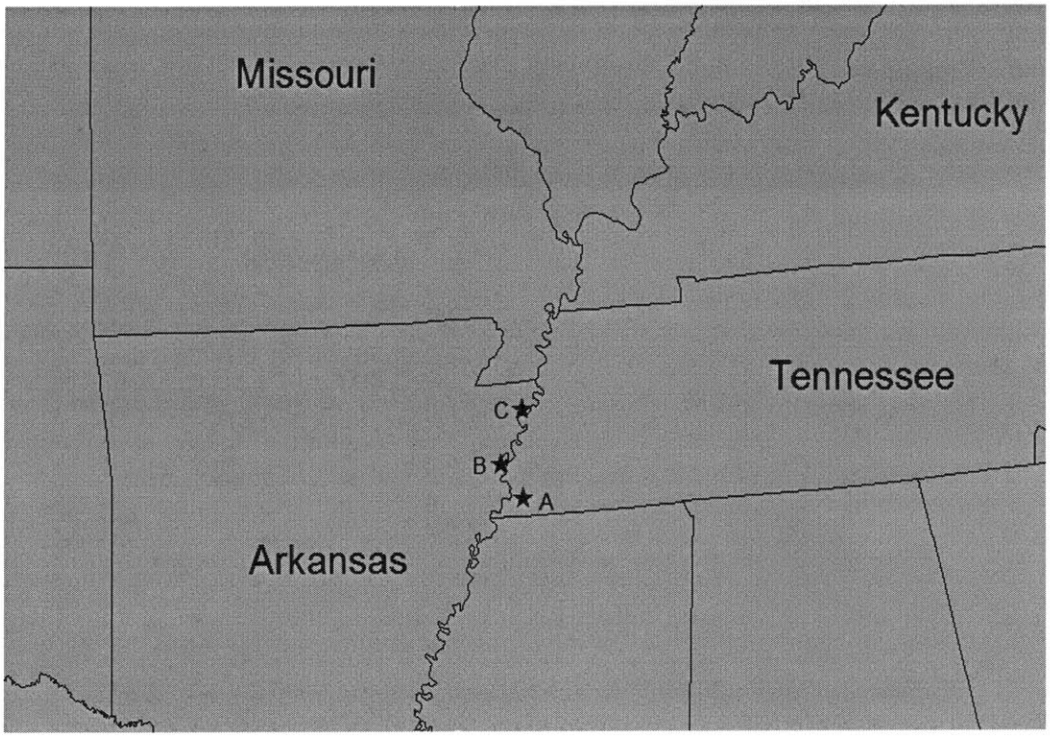

Figure 4-7: The three epicenters considered for the sensitivity analysis

Epicenter	Latitude	Longitude
A	35.10	-89.89
B	35.40	-90.14
C	35.79	-89.90

Table 4-4: Coordinates of the epicenters considered in the sensitivity analysis

	Attenuation Relationship		
	Atkinson and Boore (1995)	Frankel et al. (1996)	Toro et al. (1997)
Structural Component Losses ($B)	18.33	33.12	18.44
Non-Structural Drift Component Losses ($B)	21.57	37.59	21.22
Non-Structural Acceleration Sensitive Component Losses ($B)	11.33	20.51	10.92
Bridge Losses ($B)	1.33	1.98	1.34
Highway Link Losses ($B)	0.98	0.97	0.77
Production Losses ($B)	50.93	73.58	50.90
Consumption Losses ($B)	2.02	6.38	2.12

Table 4-5: Sensitivity of the direct and indirect losses to attenuation relationship, Epicenter A

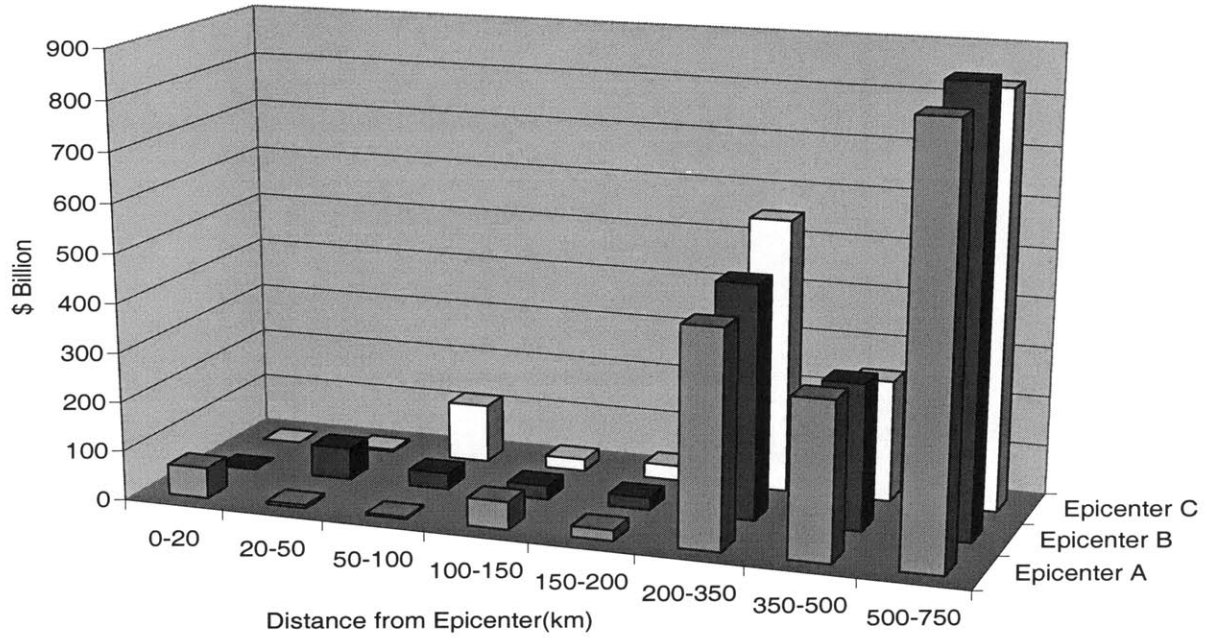

Figure 4-8: Distribution of building inventory value with distance from the epicenter

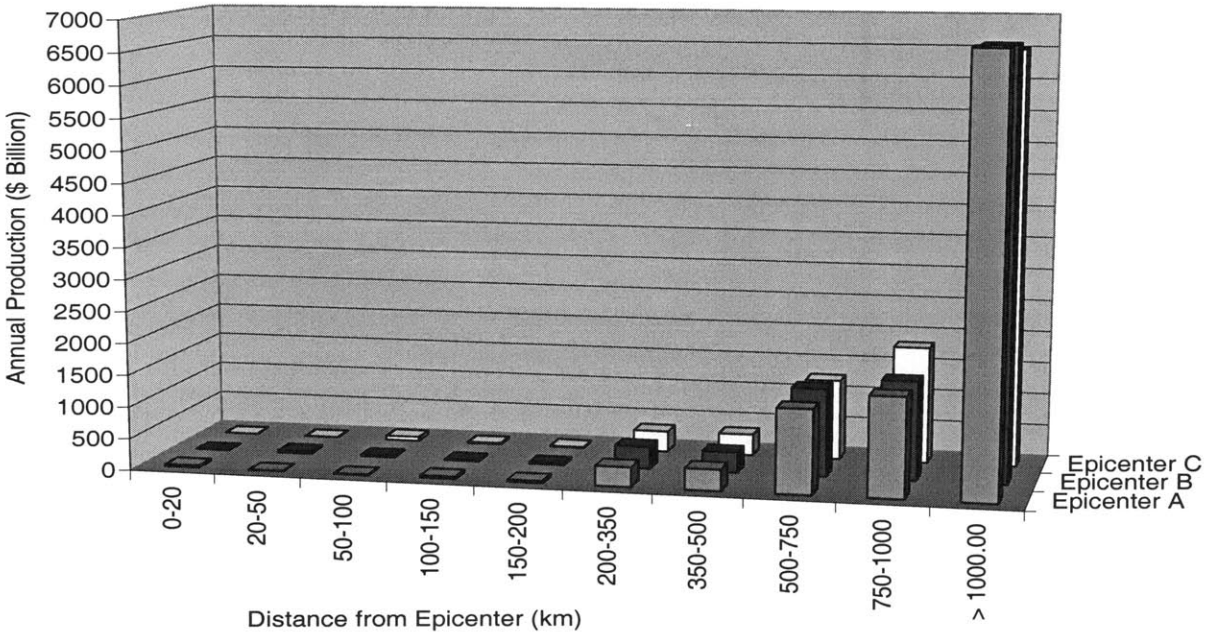

Figure 4-9: Distribution of annual production of all the economic sectors with distance from the epicenter

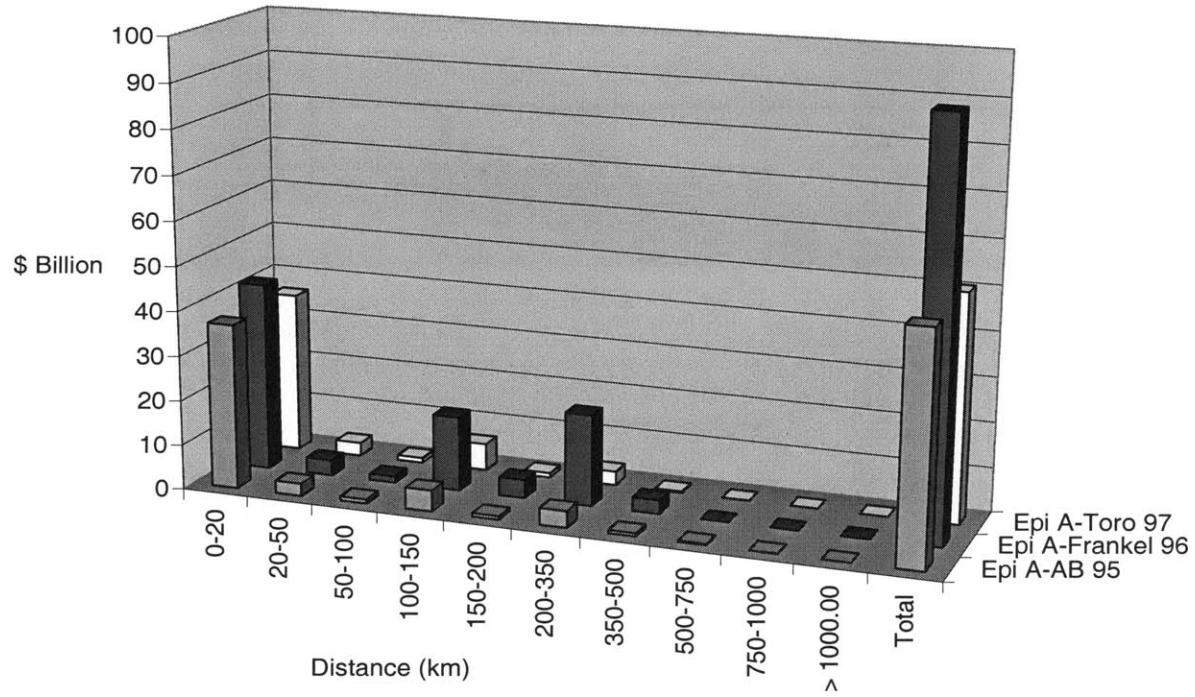

Figure 4-10: Distribution of direct building losses with distance in the 'engineering' approach, as a function of the three attenuation relations considered, Epicenter A.

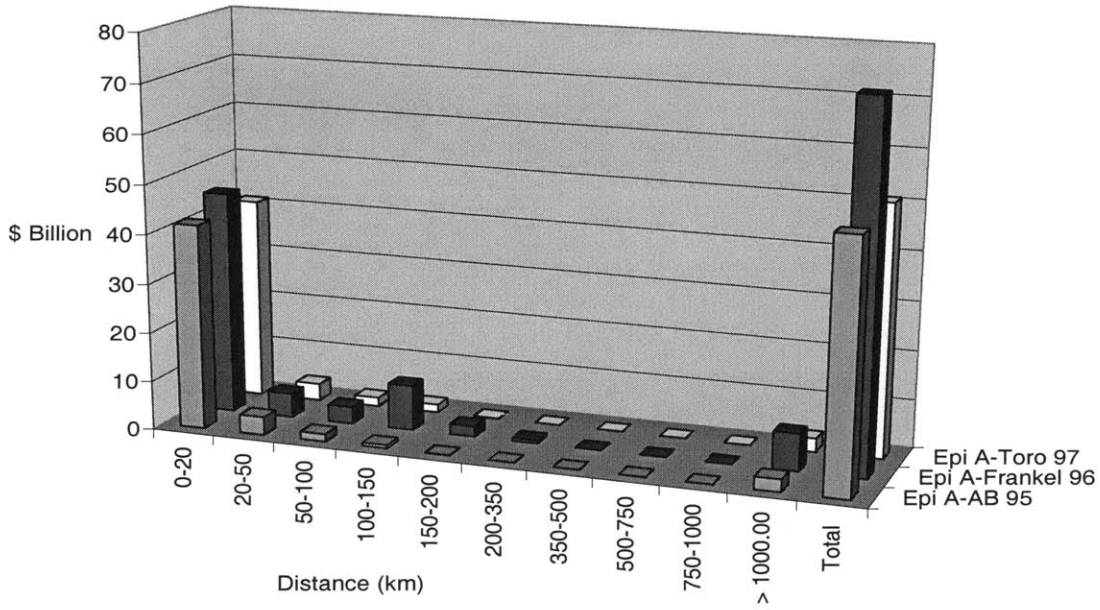

Figure 4-11: Distribution of production losses with distance in the 'engineering' approach, as a function of the three attenuation relations considered, Epicenter A.

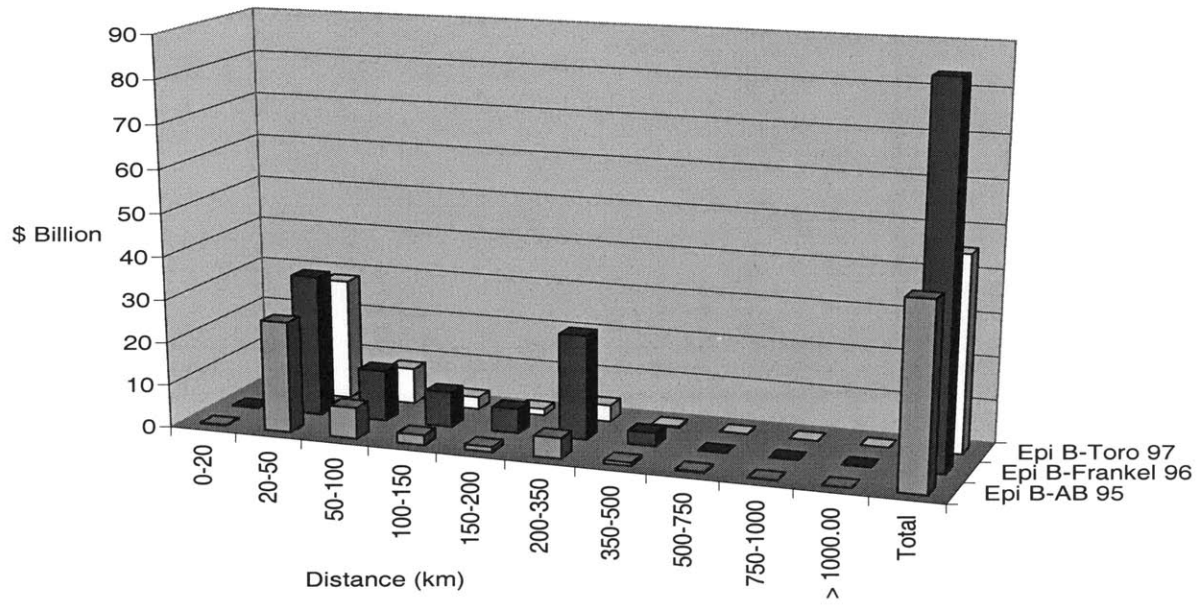

Figure 4-12: Distribution of direct building losses with distance in the 'engineering' approach, as a function of the three attenuation relations considered, Epicenter B.

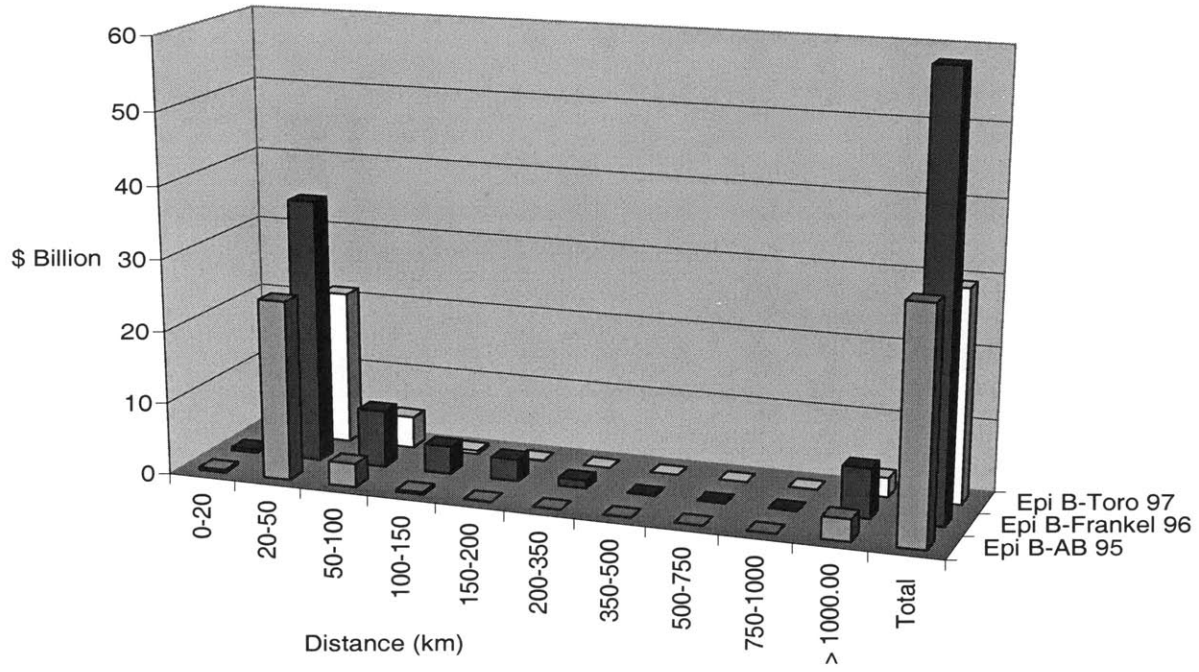

Figure 4-13: Distribution of production losses with distance in the 'engineering' approach, as a function of the three attenuation relations considered, Epicenter B.

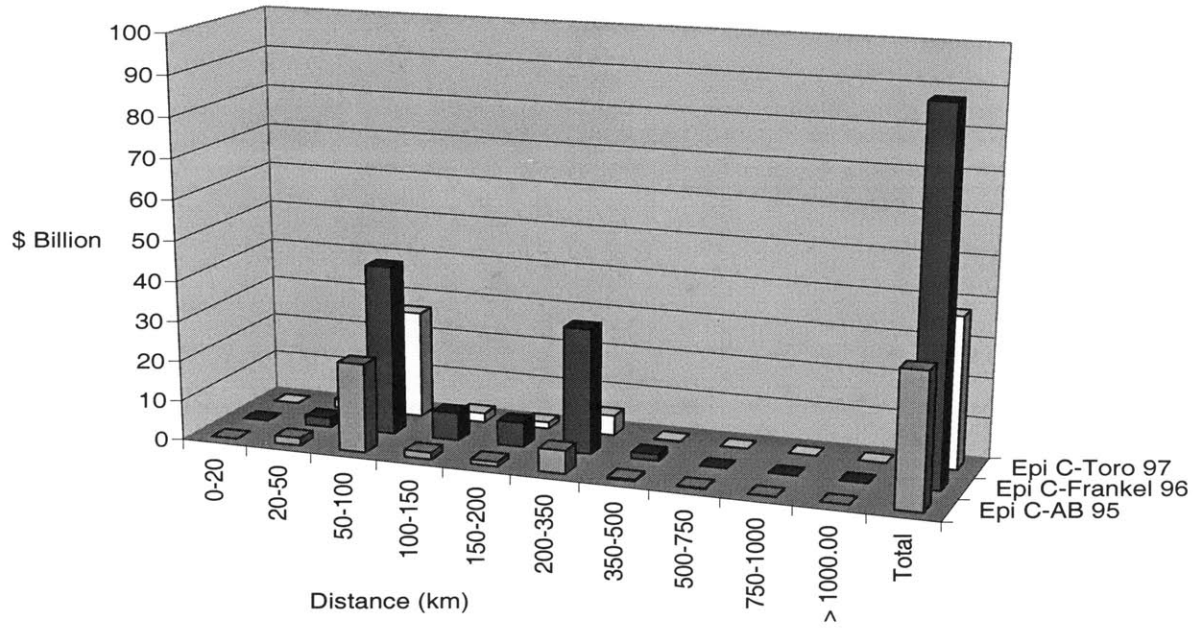

Figure 4-14: Distribution of direct building losses with distance in the 'engineering' approach, as a function of the three attenuation relations considered, Epicenter C.

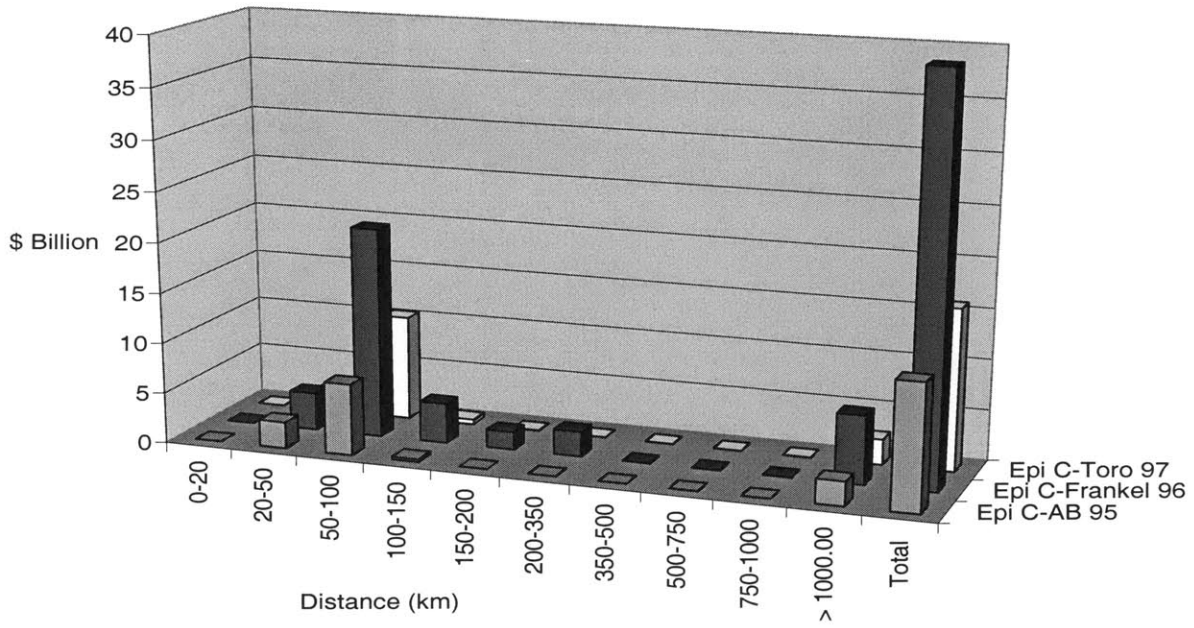

Figure 4-15: Distribution of production losses with distance in the 'engineering' approach, as a function of the three attenuation relations considered, Epicenter C.

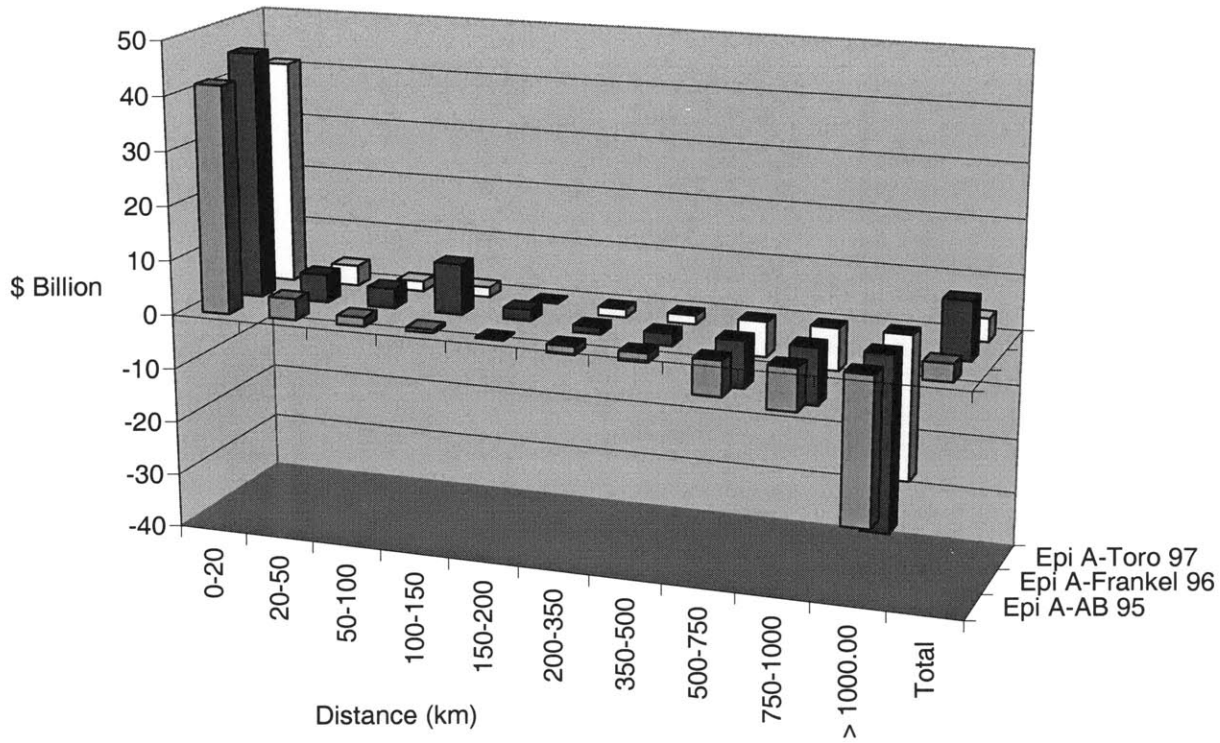

Figure 4-16: Distribution of production losses with distance in the 'engineering' approach, as a function of the three attenuation relations considered, Epicenter A (Production Loss Method 2)

4.3.2 Sensitivity to soil amplification

In this section, we study the sensitivity of the loss estimates to the soil amplification factors given in Borcherdt et al. (2002), Dobry et al. (2000) and Hwang et al. (1997a). We use the models and parameters corresponding to the engineering approach given in Table 4-1 for this sensitivity study.

Table 4-6 shows the loss estimates obtained by using the three alternative soil amplification models with Production Loss Method 1. There is an 18% and 13% increase in the direct and indirect losses respectively when changing from Dobry et al. (2000) to Borcherdt et al. (2002). The direct and indirect losses from Hwang et al. (1997a) are about 27% and 18% greater than those from Dobry et al. (2000).

With Production Loss Method 2, production losses by Borcherdt et al. (2002), Hwang et al. (1997a) and Dobry et al. (2000) are $3.21B, $2.97B and $2.48B respectively. Figure 4-17 shows the distribution of the production losses with distance for each of the three amplification models. As can be seen, Hwang et al. (1997a) predicts greater losses near the epicenter than the other two sources. However, the production gains associated with Hwang et al. (1997a) from distances beyond 200 km are greater than those by the other two sources. This results in the cumulative production losses in case of Hwang et al. (1997a) to be lesser than those from Borcherdt et al. (2002) by about 7%.

The soil amplification factors given in Dobry et al. (2000) are lesser than those given in Borcherdt et al. (2002) and Hwang et al. (1997a), for all magnitudes of ground shaking and soil types, resulting in smaller losses when using Dobry et al. (2000). For NEHRP site class D, the short-period soil amplification factors given by Borcherdt et al. (2002) are slightly greater than those given by Hwang et al. (1997a). As the geologic conditions near the epicenter correspond to NEHRP site class D, these differences in the short period soil amplification factors result in greater Peak Ground Acceleration (PGA) estimates when using Borcherdt et al. (2002) than when using Hwang et al. (1997a). Since PGA is the ground motion parameter used to estimate the acceleration sensitive component and highway link losses, Borcherdt et al. (2002) predicts slightly greater values of these losses compared to Hwang et al. (1997a).

However, for NEHRP site class D, the long-period soil amplification factors given by Borcherdt et al. (2002) are lesser than those given by Hwang et al. (1997a). As spectral acceleration at 1-second period (Sa-1sec) is the ground motion parameter used to estimate the damage to bridges, bridge losses obtained when using Borcherdt et al. (2002) are lesser than those obtained when using Hwang et al. (1997a).

	Soil Amplification Model		
	Borcherdt et al. (2000)	Dobry et al. (2000)	Hwang et al. (1997a)
Structural Component Losses ($B)	18.33	15.87	19.50
Non-Structural Drift Component Losses ($B)	21.57	18.30	24.10
Non-Structural Acceleration Sensitive Component Losses ($B)	11.34	9.45	11.32
Bridge Losses ($B)	1.33	1.00	1.67
Highway Link Losses ($B)	0.98	0.77	0.88
Total Direct Losses ($B)	**53.54**	**45.39**	**57.47**
Production Losses ($B)	50.93	45.11	53.48
Consumption Losses ($B)	2.02	1.64	1.86
Total Indirect Losses ($B)	**52.95**	**46.75**	**55.34**

Table 4-6: Sensitivity to alternative soil amplification factors, Production Loss Method 1

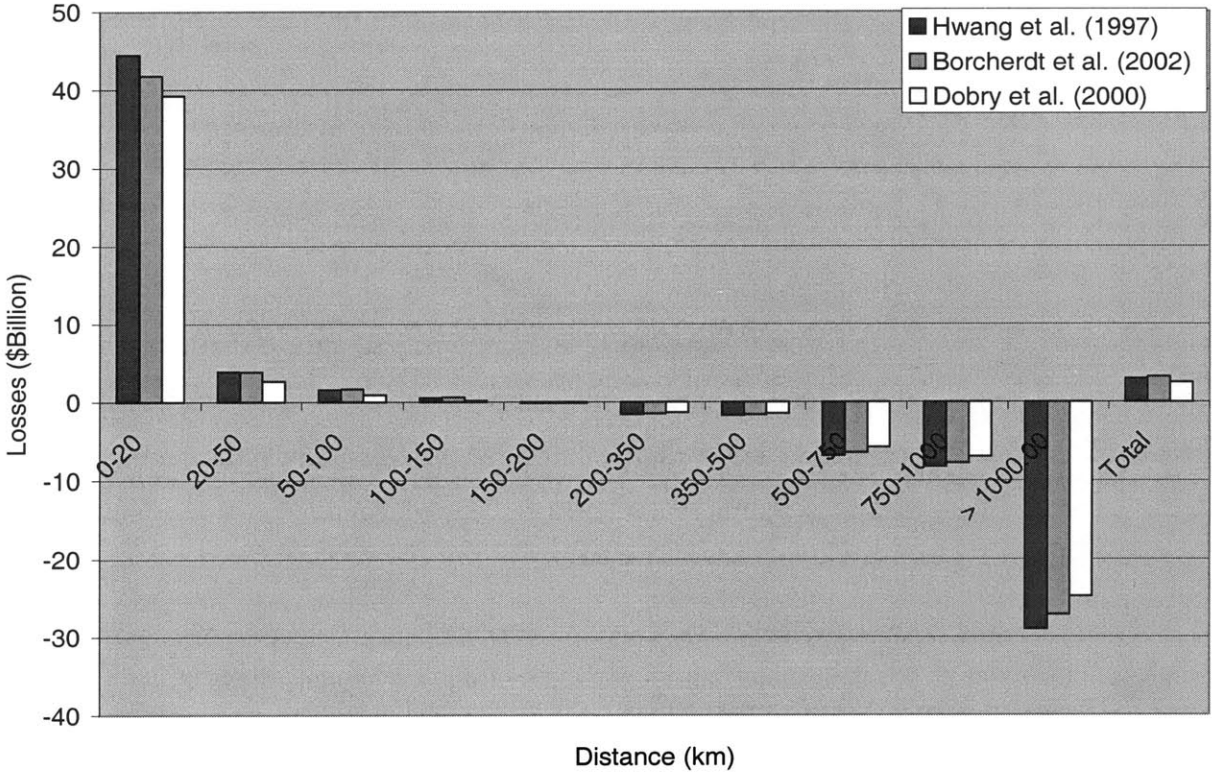

Figure 4-17: Sensitivity of the production losses to soil amplification factors, Production Loss Method 2

Spectral displacement (Sd) is the ground motion parameter used in the estimation of the structural and non-structural drift sensitive component losses. Borcherdt et al. (2002) predicts smaller values of Sd near the epicenter, compared to those predicted by Hwang et al. (1997a). This is the reason for the observed differences in structural and non-structural drift sensitive component losses, when using Borcherdt et al. (2002) and Hwang et al. (1997a).

Summary

The loss estimates given by Dobry et al. (2000) are much smaller than those given by Borcherdt et al. (2002) and Hwang et al. (1997a). The loss estimates by Borcherdt et al. (2002) and Hwang et al. (1997a) are reasonably consistent.

4.4 Sensitivity to building inventory and fragility parameters

4.4.1 Macroseismic approach

4.4.1.1 Sensitivity to alternative structural-occupancy mappings and fragility parameters

In this section, we study the sensitivity of the loss estimates to alternative macroseismic building fragility models, viz., ATC-13 and FEMA (1990), and alternative structural-occupancy mappings for the CEUS. 'Mapping 1' and 'Mapping 2' are the two mappings considered here, which correspond to the structural-occupancy mappings given in Table 3-16 and Table 3-17 respectively. Figure 4-18 shows the differences in the percentages of each structural class in the residential sector between the two mappings.

Table 4-7 and Figure 4-19 show the sensitivity of the direct losses from the different social function classes for the alternative building fragility models and structural-occupancy mappings considered here. As can be seen, Mapping 1 gives higher building loss estimates than Mapping 2. The bulk of this difference comes from the residential sector. The observed differences in the residential sector losses are mainly because Mapping 2 assumes a larger percentage of Wood Frame (W1) buildings and a smaller percentage of the Concrete Shear Wall (C2) buildings in the Residential sector. The floor area in the Residential sector occupied by buildings of type W1 is 82% in Mapping 2

compared to the 65% in Mapping 1. The percentage of buildings of the type C2, which have lower seismic resistance than W1 buildings, is 10% in Mapping 1 and 3% in Mapping 2. There are no differences in the direct losses to the industrial sectors when using the two mappings, because for the industrial sectors Mapping 1 and Mapping 2 use the same distribution of structural classes.

As can be seen in Table 4-7 and Figure 4-19, the loss estimates obtained by using the fragility parameters that are based on ATC-13 are lower than those obtained when using fragility parameters based on FEMA (1990). When using Mapping 1, one can see that ATC-13 direct losses are lower than those from FEMA (1990) by $29.8B. Out of the total difference of $29.8B, $25B comes from the residential sector, $4B from the Commercial sector and the remaining from the other sectors. The difference in the Residential sector losses is mainly due to the higher seismic resistance given in ATC-13 compared to FEMA (1990) for the structural classes W1, URML and C2. Commercial sector losses when using ATC-13, are lower because of the higher seismic resistance estimated by ATC-13 for W2, URML and S3 structural classes.

Table 4-8 compares the sensitivity of the production losses in different economic sectors for alternative building fragility models and structural-occupancy mappings when using the Production Loss Method 1 (which does not consider the increased productions due to the slack in the production capacity). From Mapping 1 to Mapping 2 losses decrease by $0.6B when using ATC-13 and by $0.2B from Mapping 1 to Mapping 2 when using FEMA (1990). When Mapping 1 is used, production losses from FEMA (1990) are about $7B greater than those from ATC-13 (about a 45% increase). This difference is due mainly to the greater damage, hence the greater loss in initial functionality of the residential, commercial and light industry sectors when using FEMA (1990).

With Mapping 1 and Production Loss Method 2 (which considers the increased productions due to the slack in the production capacity), production losses by ATC-13 and FEMA (1990) are $2.81B and $3.24B respectively. Production losses from regions within 200 km when using FEMA (1990) are greater than those when using ATC-13 by

$6.25B. However, the production gains from FEMA (1990) from regions beyond 200 km are greater than those from ATC-13 by $5.82B (as shown in Figure 4-20). As a result, there is not much difference in the production losses from ATC-13 and FEMA (1990).

Summary

- Mapping 1 and Mapping 2 differ mainly in the Residential sector and to a certain extent in the Commercial sector. However, there is no difference in the two mappings for the industrial sectors. Therefore, when the structural-occupancy mapping is changed from Mapping 1 to Mapping 2, the direct losses get affected much more than the indirect losses.
- As ATC-13 estimates higher seismic resistance for W1, W2, S3, C2 and URML structural classes, it gives lower estimates of both direct and indirect losses than those given by FEMA (1990). The difference in the ATC-13 and FEMA (1990) direct losses is about 50%. When using Production Loss Method 1, the production losses from ATC-13 are lower than those from FEMA (1990) by about 35%. However, with Production Loss Method 2, the difference is about 10%.

4.4.1.2 Sensitivity to the resistance of various structural classes

In this section, we investigate the sensitivity of the losses to the resistance of various structural classes, with alternative structural-occupancy -mappings and functionality-interaction coefficients. Sensitivities are studied for the three cases that are shown in Table 4-9. Case 1 and Case 2 are scenarios where the functionalities and the recovery rates of the economic sectors are assumed to depend on the functionalities of the residential sector, utilities and intra-nodal transportation. However, Case 3 is an optimistic scenario, where the functionality-interactions are assumed to be absent, i.e., the corresponding β and γ coefficients (which were introduced in Section 3.6.2) are all zeroes.

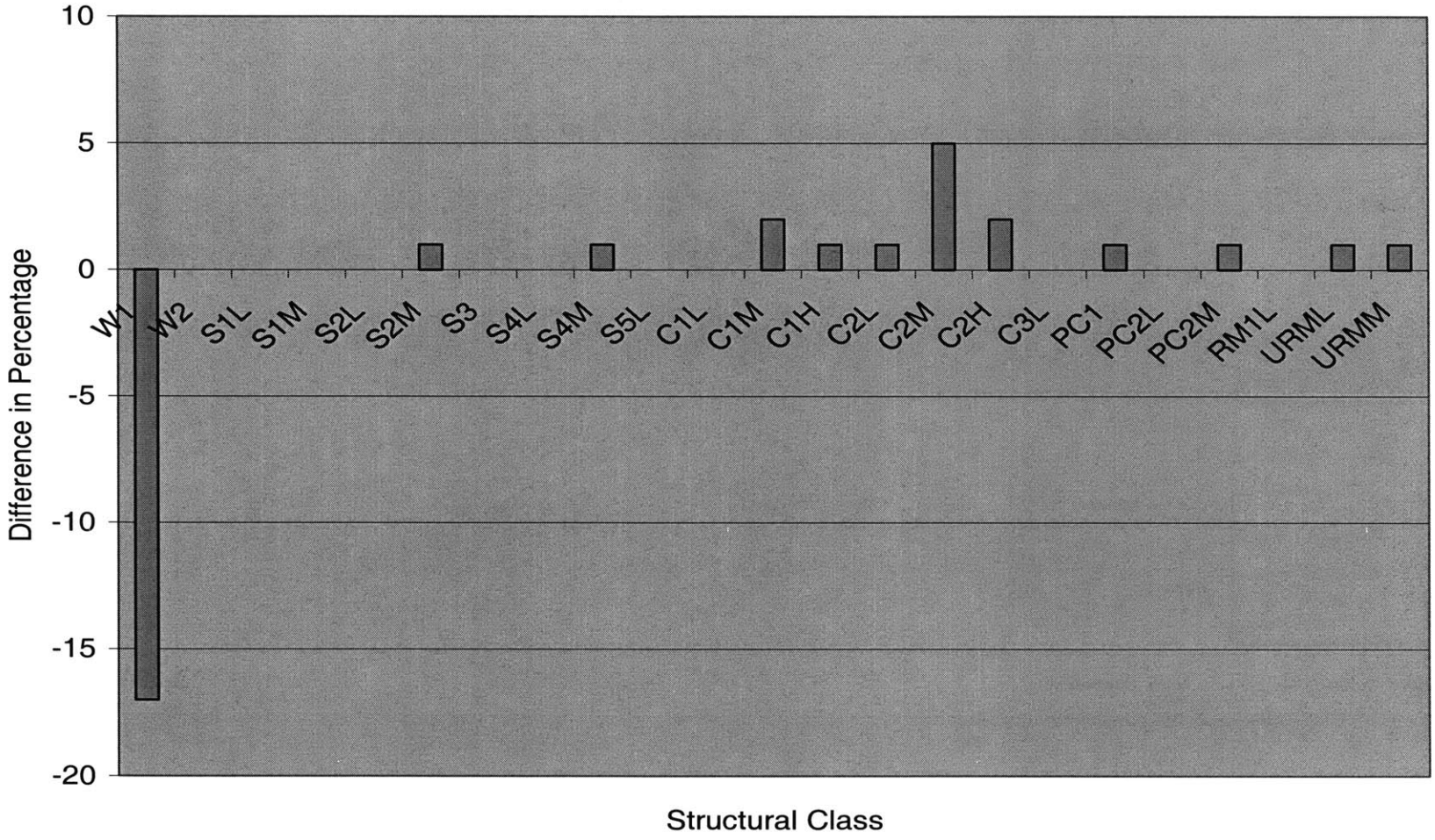

Figure 4-18: Difference in the percentage of each structural class in Mapping 1 and Mapping 2 for the residential sector (obtained by subtracting values in Mapping 1 from those in Mapping 2)

	Residential	Commercial	Heavy Industry	Light Industry	High Technology	Food and Drug	Chemical	Total
ATC13 - Mapping 1	45.8	20.9	1.5	1.4	0.0	0.3	0.3	70.2
ATC13 - Mapping 2	36.9	20.5	1.5	1.4	0.0	0.3	0.3	60.9
FEMA - Mapping 1	70.8	24.9	1.9	1.6	0.0	0.4	0.4	100.0
FEMA - Mapping 2	65.9	25.0	1.9	1.6	0.0	0.4	0.4	95.2

Table 4-7: Comparison of the building loss estimates ($B) obtained from alternative fragility models and structural-occupancy models

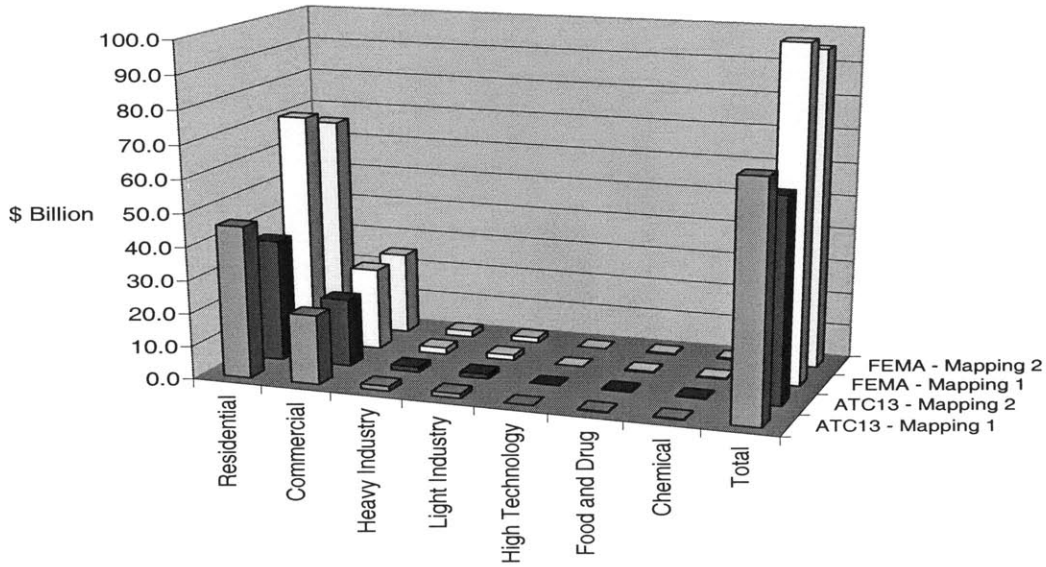

Figure 4-19: Comparison of the building loss estimates obtained from alternative fragility models and structural-occupancy models

	ATC13 -Mapping 1	ATC13 -Mapping 2	FEMA - Mapping 1	FEMA - Mapping 2
Agriculture	0.1	0.1	0.1	0.1
Mining	0.1	0.1	0.1	0.1
Construction	0.2	0.2	0.2	0.2
Food	1.1	1.1	1.5	1.5
Chemical	0.5	0.5	0.7	0.7
Primary Metal	0.2	0.2	0.4	0.4
Fabricated Metal	0.2	0.2	0.4	0.4
Industrial Machinery	0.5	0.5	0.8	0.8
Electronics and Electrical	0.9	0.9	1.2	1.2
Transportation Equipment	0.4	0.4	0.7	0.7
Non Durable Manufacturing	2.7	2.6	4.0	3.9
Durables Manufacturing	0.7	0.7	1.0	1.0
Commercial	4.0	3.7	7.5	7.4
Total	**11.6**	**11.0**	**18.5**	**18.3**

Table 4-8: Comparison of the production loss estimates ($B) obtained from alternative fragility models and structural-occupancy models, Production Loss Method 1

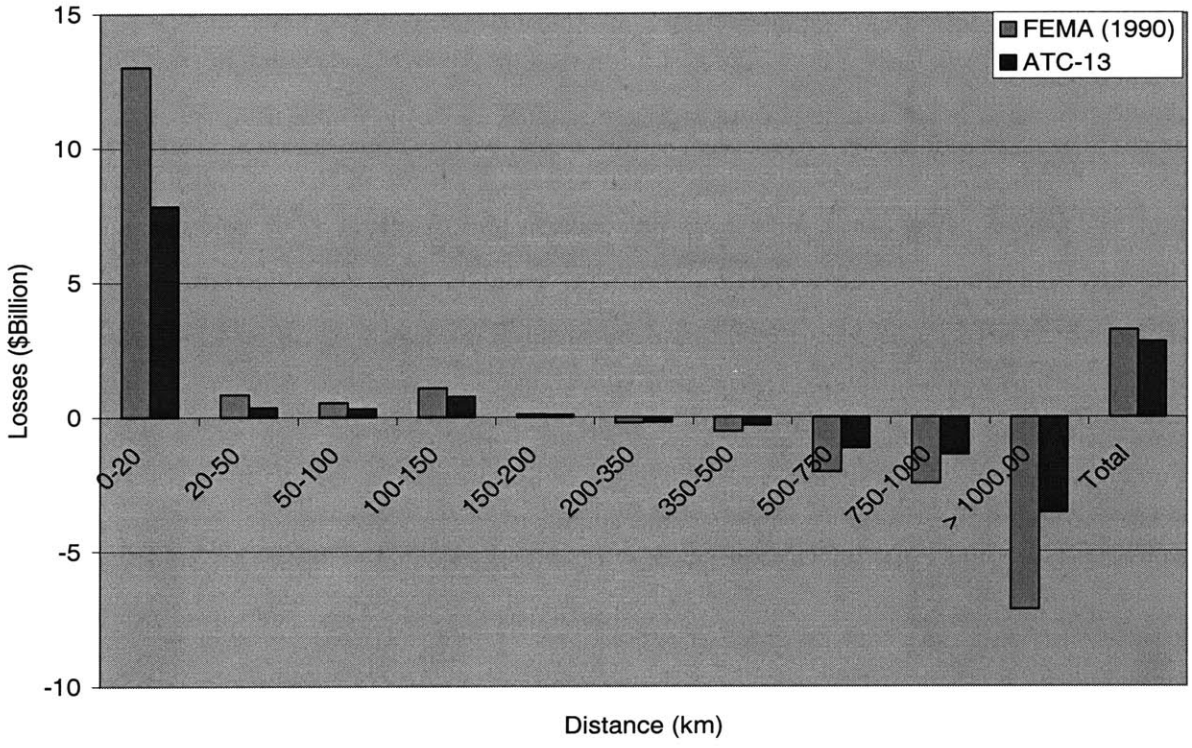

Figure 4-20: Distribution of the production losses, Production Loss Method 2

Case No.	Structural-Occupancy Mapping	Functionality-Interactions Present?
1	Mapping 1	Yes
2	Mapping 2	Yes
3	Mapping 1	No

Table 4-9: The three cases considered for the sensitivity study

Case 1

Figure 4-21 shows the sensitivity of the direct losses to a 5% change in the resistance of different infrastructure classes. For example, when the resistance of the Wood-Frame (W) buildings is increased by 5%, the percentage decrease in the direct losses is about 12%. However, when the resistance of Steel Light Frame (S3) buildings is increased by 5%, the percentage decrease in the direct losses is only 0.9%. Damages to the W and URM buildings affect the direct losses the most, followed by the damage to the buildings of the type C2. Greater sensitivity of the direct losses to Wood-Frame construction is due to the greater proportion of the Wood-Frame buildings in the residential sector, which contributes the most to the direct building losses. Sensitivity of the losses to a 5% change in the resistance of the URM buildings is about 11.5%. This high sensitivity to the fragility of URM construction is due to its presence in almost all the occupancy classes and the low resistance of URM construction. The 5% change in the resistance of C2 buildings, which account for about 10% and 12% of the total floor area of the Residential and Commercial sectors respectively, results in a change in the direct losses by about 4.5%.

Figure 4-22 shows the sensitivity of the production losses to changes in the resistance of various infrastructure classes. As can be seen, production losses are most sensitive to changes in the resistance of the Wood-Frame buildings. This large sensitivity of the production losses is due to the following reasons:

- Wood-Frame construction predominates the residential sector, on which the commercial and industrial sectors depend for human resources. Thus, the damage to the Wood-Frame construction indirectly affects the functionality and the recovery rate of all the economic sectors.

- Wood-Frame buildings exist to certain extent in the commercial and industrial sectors as well; hence their vulnerability contributes directly to the production losses.

Intra-nodal transportation is the infrastructural class that has the next greatest influence on the production losses. This is mainly due to the assumed dependence of the functionality and recovery of the economic sectors on the functionality of intra-nodal transportation. There is greater sensitivity of the production losses than the direct losses to changes in the resistance of the S3 building class. This is due to the fact that S3 has almost no presence in the residential sector, which is the main contributor to the direct losses, and has some presence in the commercial and the industrial sectors, which are the only direct contributors to the production losses. In Figure 4-22, one can also see the relatively low sensitivity of the production losses to the changes in the resistance of the utilities (electric power). As utilities become fully functional much earlier than the commercial and industrial sectors, the loss in functionality of these sectors does not have a considerable influence on the indirect losses.

Case 2

Figure 4-23 illustrates the percentage changes in the direct losses, with changes in the resistances of different structural classes, when using Mapping 2. The pattern observed here is similar to that seen in Case 1, except for the sensitivity to change in the expected mean resistance of the structural class C2. When the resistance of C2 buildings is changed by 5%, the change in the direct losses is 1.6% and 4.7% for Mapping 1 and Mapping 2 respectively. The reason for this difference is that C2 accounts for a greater proportion of the residential sector in Mapping 1 compared to that in Mapping 2. The percentage changes in the production losses, as shown in Figure 4-24, are very similar to that observed in Case 1.

Case 3

Figure 4-25 illustrates the associated sensitivities. It can be seen that with no functionality-interactions, S3 has the most influence on the production losses. The percentage change in the losses drop from about 18% in Case 1 to 4.5% here, for a 5%

change in the fragility of the W structural class. This is mainly due to the assumed independence of the functionalities and recovery rates of all the economic sectors on the residential sector, in which Wood Frame buildings predominate. The sensitivities of the losses to changes in the resistances of C2, URM and S2 are very similar in Case 1 and Case 3.

Summary

- W, URM and C2, in this order, are the buildings that have considerable influence on the direct building losses. Extent of this influence is not found to be very different for alternative structural-occupancy mappings.
- The influence that the damages to different buildings have on the production losses depends on the values taken by the functionality-interaction coefficients. When the economic sectors are assumed to be affected by the functionality of the residential sector and the lifelines, the structural classes W, S3, C2 and URM, in this order, influence the production losses. In addition, Intra-nodal transportation has a large influence on the production losses. However, when the functionality-interaction coefficients are all assumed to be zero, S3, W, C2 and URM, in this order, influence the production losses.

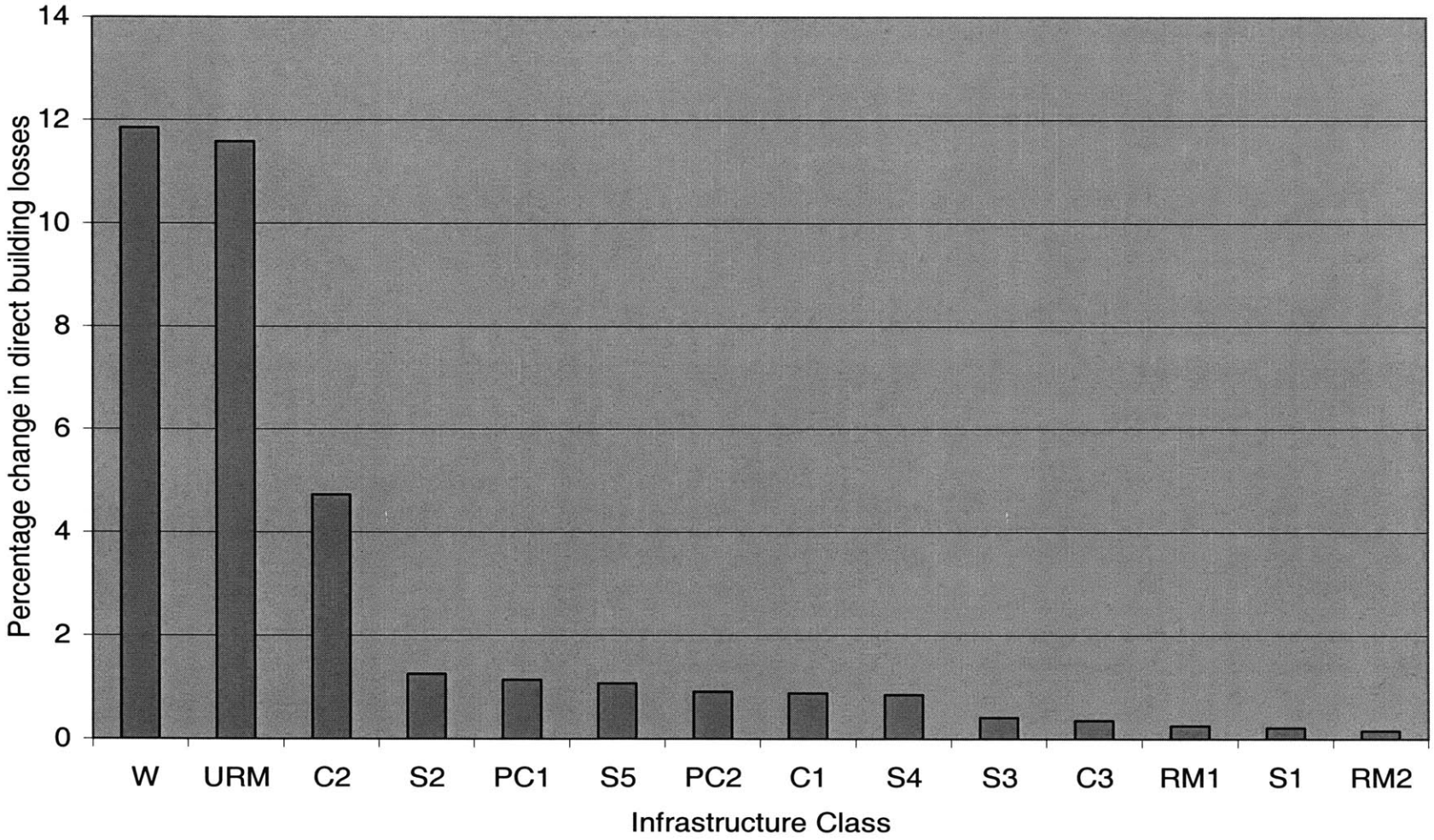

Figure 4-21: Percentage change in the direct building loss estimates with a 5% change in building resistance, Mapping 1 is considered

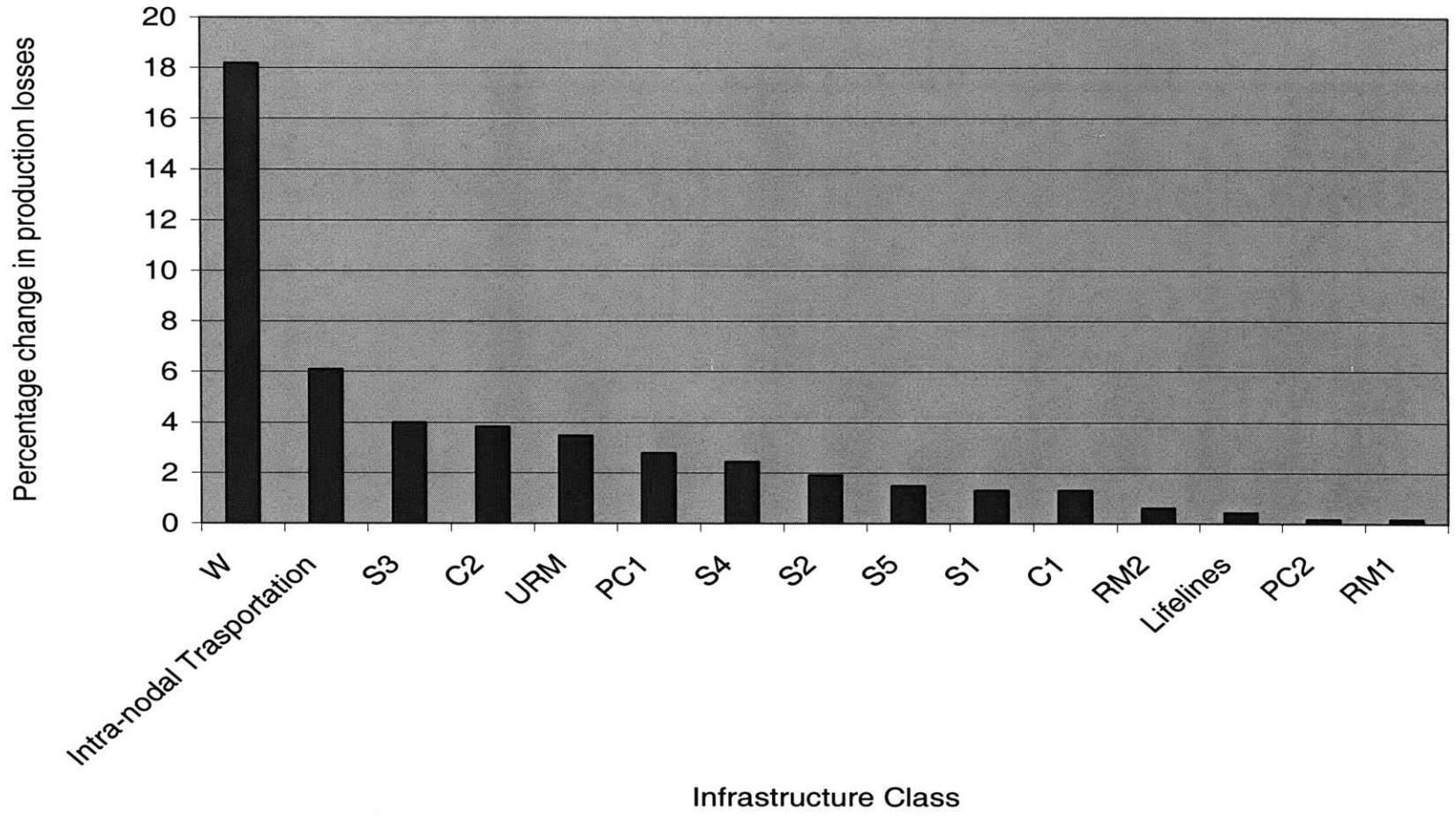

Figure 4-22: Percentage change in the production loss estimates with a 5% change in building resistance, Mapping 1 is considered

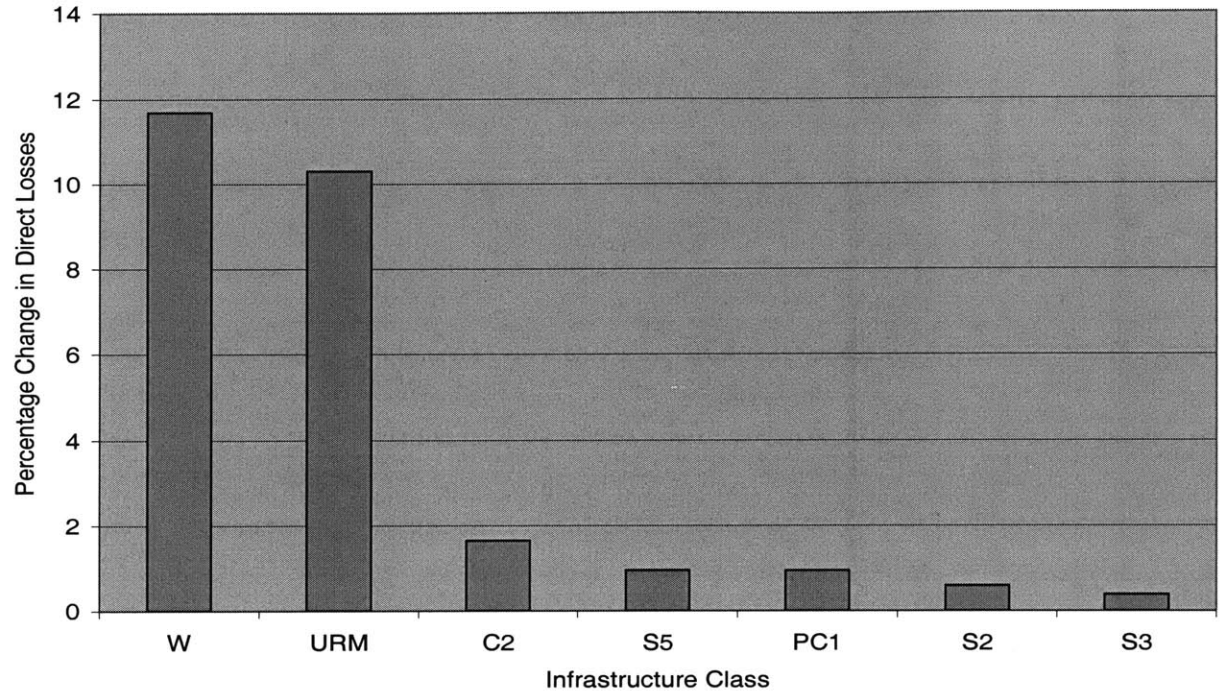

Figure 4-23: Percentage change in the direct building loss estimates with a 5% change in building resistance, Mapping 2 is considered

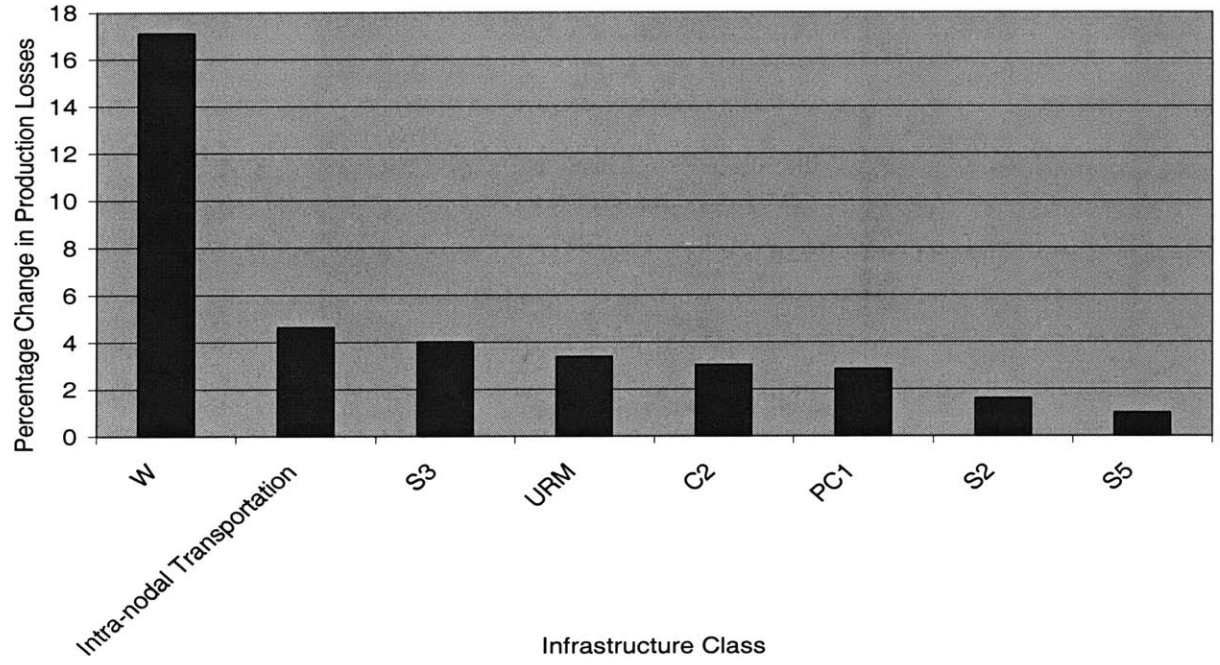

Figure 4-24: Percentage change in the production loss estimates with a 5% change in building resistance, Mapping 2 is considered

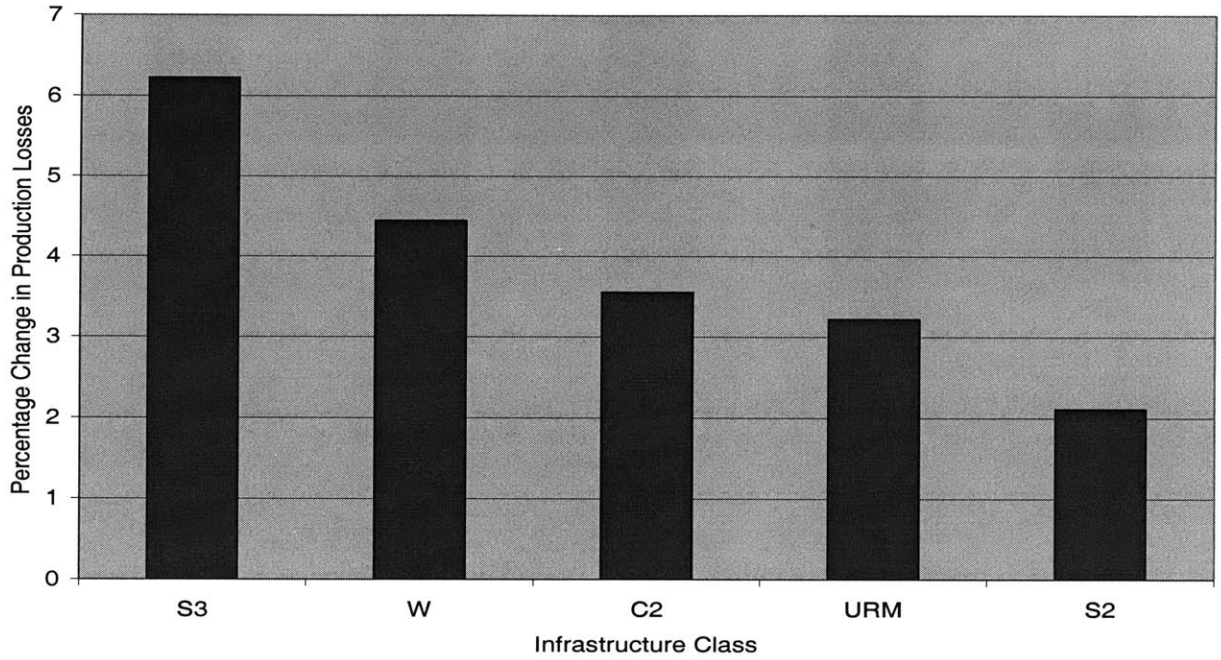

Figure 4-25: Percentage change in the production loss estimates with a 5% change in building resistance, assuming that there is no dependence of the economic sectors on utilities, intra-nodal transportation and the residential sector

4.4.1.3 Sensitivity of the losses to the mean seismic resistance, $E(M)$

Here we look at the sensitivity of the losses to the change in the expected mean seismic resistance of all the seismic vulnerability classes by $\sigma_{\overline{M}}$. Table 4-10 shows the sensitivities to the cases when the seismic resistance of all the seismic vulnerability classes are decreased and increased by $\sigma_{\overline{M}}$. As can be seen, there is a considerable change in the losses with change in $E(M)$.

Case	Percentage change in Building Losses	Percentage Change in Production Losses
$\sigma_{\overline{M}}$ -	41.92	50.13
$\sigma_{\overline{M}}$ +	-30.95	-32.84

Table 4-10: Sensitivity to the mean seismic resistance

4.4.2 Engineering approach

4.4.2.1 Sensitivity to alternative structural-occupancy mappings

In this section, we look at the sensitivity of the losses to alternative structural-occupancy mappings when using the engineering approach.

Table 4-11 gives a summary of the results obtained by using Mapping 1 and Mapping 2 (Table 3-16 and Table 3-17 respectively). Interestingly, there is a 5% decrease in the structural component losses, but about 8% increase in both the acceleration sensitive component and content losses, when using Mapping 2 instead of Mapping 1. All of the difference between the structural component losses with Mapping 1 and Mapping 2 is contributed by the residential sector, as seen in Figure 4-26. Both the residential and commercial sectors contribute to the differences in the acceleration sensitive loss estimates, as seen in Figure 4-27. There are no differences in loss estimates to any of the industrial sectors because Mapping 1 and Mapping 2 are identical for these sectors.

To better understand the above differences, the mean damage factors of three structural classes are compared at a region located about 9km from the epicenter. Table 4-12 gives the mean damage factor of different components in the three structural classes. In addition, this table shows the spectral response of each of the three structural classes in terms of: (1) the Spectral Acceleration (Sa), which is used as an input to the acceleration sensitive component and content damage estimation, and (2) Spectral Displacement (Sd), which is used as an input to the structural component and drift sensitive component damage estimation.

In Mapping 1 it is assumed that W1, C2M and URML occupy 65%, 7% and 13% of the floor area in the Residential sector. Using these values, the mean damage factors for the structural and acceleration sensitive components in the residential sector are found to be 0.79 and 0.28 respectively. On the other hand, Mapping 2 assumes that 82%, 2% and 12% of the Residential sector floor area is covered by W1, C2M and URML respectively and the corresponding mean damage factors are 0.74 and 0.33 for the structural and acceleration sensitive components, respectively. As the mean content damage factor is

	Mapping 1	Mapping 2
Structural Component Losses ($ Billion)	18.33	17.45
Drift Sensitive Component Losses ($ Billion)	21.57	21.68
Acceleration Sensitive Component Losses ($ Billion)	11.33	12.30
Contents Losses ($ Billion)	9.41	10.16
Production Losses ($ Billion)	50.93	50.37

Table 4-11: Comparison of the loss estimates obtained from the two mappings, engineering

Structural Class	Sd (inches)	Structural Component Damage	Drift Sensitive Component Damage	Sa (g)	Acceleration Sensitive Component Damage	Content Damage
W1	7.50	0.70	0.73	0.83	0.45	0.23
C2M	23.95	0.92	0.72	0.42	0.20	0.10
URML	22.50	0.96	0.89	0.40	0.19	0.10

Table 4-12: Comparison of the spectral response and the mean damage factors associated with different components in three structural classes

assumed to be half of the mean damage factor of the acceleration sensitive components, content losses increase when changing from Mapping 1 to Mapping 2. A comment about the acceleration sensitive component damage factor estimation is that even though the seismic resistance of the non-structural components is assumed to be independent of the structural class, greater mean non-structural acceleration-sensitive damage factor associated with the W1 structural class is due to a greater spectral response (in terms of Sa) associated with this structural class.

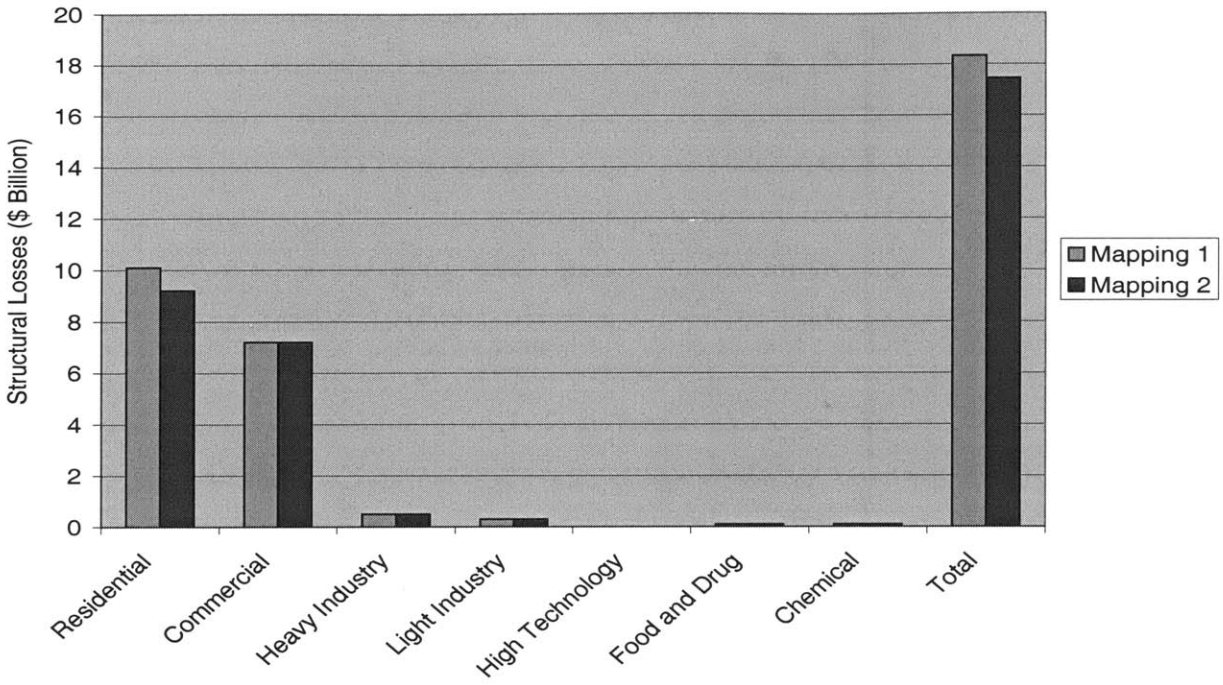

Figure 4-26: Comparison of the structural component loss estimates obtained from alternative structural-occupancy mappings, engineering approach

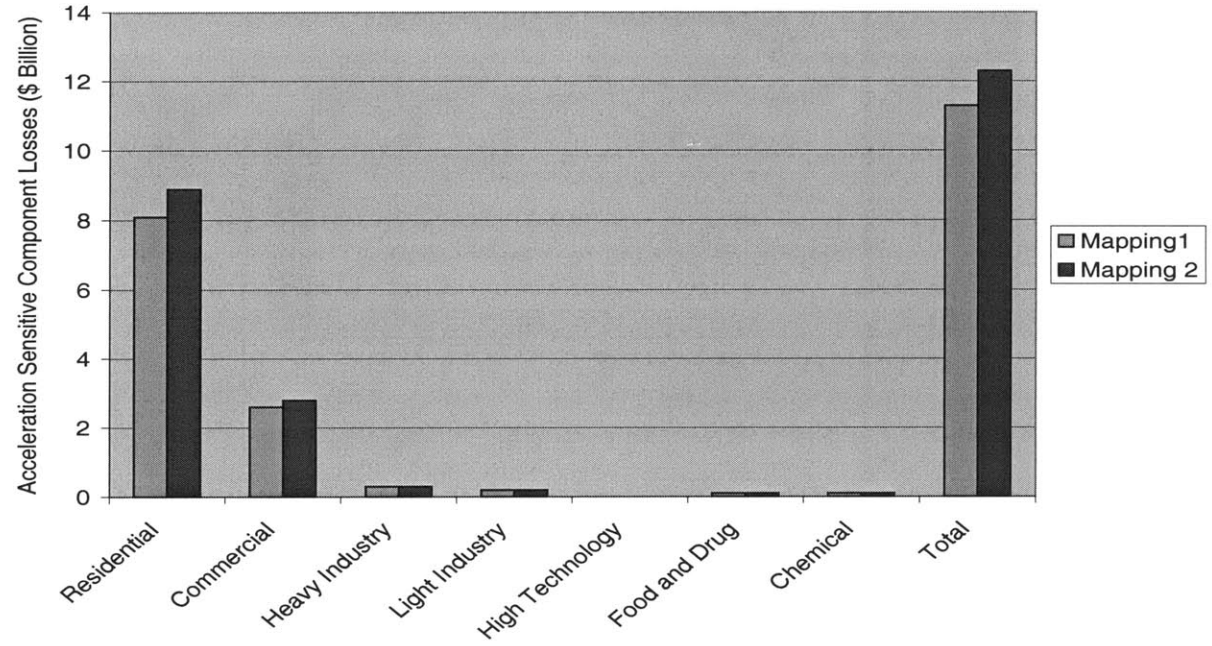

Figure 4-27: Comparison of the non-structural acceleration-sensitive component loss estimates obtained from alternative structural-occupancy mappings, engineering approach

Summary

While there is a slight increase in the structural component losses when shifting from Mapping 1 to Mapping 2, there is a slight decrease in the acceleration sensitive non-structural and contents losses. This is mainly due to the differences in the structural and non-structural acceleration sensitive damages to the Wood-Frame (W1) buildings.

4.4.2.2 Sensitivity to the resistance of various structural classes

Here we look at the sensitivity of the losses to a 5% change in the expected structural and non-structural mean resistance parameters, $E(M)_{structural}$, $E(M)_{drift-sensitive}$ and $E(M)_{acceleration-sensitive}$, of different infrastructure classes. Table 4-13 and Table 4-14 show the associated sensitivity of the building and production losses. While the change in the resistance of Wood-Frame buildings has the greatest influence on the building losses, the change in the resistance of Intra-nodal transportation has the greatest effect on the production losses. The order of influence of different infrastructure classes seen here is very similar to that seen in the macroseismic approach.

Infrastructure Class	W	C2	URM	S2	S4	S3	PC1
Percentage Change	1.93	0.73	0.56	0.29	0.14	0.07	0.06

Table 4-13: Percentage change in direct building losses to a 5% change in mean resistance of different classes, engineering approach

Infrastructure Class	Intra-nodal Transportation	W	C2	URM	S2	S4	S3
Percentage Change	1.57	0.53	0.20	0.14	0.10	0.08	0.04

Table 4-14: Percentage change in production losses to a 5% change in mean resistance of different classes, engineering approach

4.4.2.3 Sensitivity of the losses to alternative proportions of buildings in different seismic design levels

Table 4-15 has a summary of the loss estimates obtained for three scenarios. Percentage-Sets 1, 2 and 3 correspond to cases when all the buildings are assumed to be of the Moderate-Code, Low-Code and Pre-Code seismic design levels respectively. As can be seen, changing from Percentage-Set 1 to Percentage-Set 2 results in a 7.5% and 1%

increase in the direct building losses and production losses respectively. Changing from Percentage-Set 1 to Percentage-Set 3 results in a 13% and 4% increase in the direct building losses and production losses respectively. There is not much difference in the fragility parameters for the acceleration sensitive components in the Low-Code and Pre-Code levels, resulting in almost equal acceleration sensitive component losses for Percentage Sets 2 and 3.

4.4.2.4 Sensitivity of the losses to change in σ_M, the building to building variability in mean seismic resistance

Here, we compare the losses obtained by increasing the parameter σ_M corresponding to the structural and non-structural components by 25% for all the building types. Table 4-16 has a summary of the results obtained in the base-case and the case with an increased σ_M. We find a 15% increase in the building losses by increasing this parameter. As can be seen in Figure 4-28, the bulk of this difference comes from regions in the distance range of 100km-750km, where the damage factor is slightly greater because of a greater value of σ_M. With an increase in σ_M, the damages near the epicenter decrease resulting in a decrease in the direct losses near the epicenter

Figure 4-29 shows the associated changes in the production losses. The production losses are mainly contributed by the epicentral region, where the damage predictions decrease with an increase in σ_M. Therefore, there is a 4% decrease in the production losses with an increase in σ_M.

4.4.2.5 Sensitivity of production losses to weights assigned to functionality of structural and non-structural components and contents

In this section, we study the sensitivity of production losses to the weights assigned to the functionality of structural and non-structural components, and contents in the estimation of the total functionality of a facility.

Table 4-17 shows the production loss estimates obtained with three alternative sets of weights. For example, one of the sets, denoted by (1.0, 0.0, 0.0, 0.0), corresponds to the case when only the structural component functionality is assumed to have an effect on the

total functionality of the facility. As can be seen in Table 4-17, there is a 12% and 31% drop in the production losses when using the weight sets (0.85, 0.05, 0.05, 0.05) and (0.50, 0.125, 0.125, 0.25) respectively, from those obtained when using a weight set of (1.0, 0.0, 0.0, 0.0).i.e., when the total functionality of a facility is assumed to depend only on the functionality of its structural components, the production losses are much higher than when it is assumed to also depend on the functionalities of the non-structural components and contents. Reason for this difference is that the mean damage factor associated with the structural components is typically higher than that associated with the non-structural components and contents, as shown in Figure 4-30.

4.5 Sensitivity of losses to alternative transportation network damage and functionality models

4.5.1 Losses under alternative bridge fragility models

Here we study the sensitivity of the losses to bridge fragility models given in HAZUS (2000), DesRoches (2002) and Hwang et al. (2000a). Here we assume that there is no slack in the production capacity. The re-routing parameter (ρ) used in Kunnumkal (2002) to model the effect of the secondary roads is set to 0.001. By assuming ρ to be very small, we restrict the link capacities to be the minimum of the bridge and pavement capacities. We set the re-routing parameter (ρ) to a value that is as close to zero to better understand the sensitivity of the indirect (production and consumption) losses to alternative bridge fragility models.

The reason for choosing such a small value of ρ for the sensitivity study is illustrated here. For example, consider a link whose pavement is undamaged, but the only bridge on the link is partially damaged. Let the functionality of the bridge be obtained to be 0.1 and 0.3 by using the bridge fragility models in DesRoches (2002) and HAZUS (2000) respectively (due to the difference in the damage predictions made by the two models). We now consider two cases, (a) ρ is chosen to be 0.3, and (b) ρ is chosen to be 0.001. In the first case, the link functionality would be obtained to be 30% of the undamaged link capacity, irrespective of the bridge fragility model (thus nullifying the difference in the damage predictions made by DesRoches (2002) and HAZUS (2000)). However, in the

second case, where ρ is chosen to be 0.001, we would obtain the link functionality to be 10% and 30% of the undamaged link capacity when using DesRoches (2002) and HAZUS (2000) respectively. Thus, we retain the differences in the functionality predictions made by the two bridge fragility models for the indirect loss estimation when using a ρ that is close to zero.

Table 4-18 has the loss estimates obtained by using the alternative bridge fragility models. As can be seen, DesRoches (2002) predicts higher bridge losses compared to the other two sources. This is due to the differences in the mean damage factor predictions of the three bridge fragility models. DesRoches (2002) predicts almost 100% damage near the epicenter, where most of the bridge inventory is located, as shown in Figure 4-31. This results in higher losses near the epicenter, as shown in Figure 4-32 . HAZUS (2000) on the other hand predicts a damage of about 65% near the epicenter, but its damage predictions attenuate very quickly with distance compared to the other two sources, resulting in lower total bridge losses. Hwang et al. (2000a) restricts the maximum damage factor to 0.8 and predicts lower bridge losses near the epicenter compared to DesRoches (2002).

The greater production losses when using DesRoches (2002) are due to a greater reduction in productions far from the epicentral region due to the dependence, to some extent, on productions in the epicentral region. This greater reduction in the productions is in turn due to the greater bridge damage and hence a greater loss in functionality predicted by DesRoches (2002) to the highway network.

	Percentage Set 1	Percentage Set 2	Percentage Set 3
Moderate-Code Buildings	100	0	0
Low-Code Buildings	0	100	0
Pre-Code Buildings	0	0	100
Acceleration Sensitive Component Losses ($Billion)	8.65	11.32	11.33
Drift Sensitive Component Losses ($Billion)	20.93	21.16	21.57
Structural Component Losses ($Billion)	15.69	16.21	18.33
Total Building Losses ($Billion)	45.27	48.7	51.23
Production Losses ($Billion)	48.79	49.34	50.93
Consumption Losses ($Billion)	1.85	1.85	2.02

Table 4-15: Comparison of the loss estimates obtained with alternative proportion of the Moderate-Code, Low-Code and Pre-Code buildings.

	Nominal σ_M	Increased σ_M
Acceleration Sensitive Component Losses ($Billion)	11.33	14.29
Drift Sensitive Component Losses ($Billion)	21.57	24.03
Structural Component Losses ($Billion)	18.33	20.61
Total Building Losses ($Billion)	51.23	58.93
Production Losses ($Billion)	50.93	48.87
Consumption Losses ($Billion)	2.02	1.97

Table 4-16: Sensitivity of the loss estimates to changes in the parameter σ_M

Weights assigned to the component functionalities				Production losses ($Billion)
Structural Components	Acceleration Sensitive Components	Drift Sensitive Components	Contents	
1.000	0.000	0.000	0.000	50.93
0.850	0.050	0.050	0.050	44.92
0.50	0.125	0.125	0.25	35.01

Table 4-17: Sensitivity of the production losses to alternative sets of weights assigned to the functionality of the individual components of a facility

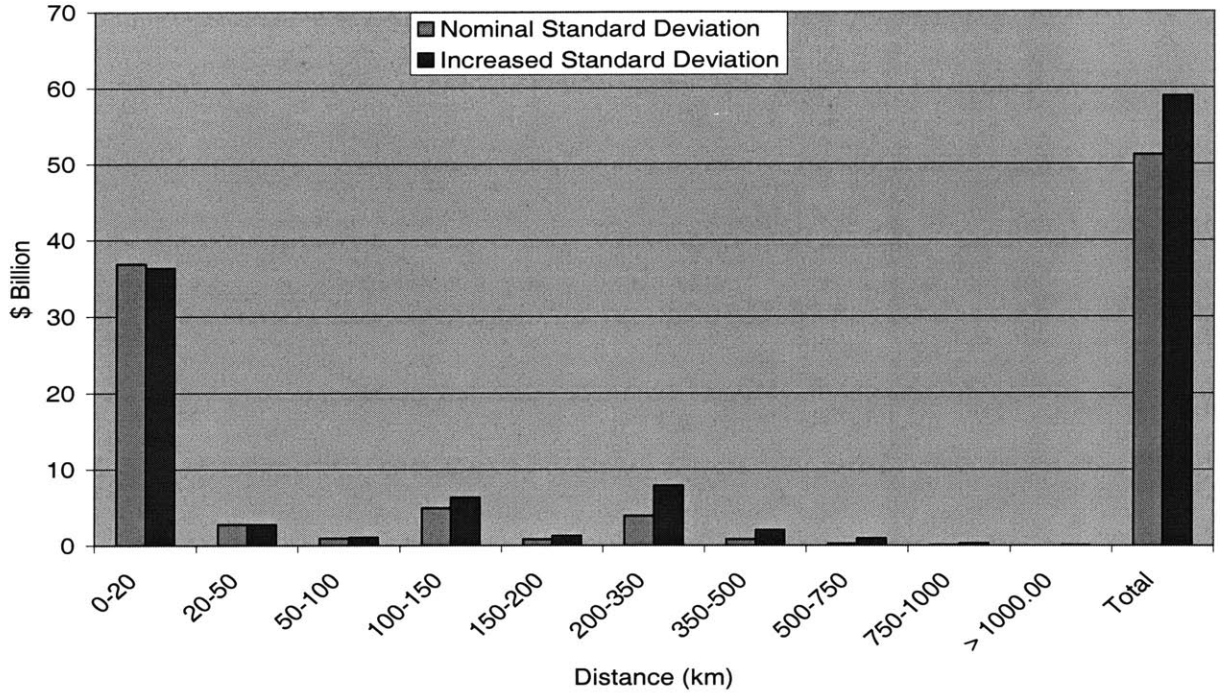

Figure 4-28: Distribution of the direct building losses as a function of the distance from the epicenter, with changes in the parameter σ_M

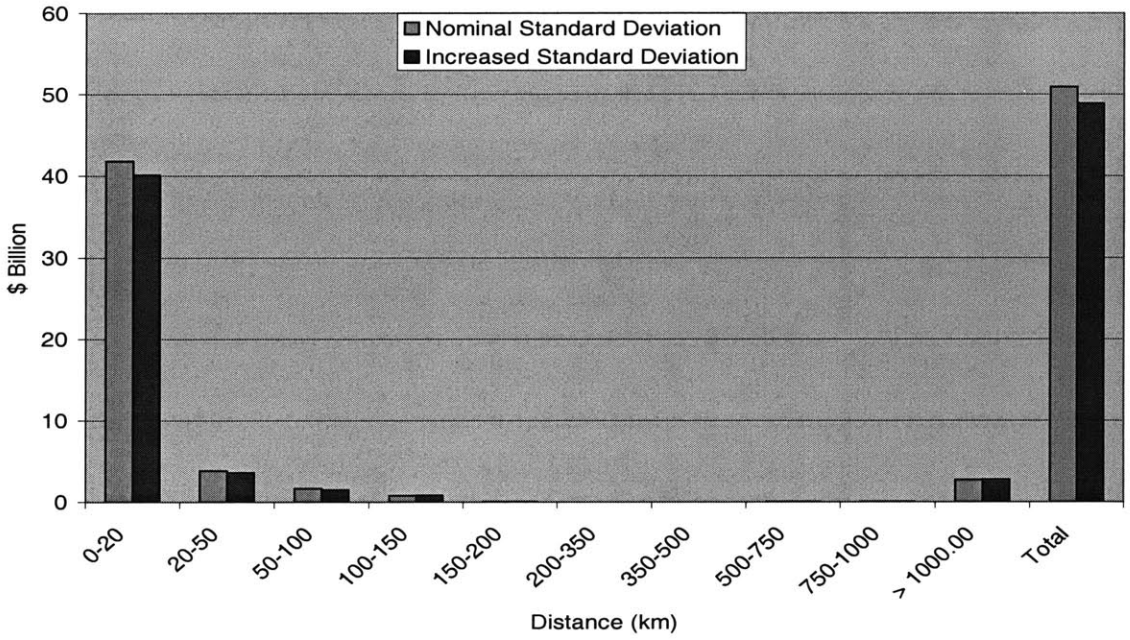

Figure 4-29: Distribution of the production losses as a function of the distance from the epicenter, with changes in the parameter σ_M

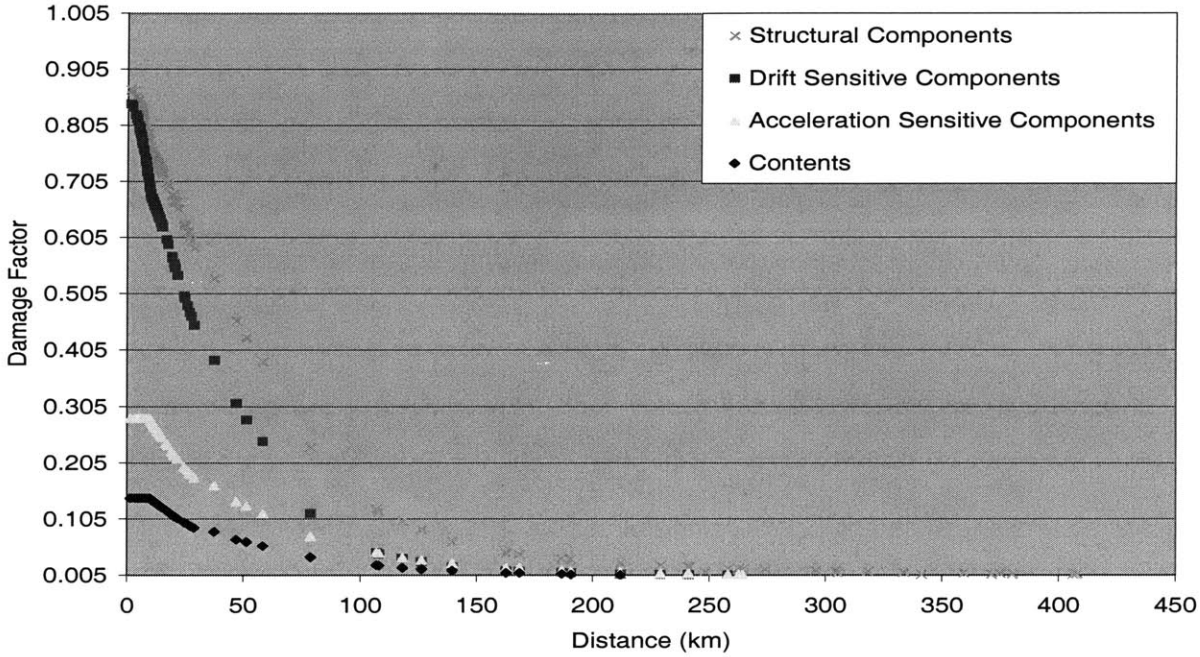

Figure 4-30: Comparison of the damage factors associated with different building components in Residential sector

4.5.2 Sensitivity of indirect losses to highway network damage and rerouting

In this section, we look at the sensitivity of production and consumption losses to changes in the highway network fragility model and the rerouting parameter (ρ). Here, we consider the scenario when there is no slack in the production capacity. Table 4-19 has a summary of the sensitivity runs. Runs 3 and 4 consider rather pessimistic scenarios, where all the bridges within the study area (<500km radius around Memphis) are assumed to be damaged due to the earthquake. It is felt that such a pessimistic scenario would give a better understanding of the effect of the rerouting parameter and the highway network functionality on the indirect losses. As can be seen, changing the rerouting parameter from 0.001 to 0.25 results in a 27% and 26% decrease in the production losses and consumption losses respectively when all the bridges are assumed to be damaged. On the other hand, with the bridge fragility model of HAZUS (2000), there is almost no change in the production and consumption losses when changing the rerouting parameter from 0.001 to 0.25. These results suggest a relatively smaller

Bridge Fragility Model	Direct Bridge Losses ($ Billion)	Production Losses ($Billion)	
		Production Loss Method 1	Production Loss Method 2
HAZUS (2000)	1.29	51.77	4.06
Hwang et al. (2000a)	1.80	53.00	5.30
DesRoches (2002)	2.98	54.87	7.17

Table 4-18: Comparison of the losses with alternative bridge fragility models

Run No.	Link Fragility Model	Bridge Fragility Model	Rerouting Parameter (ρ)	Production Losses ($Billion)	Consumption Losses ($Billion)
1	Nominal	HAZUS (2000)	0.001	52.82	29.08
2	Nominal	HAZUS (2000)	0.25	52.78	29.07
3	Nominal	All Bridges Damaged	0.001	74.1	39.7
4	Nominal	All Bridges Damaged	0.25	53.67	29.42
5	No Damage to any link	No Damage to any Bridge	---	52.32	28.79

Table 4-19: Comparison of the losses with alternative highway network fragility models and rerouting parameter, no slack in production

reduction in the functionality of the highway network when using the HAZUS (2000) bridge fragility model and a relatively smaller effect of the value of the rerouting parameter when there is a smaller loss in functionality of the highway network due to bridge damage.

There is a 29% and 27% decrease in the production and consumption losses respectively when the scenario is changed from that with complete bridge damage to a scenario where there is no highway component damage (comparing run no.'s 3 and 5). Figure 4-33 has the distribution of the production losses with distance for these two cases. As can be seen, there is not much change in the production losses near the epicenter, but beyond 100 km, there is a considerable influence of the complete bridge damage on the production losses. This is due to the inter-dependence of the economic sectors in geographically separated regions, through the transportation network.

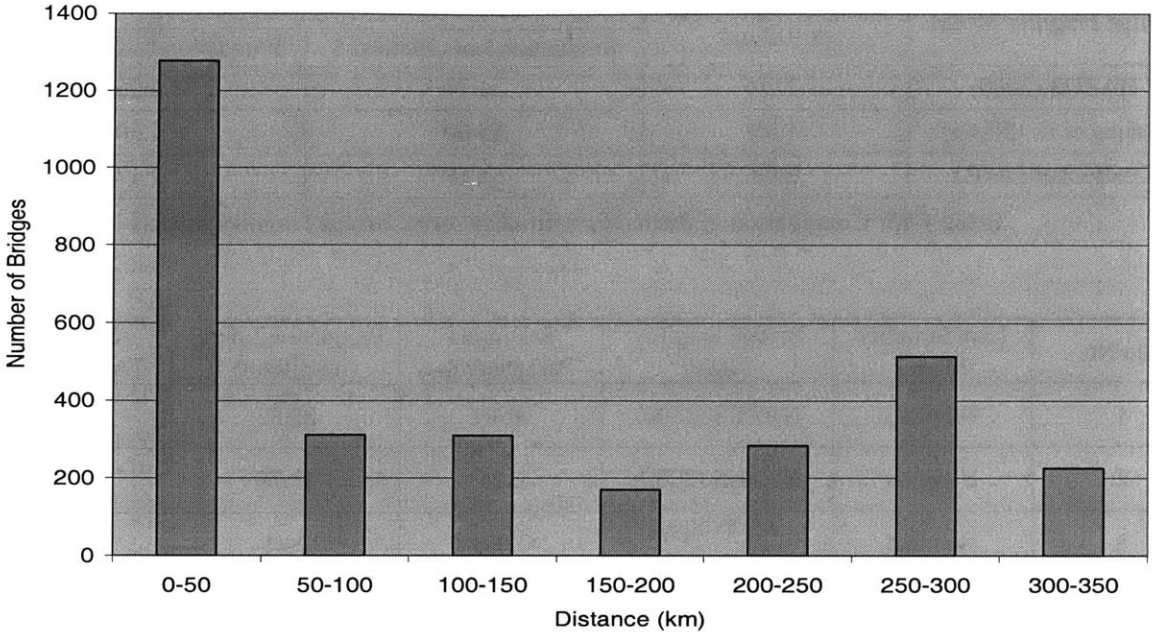

Figure 4-31: Distribution of the bridge inventory as a function of the distance from the epicenter

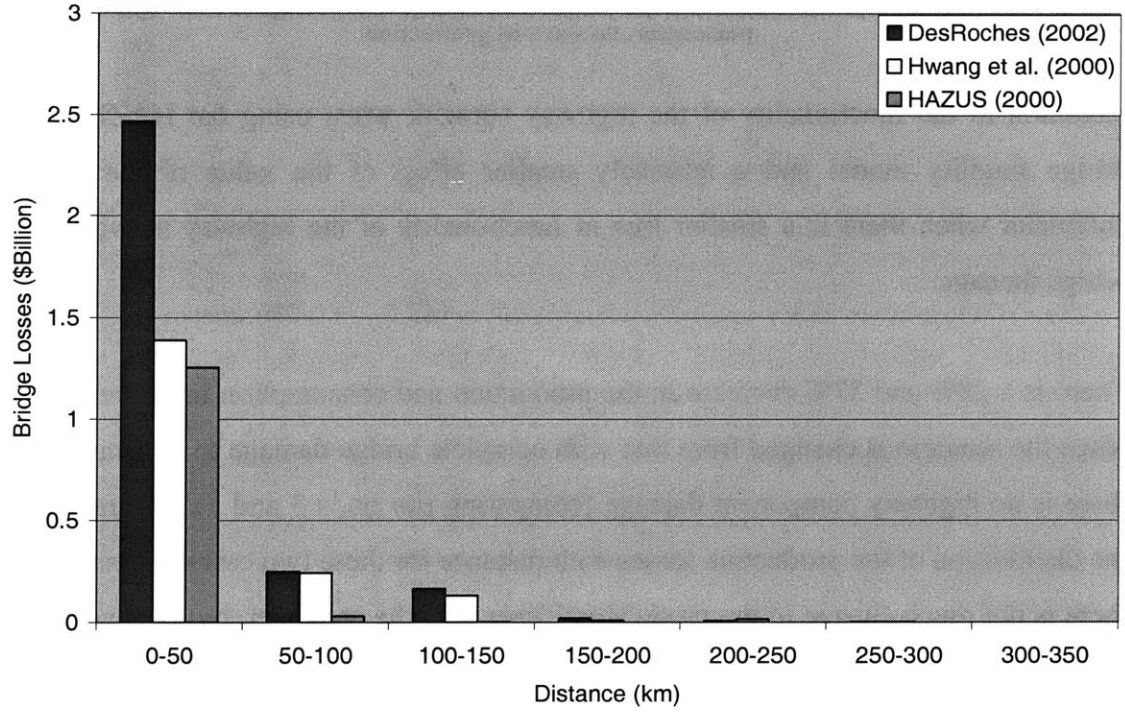

Figure 4-32: Comparison of the bridge losses estimated by alternative bridge fragility models, as a function of distance from the epicenter

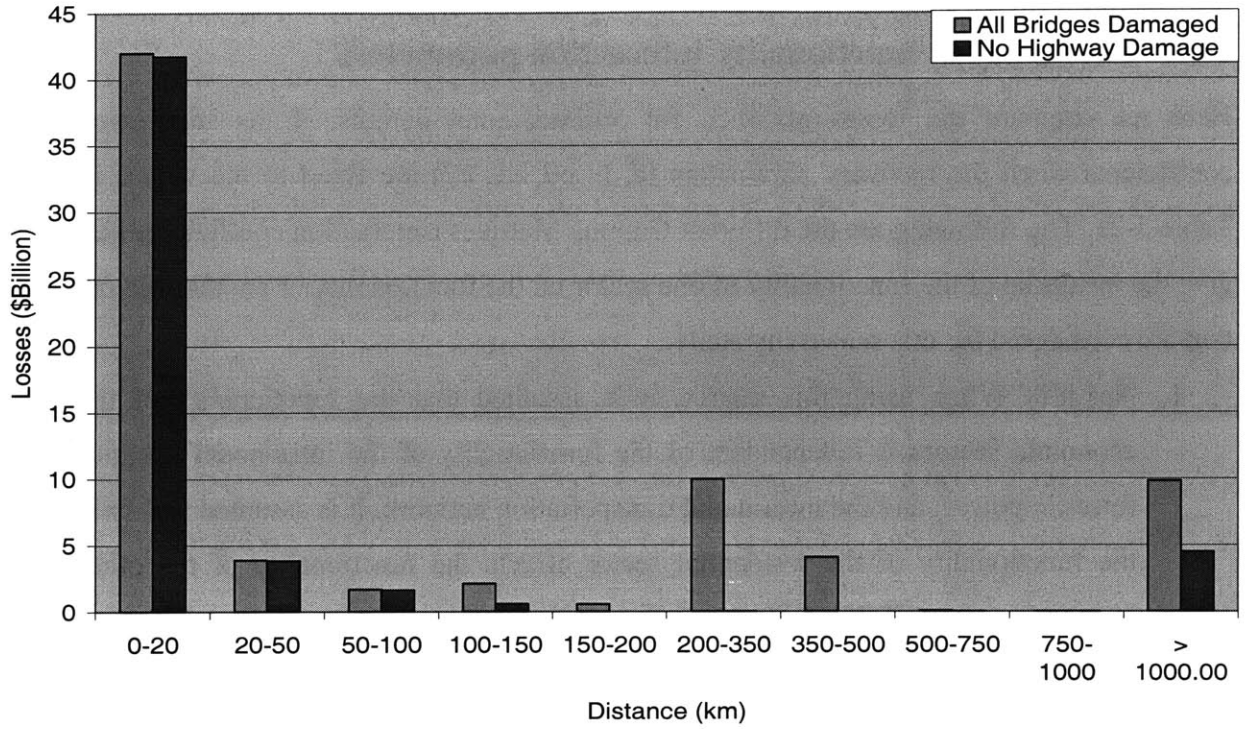

Figure 4-33: Distribution of the production losses as a function of the distance from the epicenter, when there is complete bridge damage and when there is no highway damage

Summary

- The effect of the re-routing parameter, ρ, on the indirect losses is dependent on the extent of bridge damage. For example, changing the value of ρ from 0.25 to 0.001 has a much smaller effect on the indirect losses when the bridge fragility model of HAZUS (2000) is used than when all the bridges are assumed to be damaged.
- Productions in regions far from the epicenter get affected much more than those near the epicenter, with an increase in the transportation network damage.

4.6 Sensitivity of the losses to recovery and functionality-interaction parameters

4.6.1 Sensitivity to functionality-interaction parameters

Here we compare the losses obtained for various combinations of the interaction coefficients when the recovery parameters (a, b, c0, c1, c2) are fixed to the values in Table 3-21. The following are the different Gamma Matrices (interaction coefficients that give the influence of the functionality of one sector on the functionality of another sector) that are considered for this sensitivity study:

1. **NoLifT:** When using this matrix, it is assumed that the functionality of the economic sectors is independent of the functionality of the intra-nodal lifelines (electric power) and the intra-nodal transportation network. It is assumed that only the functionality of the residential sector affects the functionality of the other economic sectors. Table 4-20 shows the corresponding gamma coefficients.
2. **NoRes:** Here it is assumed that the functionality of the residential sector does not influence the functionality of other economic sectors. Table 4-21 shows the gammas corresponding to the NoRes case.
3. **Zero**: The functionality of the economic sectors is assumed to be independent of the functionality of the residential sector, utilities and intra-nodal transportation network. Therefore all the entries in this matrix are zeroes.

The following are the different Beta Matrices (interaction coefficients that give the influence of the functionality of one sector on the recovery rate of another sector) that are considered:

1. **NoLifT:** Here, the rate of recovery of the economic sectors is assumed to be independent of the functionality of the intra-nodal utilities (electric power) and the intra-nodal transportation network. Only the functionality of the residential sector is assumed to have an effect on the rate of recovery of the economic sectors. Table 4-22 shows the betas corresponding to this matrix.
2. **NoRes:** This matrix assumes that the functionality of the residential sector does not have any effect on the rate of recovery of the other sectors. The corresponding betas are shown in Table 4-23.

	Residential	Lifelines	Transportation
Residential		0	0
Commercial	0.6	0	0
Heavy Industry	0.3	0	0
Light Industry	0.3	0	0
Food and Drug	0.3	0	0
Chemical	0.3	0	0
High Technology	0.3	0	0

Table 4-20: γ 's corresponding to NoLifT matrix

	Residential	Utilities	Transportation
Residential		0.5	0.3
Commercial	0	0.5	0.4
Heavy Industry	0	1.0	0.3
Light Industry	0	1.0	0.3
Food and Drug	0	1.0	0.3
Chemical	0	0.9	0.3
High Technology	0	0.9	0.3

Table 4-21: γ 's corresponding to NoRes matrix

	Residential	Utilities	Transportation
Residential	0.0	0	0
Commercial	0.5	0	0
Heavy Industry	0.5	0	0
Light Industry	0.5	0	0
Food and Drug	0.5	0	0
Chemical	0.5	0	0
High Technology	0.5	0	0

Table 4-22: β 's corresponding to NoLifT matrix

3. **TransReduced:** This matrix assumes that the rate of recovery of the economic sectors is dependent on the residential sector, utilities and intra-nodal transportation network. However, the parameters that control the dependence of the rates of recovery of the economic sectors on the functionality of the intra-nodal transportation network are reduced by half from the values given in Table 3-24.
4. **Zero:** Here it is assumed that the rate of recovery of the sectors is independent of the functionality of the residential, electric power and intra-nodal transportation network.

Observations

- Table 4-25 compares the production losses at various combinations of the beta and gamma matrices. The production losses decrease by about 37% when the interaction coefficients with the utilities and the intra-nodal transportation network are set to zero. As the utilities recover much earlier than the intra-nodal transportation network, the production losses are much more sensitive to the functionality of the intra-nodal transportation network than to that of the utilities. However, there is a 11% drop in the production losses when the functionality of the residential sector is assumed to have no effect on the functionality and recovery of the economic sectors. The above comparisons suggest that, when using the interaction coefficients given in Table 3-23 and Table 3-24, the functionality of the intra-nodal transportation network has the greatest influence on the production losses, followed by the functionality of the residential sector.
- It can also be seen in Table 4-25 that when the nominal β's corresponding to the intra-nodal transportation network are reduced by half, the production losses decrease by about 8%.
- When using the nominal values of the interaction coefficients, the β coefficients have larger influence on the production losses than the γ coefficients. This can be inferred by comparing Runs 1, 4 and 5.
- Production losses decrease by about 45% when the economic sectors recover independently (corresponding γ and β coefficients are zeroes), suggesting a large influence of the interaction coefficients on the production losses.
- The additive interaction model given in Kunnumkal (2001) predicts production losses that are about 32% lesser than those given by his multiplicative interaction model, due to its averaging effect (as was described in Section 3.6.1).

	Residential	Utilities	Transportation
Residential		0.1	0.6
Commercial	0	0.3	0.9
Heavy Industry	0	0.3	0.9
Light Industry	0	0.3	1.0
Food and Drug	0	0.3	1.0
Chemical	0	0.3	1.0
High Technology	0	0.3	1.0

Table 4-23: β's corresponding to NoRes matrix

	Residential	Utilities	Transportation
Residential	0	0.1	0.3
Commercial	0.5	0.3	0.45
Heavy Industry	0.5	0.3	0.45
Light Industry	0.5	0.3	0.5
Food and Drug	0.5	0.3	0.5
Chemical	0.5	0.3	0.5
High Technology	0.5	0.3	0.5

Table 4-24: β's corresponding to TransReduced matrix

Run No.	Interaction Model	Gamma Matrix	Beta Matrix	Production Losses ($ Billion)
1	Multiplicative	Nominal	Nominal	50.93
2	Multiplicative	NoLifT	NoLifT	32.04
3	Multiplicative	NoRes	NoRes	45.4
4	Multiplicative	Zero	Nominal	48.79
5	Multiplicative	Nominal	Zero	34.99
6	Multiplicative	Zero	Zero	28.13
7	Multiplicative	Nominal	TransReduced	46.97
8	Additive	Nominal	Nominal	34.7

Table 4-25: Sensitivity of the production losses to various combinations of the functionality interaction coefficients

4.6.2 Sensitivity to recovery parameters

- Figure 4-34 shows the sensitivity of the production losses, if the time to full recovery of each sector is changed by 50%. It can be seen that the recovery time of the intra-nodal transportation has the greatest effect on the production losses. This is mainly because of the large influence that this sector's functionality has on the recovery of the other economic sectors when using the nominal interaction coefficients given in Table 3-23 and Table 3-24. The recovery time of the Commercial sector comes next to that of the intra-nodal transportation in

influencing the production losses. The reason for this large influence of the Commercial sector compared to the influence of other industrial sectors is that this sector is the main contributor to the total production losses. This is in turn due to the relatively large production value associated with the Commercial sector in a majority of the geographical regions and the greater dependence of other sectors on the output from this sector.

- Figure 4-35 shows the sensitivity of the production losses to different recovery times of the Residential sector. One can see an almost linear change in the production losses with changes in the time to recovery of the residential sector.
- There is a 25% increase in the production losses when the parameter a (parameter that controls the recovery rate) corresponding to all the social function classes, is decreased by one standard deviation. On the other hand, there is a 20% decrease in the production losses when a is increased for all the classes by one standard deviation.

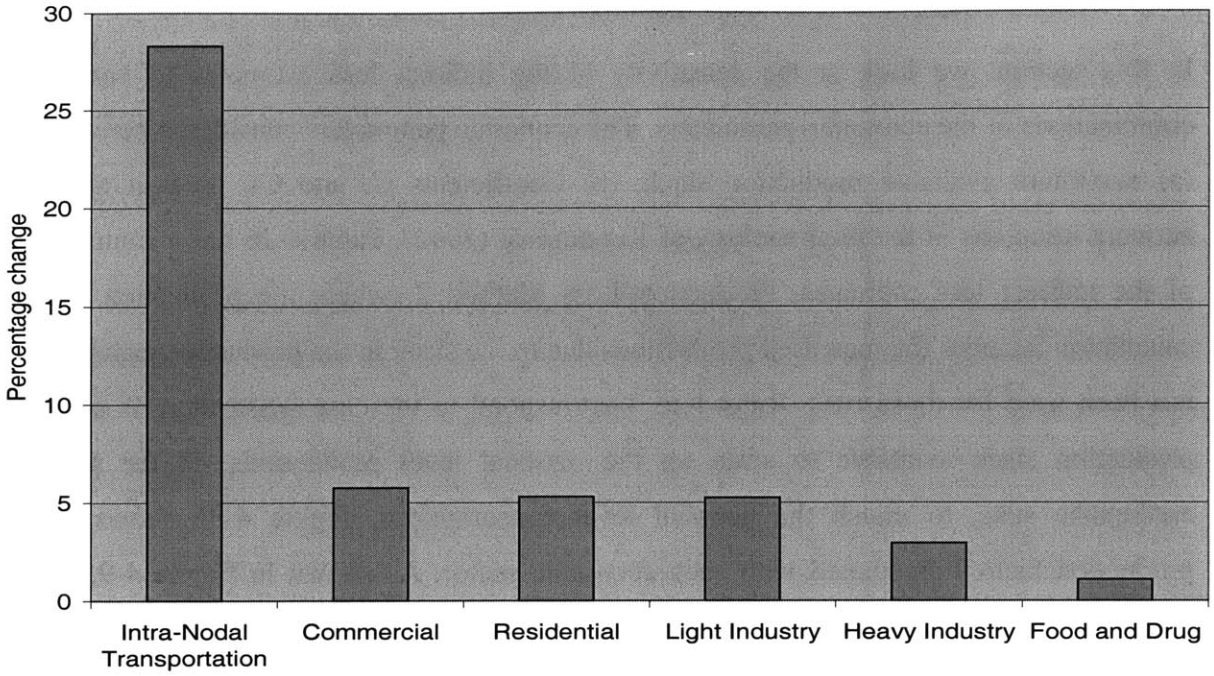

Figure 4-34: Sensitivity of the production losses to change in the nominal time to reach full-functionality by 50%

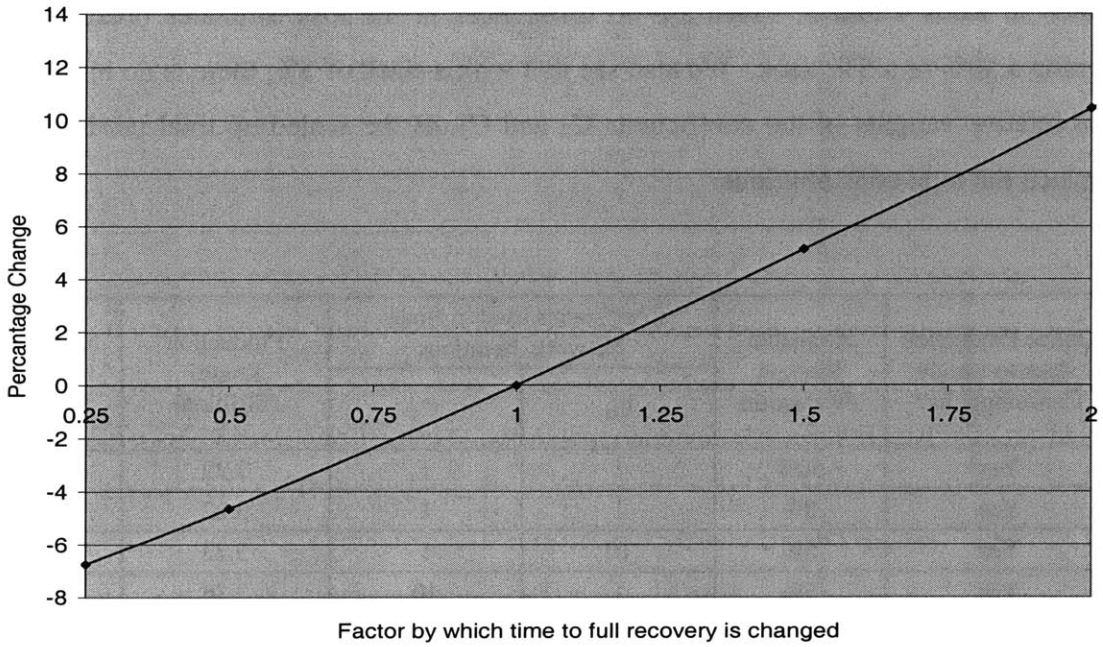

Figure 4-35: Sensitivity of the production losses to changes in the time taken by the residential sector to become fully functional, from the nominal time

4.7 Sensitivity to economic parameters

In this section, we look at the sensitivity of the indirect loss estimates to various combinations of the economic parameters. The economic parameters considered here are, (a) maximum available production slack, (b) Coefficients C_2 and C_3, used in node-network iterations of the methodology of Kunnumkal (2002). Table 4-26 has a summary of the indirect loss estimates. Production Loss Method 2 (where the production loss calculation includes the increased productions due to the slack in the production capacity) has been used for these runs. Runs 1 to 4 correspond to the case when there is some production slack available to scale up the national level productions, in the post-earthquake state, to match the national level consumptions. Figure 4-36 shows the production factors associated with each economic sector. As shown in Figure 4-9, the production in the earthquake affected region is very small compared to the total national-level production. Therefore, about 1% increase in the national productions, immediately after the earthquake, is sufficient to match the national level consumptions, which are assumed to be the same as the pre-earthquake values. This effect is seen in the losses obtained in Runs 1 and 2. There are no differences in the loss estimates obtained by assuming a 50% or a 5% slack. We also see that with a slack of 5%, there is no influence of the relative weights of the coefficients C_2 and C_3, as the scaled-up total productions can match the total consumptions.

Run No.	Utilize Production slack to match Consumptions?	Available Slack in Production	Coefficients used in Node-Network Iterations		Production Losses ($Billion)	Consumption Losses ($Billion)
			C_2	C_3		
1	Yes	50%	1	1	3.22	2.02
2	Yes	5%	1	1	3.22	2.02
3	Yes	5%	10	1	3.22	2.03
4	Yes	5%	1	10	3.34	1.98
5	No	None	1	1	52.79	29.07
6	No	None	10	1	52.79	29.07
7	No	None	1	10	102.9	50.7

Table 4-26: Sensitivity of the production losses and consumption losses to various combinations of the economic parameters, Production Loss Method 2

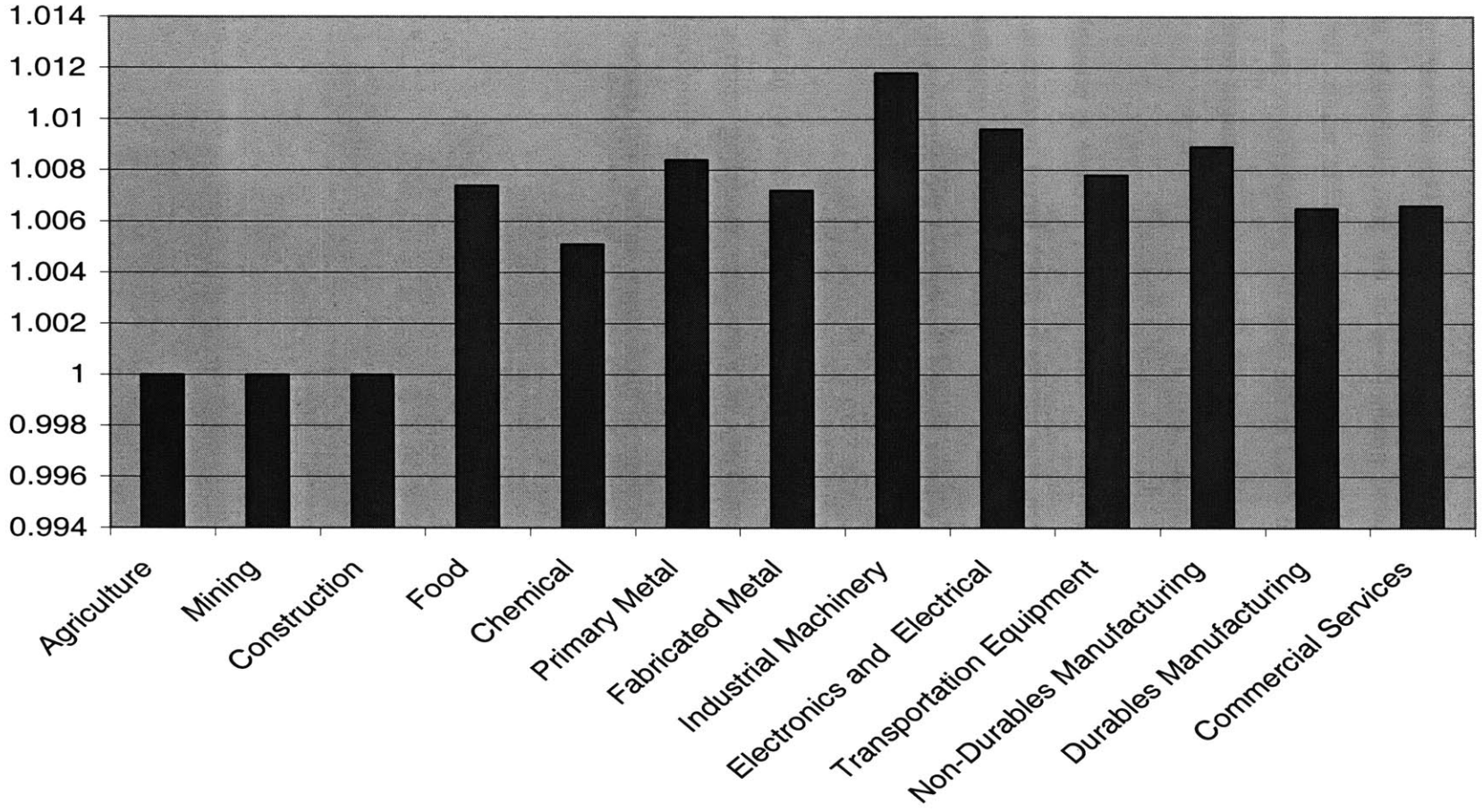

Figure 4-36: Factors by which the national-level productions of each sector are increased to match the national-level consumptions, 0.01 days after the earthquake

The indirect losses (consumption + production losses) associated with the case when there is no slack in the production capacity are much greater than those obtained when there is slack in the production capacity (comparing Runs 2 and 5). This increase in the indirect losses is mainly due to the reduced productions in the post earthquake state, which cannot match the national consumption demands. One possible reason for the difference in the loss estimates in the two cases is the assumed availability of the extra production capacity, free of any cost. In reality, using the extra capacity might result in additional costs, which are not considered in our analysis.

In Run 7, greater importance is given to keeping the consumptions as close as possible to their pre-earthquake levels. As can be seen, this results in much larger production and consumption losses, compared to the case when greater weight is placed on maximizing the productions. This is due to the ripple effects caused throughout the economy by the reduced productions.

In this chapter, we have studied the sensitivity of the losses to the uncertainty in various components. We have looked at the sensitivity to alternative modeling approaches, attenuation relations, structural-occupancy mappings, fragility parameters, functionality-interaction coefficients and some of the economic parameters. In the next chapter, we summarize our findings and suggest areas for future research.

5 Conclusion

5.1 Summary and main results

We have assessed the uncertainty in models and parameters used for earthquake loss estimation and performed sensitivity analyses using the earthquake loss methodology developed by Kunnumkal (2002). Specifically, we have considered models, inventories and relations that are applicable to the Central and Eastern United States (CEUS). A summary of our results is given next.

5.1.1 Uncertainty assessment

We have assessed uncertainty on (1) ground motion attenuation, (2) soil amplification, (3) building inventory, (4) building fragility, (5) bridge fragility, and (6) loss of functionality and recovery of social function. A summary of our findings is presented below:

- For loss estimation in the CEUS, we recommend the use of the macroseismic attenuation relation of Bollinger (1977) because this relation is based on individual damage reports rather than on subjectively drawn isoseismal contours or on "wrong regressions."
- Atkinson and Boore (1995), Frankel et al. (1996) and Toro et al. (1997) are three often used engineering attenuation relations in the CEUS. In order to account for epistemic uncertainty, we have given equal weight to each of these three relations.
- Concerning site amplification, we have assigned weights of 0.4, 0.4 and 0.2 to the amplification factors given in Borcherdt et al. (2002), Hwang et al. (1997a) and Dobry et al. (2000). We give a lower weight to Dobry et al. (2000) mainly based on the comments in Borcherdt et al. (2002), who feel that the codal values may be on a lower side.
- We have derived building fragility models in terms of instrumental ground motion parameters, using data in HAZUS (2000).
- We have obtained corresponding fragility models in terms of MMI using ATC-13 and FEMA (1990). We have assigned a weight of 0.6 to the mean resistance

estimates in FEMA (1990) and a weight of 0.4 to those in ATC-13, in recognition of the fact that ATC-13 considered specifically the California region and not the CEUS.

- We have compared different structural-occupancy models applicable for the CEUS. We have found that the estimates for the emergency response sector (Police/Fire Station) in HAZUS (2000) and French et al. (2000) are similar. However, for the residential sector, differences exist between HAZUS (2000) and Jones et al. (1996). To account for epistemic uncertainty, we propose two alternative structural-occupancy mappings for the CEUS. The basic difference between these mappings is the distribution of the residential sector inventory among different height categories and the relative proportions of various sub-sectors (single family dwellings, multi-family dwellings, etc.) within the residential sector.
- Three bridge fragility models, described in HAZUS (2000), Hwang et al. (2000a) and DesRoches (2002), have been compared. The damage estimates from HAZUS (2000) are much lower than those from the other two models. Reasons for these differences are not fully understood. For use in earthquake loss estimation, we have assigned weights of 0.2, 0.4 and 0.4 to HAZUS (2000), Hwang et al. (2000a) and DesRoches (2002), respectively, to reflect the epistemic uncertainty. Greater weights are given to Hwang et al. (2000a) and DesRoches (2002) mainly because these studies are based on the analysis of bridges in the CEUS.
- There are large epistemic uncertainties in the loss of function and recovery models and parameters, mainly due to lack of statistical data. We have compared the models of ATC-13, RMS (1994) and Kunnumkal (2001). We recommend the use of the multiplicative form of the functionality-interaction model and the recovery model and parameters given by Kunnumkal (2001). The β coefficients, which govern the dependence of the rate of recovery of the economic sectors on the functionality of the intra-nodal transportation, as given in Kunnumkal (2001), may be high. We recommend the β values that correspond to the *TransReduced* matrix of Table 4-24.

5.1.2 Sensitivity analysis

We have studied the sensitivity of the losses to various uncertain parameters, using the earthquake loss estimation methodology of Kunnumkal (2002) and scenario earthquakes in the New Madrid region. We have found that:

- The production losses obtained when using a 5% slack in the production capacity with Production Loss Method 1 (where the production loss calculation does not include the increased productions due to slack in the production capacity) and when there is no slack in production are very similar. Therefore, the sensitivity results for the "5% slack in production capacity with Production Loss Method 1" case also reflect the sensitivities when there is no production capacity slack.
- There is a considerable difference in the direct loss estimates given by the engineering and macroseismic approaches. The damage estimates in the engineering approach decay much faster with epicentral distance than those in the macroseismic approach. This is the reason for the greater direct losses produced by the macroseismic approach. However, the loss of functionality in the epicentral region is greater in the engineering approach, resulting in greater production losses in the epicentral region. When there is no slack in production, almost all of the production losses are contributed by the epicentral region. Therefore, engineering approach predicts much higher production losses than the engineering approach. However, when there is slack in the production capacity, greater production losses in the epicentral region are compensated by greater production gains from regions far away from the epicenter in case of the engineering approach. As a result, the losses from the macroseismic and engineering approach are not very different.
- There is a considerable difference in the loss estimates given by Frankel et al. (1996) and those given by Toro et al. (1997) and Atkinson and Boore (1995). These differences increase with the proportion of inventory in the range of 100-350 km due to the much higher ground motion estimates given by Frankel et al. (1996) in this distance range. The estimates by Toro et al. (1997) and Atkinson and Boore (1995) are rather similar.

- The loss estimates obtained when using the soil amplification factors of Borcherdt et al. (2002) and Hwang et al. (1997a) are rather consistent. However, the estimates when using the amplification factors in Dobry et al. (2000) are much lower.
- When using the alternative structural-occupancy mappings that were proposed in Section 3.4.2, the differences in the direct losses are much greater than the differences in the indirect losses. This is due to the fact that these mappings mainly differ in the structural class distribution for the residential sector, which mainly influences the direct losses. The effect of using alternative mappings depends on the modeling approach (engineering and macroseismic). When using the engineering approach, Mapping 1 (in Table 3-16) predicts higher structural losses and lower non-structural and contents losses than Mapping 2 (in Table 3-17). This results in a very small (<1%) difference in the total direct losses given by the two mappings. However, the difference in the direct losses when using the macroseismic approach is much larger (5%-15%).
- The losses obtained when using macroseismic fragilities based on FEMA (1990) are much greater than those based on ATC-13. There is a 50% difference in the direct losses. However, the difference between the production losses in FEMA (1990) and ATC-13 is about 35% with no production slack and about 10% with a 5% slack in the production capacity.
- Wood-Frame (W), Concrete Shear Walls (C2) and Unreinforced Masonry (URM) buildings have a greater effect on the overall (direct and indirect) economic losses, due to their greater presence in the residential sector. Steel Light Frame (S3) buildings have a large influence mainly on the indirect losses (due to their presence in the commercial and the industrial sectors).
- The production losses obtained from the engineering approach are very sensitive to the weights assigned to the structural, non-structural and contents functionalities. This is due to the differences in the damages of different building components. In general, the structural and drift-sensitive non-structural damages are much greater than the acceleration-sensitive and content damages.

- The bridge losses predicted using the fragilities in HAZUS (2000) and Hwang et al. (2000a) are less than those predicted by the fragility model of DesRoches (2002) by about 55% and 40%, respectively. The main reason for these differences is that DesRoches (2002) predicts much higher damages near the epicenter, where most of the bridge inventory in the study area is located.
- The effect of the rerouting parameter on the indirect losses has been found to be sensitive to the state of damage of the transportation network. When the bridge fragility model of HAZUS (2000) is used, increasing the rerouting parameter from 0.001 to 0.25 does not have any influence on the indirect losses. However, for the same increase in the rerouting parameter when all the bridges in the study region are damaged, the decrease in the indirect losses is about 25%.
- Damages to the intra-nodal transportation network, commercial, residential, heavy industry, light industry and food & drug processing sectors are the main factors that affect indirect losses. The functionality of the Intra-nodal transportation network has a greater influence on the production losses than the residential sector and the utilities (electric power). The lower influence of the utilities is mainly due to the fact that utilities become fully functional much earlier than the intra-nodal transportation.
- The β coefficients (parameters that give the influence of the functionality of one sector on the recovery rate of another sector) have a relatively larger influence on the production losses than the γ coefficients (parameters that give the influence of the functionality of one sector on the functionality of another sector).
- Production losses decrease by about 45% when the economic sectors are assumed to recover independently i.e., when γ and β coefficients are changed from their nominal values to zeroes, showing a large dependence of production losses on the functionality-interaction coefficients.

5.2 Future research directions

- The sensitivity analysis in this thesis could be used a starting point for a more comprehensive uncertainty propagation analysis. Parameters and models that are

not found to have much influence on the losses could be used at their best estimate values so that the analysis is simplified and those that have significant influence on the losses should be understood better so that the uncertainty in these components can be reduced.

- From the sensitivity studies, we have observed that Wood-Frame (W), Concrete Shear Walls (C2), Unreinforced Masonry (URM), Steel Light Frame (S3) are the building types that affect the losses the most. Future research should focus on gaining a better understanding of the seismic resistance characteristics of at least some of these building types so that the uncertainty associated with the damages to these buildings decrease, resulting in a decrease in the overall uncertainty in the losses.
- Business-interruption losses from the Commercial, Heavy Industry, Light Industry and Food & Drug Processing sectors contribute significantly to the overall business-interruption losses. Damages to the residential sector affect not only the direct building losses, but also the overall business-interruption losses due to the assumed dependence of the economic sectors on human resources. Hence, to obtain more reliable loss estimates, future research should focus on refining models for the estimation of the damage, functionality, and recovery of at least some of the above five sectors.
- Business interruption losses have been found to be very sensitive to the weights given to the structural, non-structural and contents functionalities in the estimation of the total functionality of a facility. Future research should investigate the effect that the functionalities of various components have on the overall functionality of a facility.
- Large uncertainty exists regarding the influence that functionalities of the residential sector and lifelines such as water supply, electric power and transportation have on the functionalities and rates of recovery of the economic sectors. Future research should focus on gaining a better understanding of the extent of the dependence of the economic sectors on lifelines and the residential sector. Moreover, to improve the accuracy of the business-interruption related

losses, the models used to estimate the damage, and loss-of-function and recovery of lifelines should be refined.

- Additional sensitivity studies in future could include the use of alternative seismic vulnerability classes and economic sector classifications.
- Kunnumkal (2002), which has been used as the basis for the sensitivity studies in this thesis, could be improved in some aspects. These include:
    - *The transportation network models*: Cross-hauling of commodities, passenger flows and network congestion can be modeled in the methodology. However, to model cross-hauling and passenger flows one needs to consider OD flows or a path-based formulation, which is generally harder than a link-based formulation. Network congestion could be modeled by assuming a non-linear cost function. However, this could increase the complexity of the problem.
    - *Slack in the production capacity*: Accurate estimates of slack in the production capacities of different economic sectors in different regions should be ascertained in order to obtain reliable estimates of the indirect losses (as has been seen, the indirect losses for the case with no slack in production capacity are much different for a case with a 5% slack in production capacity). In addition, the cost, if any, associated with the use of slack in the production capacity needs to be incorporated in the loss estimation methodology.
    - *Post-earthquake consumptions*: Kunnumkal (2002) assumes that the post-earthquake domestic consumptions are same as the pre-earthquake values. Future research should understand the influence of the earthquake damage on the domestic consumptions to better model the indirect impact estimation.

Bibliography

Anderson, J.G. (1978). "On the attenuation of Modified Mercalli Intensity with distance in the United States." *Bulletin of Seismological Society of America*, 68(4): 1147-1179.

ATC-13 (1985). "Earthquake damage evaluation data for California." ATC-13. Redwood City, CA: Applied Technology Council (ATC).

Atkinson, G.M., and Boore, D.M. (1995). "New ground motion relations for eastern North America." *Bulletin of Seismological Society of America*, 85, 17-30.

Atkinson, G.M., and Boore, D.M. (1997). "Some comparisons between recent ground-motion relations." *Seismological Research Letters*, 68(1), 24-40.

Bernreuter, D.L. (1981). "Seismic hazard analysis: Application of methodology, results, and sensitivity studies." *U.S. Nuclear Regulatory Commission Report NUREG/CR-1582*, Vol. 4, Washington, D.C.

Bollinger, G.A. (1977). "Reinterpretation of the intensity data for the 1886 Charleston, South Carolina, earthquake." *U.S. Geological Survey Professional Paper*, 1028, 17-32.

Boore, D.M., Joyner, W.B. and Fumal, T.E. "Estimation of response spectra and peak accelerations from western North American earthquakes: An interim report, Part 2." *U.S. Geological Survey Open-File Report*, 93-509.

Borcherdt, R.D., (2002). "Empirical evidence for site coefficients in building code provisions." *Earthquake Spectra*, 18(2), 189-217.

Bureau of Transportation Statistics (2000). "National Transportation Atlas Database." CDROM.

Campbell, K. W. (1986). "An empirical estimate of near-source ground motion for a major, m_b=6.8, earthquake in the eastern United States." *Bulletin of Seismological Society of America*, 76(1), 1-17.

Chandra, U. (1979). "Attenuation of intensities in the United States." *Bulletin of Seismological Society of America*, 69(6), 2003-2024.

Cho, S., Gordon, P., Richardson, H.W., Moore II, J.E. and Shinozuka, M. (2000). "Analyzing transportation reconstruction network strategies: a full cost approach." *Review of Urban and Regional Development Studies*, 13(3).

Cornell, C.A. and Merz, H. (1974). "Seismic risk analysis of Boston." *Journal of the Structural Engineering Division*, ASCE, 101: 2027-2043.

Cramer, C. H. (2001). "A seismic hazard uncertainty analysis for the New Madrid seismic zone." *Engineering Geology*, 62, 251-266.

Crouse, C.B. and McGuire, J.W. (1996). "Site response studies for purpose of revising NEHRP seismic provisions." *Earthquake Spectra*, 12, 407-439.

DesRoches, R. (2002). "Bridge fragility." Personal Communication.

Dobry, R., Borcherdt, R.D., Crouse, C.B., Idriss, I.M., Joyner, W.B., Martin, G.R., Power, M.S., Rinne, E.E., and Seed, R.B. (2000). "New site coefficients and site classification system used in recent building seismic code provisions." *Earthquake Spectra*, 16(1), 41-67.

Dutton, C. E. (1889). "The Charleston earthquake of August 31, 1886." *USGS, Ninth Annual Report*, 1887-88, 203-528.

EPRI (1993). "Guidelines for determining design basis ground motions, early site permit demonstration program, Vol.1." *RP3302*, Electric Power Research Institute, Palo Alto, California.

FEMA (1990). "Estimated future earthquake losses for St. Louis City and County, Missouri." *Report 192*, Earthquake Hazards Reduction Series 53, Federal Emergency Management Agency, Washington, D.C.

Federal Highway Administration (FHWA) (1995). " Seismic retrofitting manual for highway bridges." Technical Report FHWA-RD-94-52, Office of Engineering and Highway Operations Research and Development, Federal Highway Administration, McLean, VA.

Frankel, A.D., Mueller, C.S., Barnhard, T.P., Perkins, D., Leyendecker, E.V., Dickman, N.C., Hanson, S.L., and Hopper, M.G. (1996). "National seismic-hazard maps: documentation June 1996." *USGS, Open-File Report 96-532*.

French, S. and Olshansky, R. (2000). "Inventory of Essential Facilities in Mid-America," *Project SE-1 Final Report*, Mid-America Earthquake Center, Urbana, IL.

Gupta, I.N. (1980). "A note on correlation of Modified Mercalli Intensity with peaks of far-field ground motion." *Bulletin of Seismological Society of America*, 70(3), 925-932.

Gupta, I.N. and Nuttli, O.W. (1976). "Spatial Attenuation of Intensities for Central U.S. Earthquakes." *Bulletin of Seismological Society of America*, 66, 743-751.

Gupta, U. (2001, June). "Earthquake loss estimation including transportation network Damage." *Master's thesis*, MIT, Cambridge, MA.

Hanks, T.C. and Cornell, C.A. (1994). "Probabilistic seismic hazard analysis: A beginner's guide." *Proceedings of the Fifth Symposium on Current Issues Related to Nuclear Power Plant Structures, Equipment and Piping*, I/1-1 to I/1-17, North Carolina State University, Raleigh, N.C., 1994.

HAZUS (2000). HAZUS Technical Manuals. National Institute of Building Sciences (NIBS), Washington, D.C.

Howell, B. F. and Schultz, T.R. (1975). "Attenuation of Modified Mercalli Intensity with distance from the epicenter." *Bulletin of Seismological Society of America*, 65, 651-665.

Hwang. H., Lin, H. and Huo, J.R. (1997a). "Site coefficients for design of buildings in eastern United States." *Soil Dynamics and Earthquake Engineering*, 16, 29-40.

Hwang. H., Lin, H. and Huo, J.R. (1997b). "Seismic performance evaluation of fire stations in Shelby County, Tennessee." *Earthquake Spectra*, 13(4), 739-758.

Hwang, H., Jernigan, J.B., and Lin, Y.W. (2000a). "Evaluation of seismic damage to Memphis bridges and highway system." *Journal of Bridge Engineering*, ASCE, 5(4), 322-330.

Hwang, H.M., Jernigan, J.B., Billings, S., Werner, S.D. (2000b). "Expert opinion survey on bridge repair strategy and traffic impact." In *Post-Earthquake Highway Response and Recovery Seminar*, St. Louis, MO.

Jones, B.G. (1994). "Development of a Methodology for Making Indirect Estimates of the Built Physical Environment." Research Accomplishments, 1986-1994. Buffalo, New York: National Center for Earthquake Engineering Research, 107-120.

Jones, B.G. and Malik, A.M., (1996). "The Building Stock in Memphis: Relating Structural Type and Use," *Proceedings of the Eleventh World Conference on Earthquake Engineering*, Elsevier Science, Ltd., Oxford.

Joyner, W.B. and Boore, D.M. (2000). "Recent developments in earthquake ground-motion estimation." *Proceedings of the Sixth International Conference on Seismic Zonation*, Earthquake Engineering Research Institute, Oakland, CA, Vol. II, 679-685.

Karaca, E. (2003). "Bridge damage comparisons." Personal Communication.

Kim, T.J., Ham, H., and Boyce, D.E. (2002). "Economic impacts of transportation network changes: Implementation of a combined transportation network and input-output model." *Papers in Regional Science*, 81, 223-246.

Kircher, C.A., Nassar, A.A., Kustu, O. and Holmes, W.T. (1997). "Development of building damage functions for earthquake loss estimation." *Earthquake Spectra*, 13(4), 663-682.

Kunnumkal, S. (2001). "Interactions and Restoration of Earthquake Damage Components." Personal Communication.

Kunnumkal, S. (2002). "Multi-Resolution Analysis of Earthquake Losses: From City Block to National Scale." *Master's thesis*, MIT, Cambridge, MA.

LLNL (1984). "Development of eastern U.S. ground motion models." *Seismic Hazard Characterization of the Eastern United States: Methodology and Interim Results for Ten Sites*, Vol. NUREG/CR-3756, Lawrence Livermore National Laboratory.

Mahaney, J. A., Terrence F. P., Bryan E. K., and Sigmund A. F. (1993). "The Capacity Spectrum Method for Evaluating Structural Response during the Loma Prieta Earthquake". *Proceedings of the 1993 United States National Earthquake Conference*, Memphis, Tennessee, Vol. 2, 501-510.

Murphy, J.R. and O'Brien, L.J. (1977) "The correlation of peak ground acceleration amplitudes with seismic intensity and other physical parameters." *Bulletin of Seismological Society of America*. 67, 877-915.

Newmark, N.M. and Hall, W.J. (1976). "Seismic design spectra for nuclear reactor facilities." *Proceedings of the Fourth World Conference on Earthquake Engineering*, Elsevier Science, Ltd., Oxford.

Nuttli, O. W. (1973). "The Mississippi valley earthquakes of 1811 and 1812: intensities, ground motions and magnitudes." *Bulletin of Seismological Society of America*, 63, 227-248.

Nuttli, O.W. and Hermann, R.B. (1984). "Ground motion of Mississippi valley earthquakes." *Journal of Technical Topics in Civil Engineering*, ASCE, 110 (1), 54-69.

Nuttli, O.W. and Hermann, R.B. (1984). "Scaling and Attenuation Relations for Strong Ground Motion in Eastern North America." *Proc. of the Eighth World Conference on Earthquake Engineering,* 305-309.

Okuyama,Y., G.J.Hewings, T.J.Kim, D.F.Boyce, H.Ham, and J.Sohn (1999). "Economic Impacts of an Earthquake in the New Madrid Seismic Zone. A Multiregional Analysis." *Proceedings, 5th U.S Conference on Lifeline Earthquake Engineering*, Seattle, WA, U.S Geological Society.

RMS (1994). "Development of a Standardized Earthquake Loss Estimation Methodology." Volume II. Draft Technical Manual - 95% Submittal. Prepared by Risk Management Solutions, Inc., Menlo Park, CA.

Rodriguez-Marek, A., Bray, J.D. and Abrahamson, N. (1999). "Characterization of site response general categories." *PEER Report 1999/03*. Pacific Engineering Research Center, Berkeley, CA.

Silva, W., Darragh, R., Gregor, N., Martin, G., Abrahamson, N. and Kircher, C. (2000). "Reassessment of site coefficients and near-fault factors for building code provisions." *USGS EHRP Program Report 98-HQ-GR-1010.*

SSHAC (1996). "Probabilistic seismic hazard analysis: A consensus methodology, Senior Seismic Hazard Analysis Committee (R. Budnitz, G. Apostolakis, D. Boore, L. Cluff, K. Coppersmith, A. Cornell, P. Morris)." U.S. Department of Energy, U.S. Regulatory Commission, Electric Power Research Institute.

Sohn, J., G.J.D. Hewings, T.J. Kim, J.S. Lee, and S.Jang (2001, November). Economic Assessment of Earthquake Impacts on Transportation Networks: A Scenario Analysis. *REAL 01-T-16.*

Toro, G. R., Abrahamson, N.A., Schneider, J.F. (1997). "Model of strong ground motions from earthquakes in central and eastern North America: Best estimates and uncertainties." *Seismological Research Letters*, 68(1), 41-57.

Toro, G. R. and Silva, W.J. (2001). "Scenario earthquakes for Saint Louis, MO, and Memphis, TN, and seismic hazard maps for the central and eastern United States region including the effect of site conditions." *Technical report*, Risk Engineering, Inc., Boulder, CO.

Trifunac, M.D. and Brady, A.G. (1975). "On the correlation of seismic intensity scales with the peaks of recorded strong ground motion." *Bulletin of Seismological Society of America*, 65 (1), 139-162.

Uniform Building Code (1997). "Uniform Building Code." Whittier, California: International Conference of Building Officials.

Werner, S., C. Taylor, J.M. II, J. Walton, and S. Cho (2000). "A risk-based methodology for assessing the seismic performance of highway systems." *Technical Report*, Multidisciplinary Center for Earthquake Engineering Research, Buffalo, New York.